The Lunar Atmosphere: History, Status, Current Problems, and Context

S. Alan Stern
Space Science Department
Southwest Research Institute

For Submission to Reviews of Geophysics, 1997

Running Title: The Lunar Atmosphere

Send correspondence to:

Alan Stern
Southwest Research Institute
1050 Walnut St., No. 426
Boulder, CO 80302

astern@swri.edu

[303]546-9670 (voice)
[303]546-9687 (fax)

ABSTRACT

After decades of speculation and fruitless searches, the lunar atmosphere was first observed by Apollo surface and orbital instruments between 1970 and 1972. With the demise of Apollo in 1972, and the termination of funding for Apollo lunar ground station studies in 1977, the field withered for many years, but has recently enjoyed a renaissance. This reflowering has been driven by the discovery and exploration of sodium and potassium in the lunar exosphere by groundbased observers, the detection of metal ions derived from the Moon in interplanetary space, the possible discoveries of H_2O ice at the poles of the Moon and Mercury, and the detections of tenuous atmospheres around more remote sites in the solar system, including Mercury and the Galilean satellites. In this review we summarize the present state of knowledge about the lunar atmosphere, describe the important physical processes taking place within it, and then discuss related topics including a comparison of the lunar atmosphere to other surface boundary exospheres in the solar system.

1.0 OVERVIEW

Owing to the lack of optical phenomena associated with the lunar atmosphere, it is usually stated that the Moon has no atmosphere. This is not correct. In fact, the Moon is surrounded by a tenuous envelope with a surface number density and pressure not unlike that of a cometary coma.[1] Since the lunar atmosphere is in fact an exosphere, in which particle-particle collisions are rare, one can think of its various compositional components as "independent atmospheres" occupying the same space.

This review of the lunar atmosphere is structured as follows: In §1 we will describe the history and provide an overview of the current state of knowledge about the lunar atmosphere. In §2 we discuss the structure and dynamics of the lunar atmosphere. In §3 we provide a more detailed look at the production and loss mechanisms of the lunar atmosphere. In §4 we provide a comparison of the lunar atmosphere to tenuous exospheres around other bodies in the solar system, with particular emphasis on comparison to Mercury. In §5, we examine some special topics. Finally, in §6, we summarize the major outstanding issues concerning lunar atmospheric science, ca. 1998, and describe some of the important future experiments that would shed light on this tenuous but fascinating aspect of Earth's nearest neighbor.

Before beginning, we caution the reader that this review could not possibly cover every topic relating to the lunar atmosphere in the depth it deserves, and tough choices had to be made about both the breadth and depth of the discussions that follow. Our approach

[1] However, the composition is quite different from that of any comet.

has been to review the "big picture," and to leave much of the fascinating nitty gritty to referenced papers in the literature. Any deficiencies that this approach has caused are the responsibility of this author.

1.1 A Brief Pre-Apollo History of Quantitative Atmospheric Searches

Although the lunar atmosphere was not detected until the Apollo era, scientifically based searches for the lunar atmosphere extend back to telescopic observations by Galileo. Based on the fact that optical phenomena like hazes, refraction, and clouds were not detectable, even with primitive instruments, it has been known for centuries that the lunar atmosphere must be extremely tenuous, at best.

Limiting ourselves to only key work done in this century, the record of successively more constraining research results is as follows: Fessenkov (1943) reported a search for polarization effects near the lunar terminator to set an upper limit on the surface (i.e., base) pressure of the lunar atmosphere near 10^{-4} bars. Using a Lyot polarimeter, Dollfus (1952, 1956) later reported successive upper limit pressures of $\approx 10^{-9}$ bars and $\approx 10^{-10}$ bars, respectively. Even during the early space age period prior to the Apollo lunar landings, theorists developed a convincing case that any ancient lunar atmosphere or plausible present-day source would have been rapidly lost to space through nonthermal loss processes, including blowoff, charge exchange, photoionization, and solar-wind scavenging (e.g., Herring & Licht 1959; Singer 1961; Hinton & Taeusch 1964).

Later still, occultation tests searching for the refraction of radio signals from lunar spacecraft and radio stars were eventually able to set an upper limit of 40 e^- cm^{-3} on the near-surface ion density based on studies using Pioneer VII (Pomalaza-Diaz 1967); Johnson (1971) coupled these data with a model of the expected ionization fraction of the lunar atmosphere to set various species-dependent surface pressure limits, including $\sim 3 \times 10^{-9}$ bars for hydrogen, $\sim 8 \times 10^{-10}$ bars for He, and $\sim 8 \times 10^{-12}$ bars for Ar. Limits like these were the state of the art until Apollo instruments were flown to the Moon to make more sensitive searches.

1.2 Lunar Transient Phenomena

In addition to the kinds of searches described above in §1.1, there has, particularly in the latter half of the twentieth century, been an ongoing effort to search for evidence of sporadic outgassing from the Moon. Such phenomena are collectively termed "Lunar Transient Phenomena" (LTPs) which we discuss briefly here.

There is a long history of documented reports (stretching back to at least 557 B.C.!) of groundbased sightings of discrete LTPs. In the modern era, interest was dramatically enhanced by (i) 1955 Mt. Wilson patrol images which apparently showed luminescent areas

on or over the crater Alphonsus, and (ii) Kozyrev's November 1958 spectrographic sequence showing a transient spectral emission from the central peak of Alphonsus (Kozyrev 1959, 1962).[2]

Both Middlehurst (1967) and later Cameron (1972) made in-depth studies of hundreds of reported LTP events. They found that two-thirds of the reported events occurred over the crater Aristarchus, a site where the orbiting Apollo 16 Command Service Module (CSM) detected radon emission. Although the lack of a sufficiently systematic patrol for LTPs makes the systematics of statistical tests hard, Cameron (1972, 1974) demonstrated that no statistically significant correlations of reported events occur with lunar phase or solar wind activity. However, Cameron has made the relatively convincing claim that the geographical distribution of LTP sites appears correlated with mare/highland boundaries.[3] Quite recently, Buratti et al. (1998) have recently used Clementine mission imagery to study seven sites where LTP reports have clustered, and found that several sites of repeated LTPs appear to be associated with sites of geologically recent landslide or downslope slumping.

Despite the fact that no definitive data set exists to prove that LTP reports represent true optical events (e.g., a two-site image series or simultaneous images and spectra), a significant number of lunar observers regard LTPs as real, and a manifestation of atmospheric activity. Because we will not discuss LTPs in greater detail within this review, interested readers are directed to the LTP surveys and discussions in Middlehurst (1967), Cameron (1972, 1975, 1978), and most recently Buratti et al. (1998). Despite the lack of space for further discussions on this topic here, we recognize its importance and encourage observers to provide convincing detections, which would surely open up a valuable new avenue of lunar atmosphere research.

1.3 Apollo Observations of the Lunar Ionosphere

In this subsection, we describe the Apollo-era studies of ions in the lunar environment. In the following two subsections, we will describe the Apollo-era discoveries of neutral gases in the lunar atmosphere, and of electrostatically suspended lunar dust. Following that, we will discuss more recent observational studies of the lunar atmosphere, beginning with the late-1980s discovery and subsequent study of sodium and potassium neutrals in the lunar atmosphere, which we describe in §1.6.

Observations of ions in the lunar environment were carried out beginning in late 1969 and

[2] Kozyrev attributed this emission to $\sim 4 \times 10^{12}$ g of C_2 fluorescing in sunlight, but this interpretation is not secure.

[3] This is an intriguing conclusion, owing to the Apollo 15 and 16 Rn gas detections which were also correlated with mare/highland boundaries, as we describe in §1.3.

extending to 1977 by the three surface-based Supra-Thermal Ion Detector Experiments (SIDE) emplaced by Apollos 12, 14, and 15, and the Charged Particle Lunar Environment Experiment (CPLEE) emplaced by Apollo 14.

Each SIDE instrument (Freeman 1972) consisted of two detectors, a mass analyzer (measuring six mass-to-charge bands from 0.2 eV/q to 48.6 eV/q), and a total ion detector (measuring 20 m/q bands from 0.01 KeV/q to 3.5 KeV/q). A key operating aspect of this device was that it could only detect ions accelerated into its aperture by an external electric field. As a result, the instrument could only detect ions within its field of view,[4] and the SIDE instruments only statistically sampled the lunar ion environment.

The goals of the SIDE experiment were to detect and characterize ions created from lunar atmosphere neutrals, ions in the solar wind as they interacted with the Moon, and the strength of the lunar surface electric field. As described by Benson et al. (1975), SIDE observations did in fact detect lunar atmosphere-generated ions, solar wind (and even terrestrial, planetary wind) ions, ions created by various Apollo spacecraft and debris sources, and ions time correlated with seismic detector signals that were later attributed to meteoroid impacts. Almost all of these signatures were detected during the lunar day.[5] The SIDE instruments also measured near-surface dayside electric fields of +5 to +10 V, and nightside fields of −10s to −100s of V; a Debye screening length of λ=1 km was derived.

Based on the results obtained by the SIDE instruments, it was learned that the lunar ionosphere is directly coupled to the interplanetary electric field. As a result, ion fluxes are nonthermal, highly directional, and highly variable. As in the neutral atmosphere, interactions with the lunar surface control the chemistry, and atmospheric (i.e., ion) collisions are rare. Near the surface a dayside ion sheath of height a few 10^2 m and a density of order 10^4 cm^{-3} exists (Reasoner & Burke 1972). Above this layer is a deep region of ions whose source is the neutral lunar atmosphere. Once formed, these ions are driven either toward (i.e., into) or away from the Moon as they are accelerated along interplanetary electric field lines; Figure 1.1 details some aspects of the lunar ionosphere.

Concerning ionized gas detections, all three SIDE instruments routinely detected m/q=20–28 and 40–44 ions generated by V×B drift into the instrument apertures around times of local terminator surface crossings. These signals, with typical fluxes of $\sim 10^5$ cm^{-2} s^{-1} sr^{-1} (and solar wind correlated excursions to $\sim 10^5$ cm^{-2} s^{-1} sr^{-1}) were attributed to ionized

[4] The instrument field of view was 6×6 deg, aligned to view 15 deg from the local vertical.

[5] Although ion outbursts were detected during the lunar night with fluxes of $\sim 10^4$ cm^{-2} s^{-1} sr^{-1} and m/q<10 eV/amu, such events were attributable to solar wind ions transported into the SIDE field of view by fluid turbulence effects.

^{40}Ar from the native lunar atmosphere (cf., §1.5). Benson et al. (1975) and Freeman & Benson (1977) found that a neutral gas source of roughly 10^5 cm^{-3} Ar atoms would be required to explain the m/q=40–44 ions, which is consistent with Apollo 17 site neutral mass spectrometer measurements of neutral Ar (again, cf., §1.5); for Ar, the SIDE data imply an exponential atmosphere with a barometric (i.e., thermal) scale height near 40 km.

Despite the fact that ions generated from the neutral atmosphere were so often observed at terminator crossings, only one possible sporadic gas emission event was observed during the lunar daytime. The lack of such events significantly constrains the lunar internal outgassing rate. Vondrak (1974) used the lack of SIDE-detectable gas transients, with an equivalent neutral gas detection threshold near 3×10^{-10} g cm^{-2} (or $0.5–2\times10^{-12}$ molecules cm^{-2}), to eliminate the possibility of any gas release events of magnitude larger than a few 10^7 g on the lunar front side during the period of SIDE operations. Vondrak (1977) noted that the SIDE event detection threshold should have been capable of detecting the November 1958 Kozyrev LTP event at Alphonsus.

The single, exceptional event detected by SIDE investigators was the 14-hour long, post-sunrise event of 7 March 1971 observed by the Apollo 14 SIDE. This event occurred shortly after the first sunrise at the Apollo 14 site after the instrument was emplaced; it was never repeated. The 7 March 1971 event signature displayed a complex time history of water vapor ions. Although it was initially attributed to a possible indigenous lunar source (Freeman et al. 1973); Freeman & Hills (1991) later concluded that the most probable source of these water ions was Lunar Module (LM) derived water evolving out of the local regolith as it warmed after sunrise. Accordingly, this well-known event is now generally accepted to be an exploration generated, as opposed to a indigenous lunar event.[6]

1.4 Apollo Observations of the Neutral Lunar Atmosphere

As a part of the Apollo lunar science program, three cold cathode gauges (CCG) instruments and a mass spectrometer (called LACE) were deployed on the lunar surface. Additionally, two mass spectrometers, two alpha particle spectrometers, and a UV spectrometer were placed in orbit for brief periods during 1971–1972. These instruments were designed to measure various compositional and bulk properties of the neutral lunar atmosphere. We begin this subsection with a review of the results of the surface instruments in this suite, and then proceed onto the results obtained by orbital instruments.

Cold Cathode Gauges were emplaced on the lunar surface at the Apollo 12, 14, and 15

[6] While we find Freeman and Hill's arguments concerning the probable cause of the 7 March 1971 Apollo 14 SIDE event well taken, we point out that no similar post-landing events were detected by the Apollo 12 and 15 SIDE instruments.

sites in December 1969, January 1971, and July 1971, respectively. These devices were capable of measuring total atmospheric pressure. The Apollo 12 instrument failed after less than one day of operation, but the Apollo 14 and 15 instruments operated until the mid-1970s.

Contamination in the area of the Apollo surface detectors severely constrained the CCG's ability to make precise measurements during the lunar daytime when outgassing from the LM descent stage and other abandoned equipment was significant. As a result, the CCGs determined only upper bounds of 2×10^7 molecules cm^{-3} near the surface in the local daytime environment as the instrument saturated near sunrise; however, during the cold lunar night when outgassing from nearby equipment was not a significant factor, they detected the nighttime lunar atmosphere. Because the derived densities were dependent on the (then) unknown composition of the atmosphere, investigators quoted densities for the assumption of N_2 gas; this resulted in a derived 2×10^5 molecules cm^{-3} at night, with factor of two uncertainties owing to the true composition (cf., Johnson et al. 1972).

In addition to CCG measurements, the final Apollo mission, Apollo 17, also deployed the LACE mass spectrometer on the lunar surface. This instrument mass range 1–110 amu, sensitivity: 1 count s^{-1} equivalent to $\approx$200 cm^{-3}) was an improved version of the CCGs, but unfortunately only operated for only 9 months. Like the CCGs that preceded it, LACE was routinely swamped by artifacts emanating from the nearby Lunar Module descent stage and other abandoned equipment during the lunar daytime (Hoffman et al. 1973). Despite this, LACE obtained firm detections of two species, argon and helium, during the lunar night; possible pre-sunrise detections of other species were also obtained. Initial reports of daytime ^{20}Ne detection by LACE were later revealed to be consistent with a contamination source of $H_2{}^{18}O$ from Apollo equipment (Hodges et al. 1973).We now describe each LACE signature, in turn.

Argon, which is adsorbable on the cold trapped ($\sim$100 K) lunar surface at night was observed to follow a diurnal pattern with a nighttime minimum near 2×10^2 cm^{-3}, followed by a rapid increase around sunrise to values as high as 3×10^4 cm^{-3} before LACE became saturated by gas evolving off the warming lunar surface (Hodges et al. 1972a). This is shown in Figure 1.2. The identification of Ar as endogenic was based on the fact that the typical ^{40}Ar:^{36}Ar ratio was found to be 10:1, far different from the ^{40}Ar:$^{36}Ar \ll 1$ ratio of the solar wind; the dominant lunar Ar source, ^{40}Ar, results from the decay of ^{40}K.

In modelling the LACE argon data, Hodges et al. (1973) reported evidence for a time variable lunar ^{40}Ar source of $1\text{–}4\times10^{21}$ s^{-1}, which they attributed to possible indications of a variable release rate from the deep interior.

In an important recent advance, Flynn (1997) has claimed a detection of lunar Ar at 1048 Å using the ORFEUS-SPAS satellite in Earth orbit during December 1996. This represents

both the first detection of lunar Ar by remote sensing, and the first daytime measurement of lunar argon. Flynn's derived Ar daytime surface number density is much higher than predicted, near 10^5 cm^{-3}.

As noted above, LACE also positively detected helium (during the lunar night), in the form of ^{4}He, which has no counterpart in the suite of artifactual contaminants.[7]

As shown in Figure 1.3, LACE observed nighttime helium maxima varying in the range of 2–4$\times 10^4$ cm^{-3}. Based on this number density, the total ^{4}He content of the lunar atmosphere, including ^{4}He in satellite orbits, is $\sim 10^{30}$ atoms, or 7×10^6 g (7 tons). LACE observations demonstrated that the helium number density regularly rose and fell by a factor of 20 during the lunar diurnal cycle, following the expected $n \sim T^{-5/2}$ exospheric model for noncondensable species (Hodges & Johnson 1968). Superimposed on this diurnal cycle were fluctuations well correlated with fluctuations in the geomagnetic index K_p, and hence the solar wind, such that the solar wind α-particle flux ϕ_α required to generate the observed lunar helium follows $\phi_\alpha = (5.6 \pm 1.9 + 0.44 K_p) \times 10^6$ cm^{-2} s^{-1} (Hodges 1975). The correlation of K_p with He abundance is discussed again in §3.2.

Searches by LACE for other candidate species, including N_2, CH_4, CO, CO_2, and NH_3 were undertaken at night when the contamination level from discarded equipment and the Lunar Module were low, but no definitive detections of native sources were made. Typical nighttime upper limits of order 10^3 cm^{-3} were achieved. The absence of solar wind H, C, and N in the LACE and other data sets has been attributed to the reduction of these species on the surface to H_2, CH_4, and NH_3, respectively (e.g., Hodges 1975). Hodges et al. (1973) used LACE data to set an upper limit of 8×10^4 cm^{-3} on the maximum diurnal lunar H_2 abundance; this nighttime constraint is consistent with the Apollo 17 UVS daytime H_2 upper limit of 1.4×10^3 cm^{-3}.

Finally with regard to LACE, we discuss the possible detection of species with masses at 15–16 amu, 28 amu, and 44 amu (Hoffman & Hodges 1975b). Signals at these mass channels were obtained in pre-sunrise data, indicating either O or CH_4 for the '16 amu' signal, N_2 or CO for the 28 amu signal, and CO_2 for the 44 amu signal.[8] In all three cases, the signal increase begins several hours before sunrise, and continues to rise until the instrument became background saturated around sunrise. Hoffman & Hodges (1975b) analyzed these

[7] Except possibly He outgassed from the ALSEP nuclear power supply, however, the correlation of [He] with geomagnetic index argues that this contribution must be small. By contrast, ^{3}He, like H, and H_2 could not be detected in this instrument owing to internal backgrounds in mass channels 1, 2, and 3; (R.R. Hodges, pers. comm. 1997).

[8] O is considered likely because it should naturally oxidize, e.g., with Fe to FeO (Hodges, pers. comm. 1997); also, the Apollo 17 UVS set a strict upper limit of 500 cm^{-3} on O, at odds with the LACE "detection" at 16 amu.

signals in terms of specific atmospheric spieces and reported model-dependent sunrise concentrations near 1×10^4 cm^{-3}, 8×10^2 cm^{-3}, 1×10^3 cm^{-3}, and 1×10^3 cm^{-3} for CH_4, N_2, CO, and CO_2, respectively. Because these possible detections could not be confirmed, they unfortunately can only be considered tentative.[9]

We now turn to orbital measurements of neutral species. The first clear orbital detections of native lunar gas were obtained from the Apollo 15 (July–August 1971) and 16 (April 1972) orbital Alpha Particle Spectrometer experiments (Gorenstein et al. 1973), which were designed to detect alpha particles from the noble gas ^{222}Rn, and its daughter product ^{210}Po (themselves decay products in the Ur and Th decay chains), as an indicator of either lunar internal outgassing or sites of high concentrations of radioactive decay products.[10] See Figure 1.4.

^{222}Rn was detected at an average level about 10^{-3} that of terrestrial emissions. This lunar Rn emission was found to be concentrated over a small number of localized sites ("hot spots") of scale ~150 km in diameter, most notably the Aristarchus/Marius Hills region, Grimaldi, and possibly Alphonsus and Tsiolkovsky. Both the Aristarchus/Marius Hills region and Grimaldi have been frequently reported to be sites of lunar transient optical phenomena (LTPs, cf., §1.2 above). Interestingly, both of these regions were experiencing lunar night when Rn was detected over them. Bjorkholm et al. (1973) demonstrated that the Rn emission they detected could not have plausibly come from a surface enriched in radioactive decay products, because Apollo orbital gamma ray spectrometers would have found a correlated emission source in their data. Based on this, they concluded that the Rn must have originated from outgassing from localized source regions.

As noted above, ^{210}Po, which is a daughter product of ^{222}Rn decay, was also detected by the Apollo 15 and 16 alpha particle spectrometers. The ^{210}Po emission was correlated with mare/highland boundaries (Gorenstein et al. 1974). Importantly, the polonium was detected in disequilibrium excess concentrations compared to ^{222}Rn. The combination of Rn and Po in the radioactive disequilibrium ratio seen by the Apollo 15 and 16 alpha particle instruments provides evidence for both ongoing (due to the ^{222}Rn's 3.8 d half-life) and more long-term outgassing (due to the Pb precursor of ^{210}Po's 21 yr half-life).

The Apollo 15 and 16 spacecraft also carried mass spectrometers into lunar orbit, which should have been capable of measuring the global distribution of many species. However, these instruments were heavily contaminated by effluents from the Apollo Com-

[9] The Apollo 17 UVS was capable of making comparative measurements of CO, but its upper limit (see Table 1.1) was far higher than the concentrations implied by the LACE data.

[10] Turkevitch et al. (1970) reported some previous but less secure evidence for Rn emission in Surveyor lander alpha particle spectrometer data.

mand/Service Modules on which they flew. No detections or particularly useful upper limits were therefore obtained from these instruments (Hodges et al. 1972b; Hodges, pers. comm. 1991).

Later in 1972, a high-throughput UV spectrometer with a 1180–1680 Å bandpass was operated in lunar orbit for 6 days aboard Apollo 17 (Fastie et al. 1973). Although searches for resonance fluorescence lines of H, O, C, N, Kr, Xe, H_2, and CO were made, no detections were obtained. Feldman & Morrison (1991) later re-analyzed the Apollo 17 UVS data set and used modern resonance fluorescence g-factors to obtain revised upper limits on all of these species, as well as atomic S. These results are summarized in Table 1.1.

In addition to direct observations, an additional set of orbitally-derived atmospheric constraints were derived during the Apollo era by Siscoe & Mukherjee (1972) and Mukherjee (1975), who exploited the absence of evidence in Explorer 35 data for solar wind mass loading by the lunar atmosphere. Their results, which assume a T=300 daytime exosphere, provide upper limits on H, H_2, He, Ne, O_2, N_2, NO, CO, CO_2, N_2O, and CH_4 in the range 10^3–10^4 cm^{-3}. The Explorer 35 and Apollo 17 results continue to provide the best available constraints into what molecular species may reside in abundance in the lunar atmosphere.

1.5 Suspended Dust in the Lunar Atmosphere

Although this subject is largely beyond the scope of this review, it is worthwhile to briefly discuss the evidence for suspended dust above the lunar surface, and hence "in the lunar atmosphere."

The discovery of this dust was made in post-sunset Surveyor lunar lander TV camera images of the lunar horizon (e.g., Norton et al. 1967; Shoemaker et al. 1968). Surprisingly, these Surveyor images revealed the presence of a near-surface (e.g., scale height ~10–30 cm) glow that was observed to persist for several hours after sunset, and to have a brightness near $10^{-6}B_\odot$. Rennilson & Criswell (1974) eliminated the possibility that this signature was caused by gas, based on scale height and density constraints, and instead interpreted the cause of the forward-scattered light as a population of 5–10 μm grains with a column density of ~50 g cm^{-2}.

Additional information relating to the source of this phenomenon was obtained by the Apollo 17 Lunar Ejecta and Micrometeoroids (LEAM) surface experiment (e.g., Berg 1976), which operated for several years. For several hundred hours around lunar sunrise (indeed, beginning as much as 150 hours prior), signals from LEAM were found to be dominated by a population of low-energy impacts. A considerably smaller and shorter-lived pulse of signals was also seen at each sunset. The LEAM signature was attributed to electrostatically levitated (Gold 1955; McCoy 1976), or possibly photoemission-levitated,

submicron dust particles in transport across the terminator by the large (e.g., 0.2–1 V cm^{-1}) electric fields generated there by the highly resistive nature of the surface (cf., Berg 1976, 1978; Criswell 1973; Zook et al. 1994, 1995).

Optical evidence for even higher-altitude lunar dust was later obtained from horizon glow studies by (1) the Lunokhod 2 dual-channel (2700 Å, 5400 Å) photometer (e.g., Severney et al. 1974), (2) the Apollo 16 surface far-UV spectrographic camera (Carruthers & Page 1972), (3) Apollo 15 and 17 orbital photography, (4) Apollo crew visual sightings of lunar sunrise "streamers" (McCoy & Criswell 1974; cf., Figure 1.5), and (5) Clementine imagery (Zook et al. 1994, 1995). Estimates of the brightness of these glow signatures, which have been estimated to have a scale height of tens of kilometers, vary between $10^{-13}B_{\odot}$ and $4\times10^{-12}B_{\odot}$. Zook et al. (1995), like others, point out that the brightness signature of this glow is $\sim10^5$ times too great to be explained by micrometeoroid-generated ejecta from the lunar surface.

Summarizing, a suite of data sets seem to indicate that there could be as many as three separate lunar glow signatures. These are (1) a low-altitude (cm–m scale) dust layer generated by terminator phenomena; (2) a low-altitude (meters to hundreds of meters in height) daytime dust layer detected from the far UV to 5400 Å, generated by an as yet unspecified phenomenon; and (3) a high-altitude dust or dust+gas phenomenon.[11] Future studies of these interesting, and possibly time-varying, phenomena should prove useful, particularly if the relative contributions of dust and gas to the optical signatures can be determined, and if the dust columns and vertical distributions can be more accurately determined.

1.6 The Groundbased Discoveries and Study of Na and K

The close of the Apollo flight program in 1972 and the termination of ALSEP data collection in 1977 created a hiatus in observations of the lunar atmosphere that lasted about a decade. This hiatus was caused primarily by the fact that at the time the Apollo data collection ended, none of the then-known lunar atmospheric species could be detected by groundbased or spacebased optical remote sensing techniques.

However, a major breakthrough was achieved in 1988 with the 1987 discovery of D_2-line emission from atomic K and then Na in the lunar exosphere (Potter & Morgan 1988a; an independent discovery of lunar Na was also made by Tyler, Kozlowski, & Hunten 1988). The detection of these species was achieved via long-slit, high-resolution (R>50,000) spectroscopy, motivated by the 1985–1986 discoveries of Na and K in Mercury's exosphere

[11] There is also the possibility that the Apollo visual observations and orbital photography of LHGs with scale heights of 10s of km could have involved visual detection of the then-unknown 3–10 kR-class Na/K emissions.

by the same groups (cf., Hunten et al. 1988 for a review). The high spectral resolution used in these detection observations was needed to provide suitable contrast between the weak lunar Na signal and instrument-scattered light from the far stronger surface reflection.

Potter & Morgan (1988a) found subsolar limb brightnesses of 3.8±0.4 kilorayleighs (kR) for Na and 1.8±0.4 kR for K; these brightnesses correspond to estimated zenith column densities at the subsolar point of $N_{Na}=8\pm3\times10^8$ cm^{-2} and $N_K=1.4\pm0.3\times10^8$ cm^{-2}. Measured scale heights of $H_{Na}=120\pm42$ km and $H_{Na}=90\pm20$ km in this data set were used to derive estimated surface number densities of $n_{Na}=67\pm12$ cm^{-3} and $n_K=15\pm3$ cm^{-3}. Figure 1.6 shows some of the earliest published Potter & Morgan Na data. The derived scale heights indicated that the observed Na was approximately in thermal equilibrium with the surface. The 6±3 Na/K abundance ratio obtained from these data is close to the Na/K abundance ratio in lunar soils (Williams & Jadwick 1980; Taylor 1982). The independent discovery of lunar Na by Tyler et al. (1988) found quantitatively similar brightnesses, scale heights, and abundances.

Given the fact that the combined number density of Na and K in the lunar atmosphere is only $\sim10^2$ cm^{-3}, these constituents are only trace species in the lunar atmosphere. However, the detectability of Na and K from Earth makes them highly valuable probes of the lunar atmosphere. As such, many dozens of spectroscopic and later imaging observations of these species have been reported by members of the two discovery groups, as well as by Flynn & Stern (1996). The most important results of these observations may be briefly summarized as follows.

We begin with the spectroscopic results. Early on, Potter & Morgan (1988b, 1991) detected Na at altitudes as great as 1500 km (0.9 R_M), indicating the presence of a second, no-thermal population of sodium atoms in the lunar atmosphere with H≈600 km (cf., Morgan & Shemansky 1991); cf., Figure 1.7. Similarly, Kozlowski et al. (1990) measured K abundances up to 190 km above the surface, and found the Na vertical profile to also be best fit by a two-temperature component atmosphere ($H_1=52$ km, $T_1=395$ K, $H_2=329$ km, $T_2=2500$ K). Sprague et al. (1992) confirmed the high-altitude Na with observations up to 610 km. Both Potter & Morgan (1992) and Sprague et al. (1992) reported evidence for a systematic increase in Na scale height with lunar latitude, indicating a change in source process with solar zenith angle. Hunten et al. (1992) then reported that observations made on 12, 13, and 14 October 1990 revealed a 60% growth over this period of the Na signal above the lunar south pole, despite the fact that the Na signal above the equator on the same three dates remained constant within their detection limits. Potter & Morgan (1994) reported a systematic decrease in Na column abundance away from full Moon, but was not made clear how much of this result is simply due to geometrical circumstances (i.e., line of sight effects). Potter & Morgan (1997) reported empirical evidence showing that the Na abundance decreases with solar zenith angle χ like $\cos^2(\chi)$. Their findings (see Figure

1.8) indicate that because strictly flux-dependent sources should decline only like $\cos(\chi)$, the Na source responsible for the steep falloff must have some additional dependence on flux, temperature, or some other parameter depending on the solar zenith angle. As we describe further in §3.2, Potter & Morgan suggested that chemical sputtering may be the culprit, since the falloff depends on incident flux like $\cos(\chi)$ and then exponentially on temperature for the release rate. Further interpretations of these findings will be discussed in §2 and §3.

We now turn to imaging studies. Beginning with the pioneering work of Mendillo and co-workers, most notably Baumgardner (Mendillo et al. 1991), two-dimensional, direct imaging of the lunar Na has also been undertaken. Mendillo's team uses a Lyot-stop coronagraph with a 6 deg field of view (FOV) and a narrow-band Na D-line interference filter to image Na at altitudes $>1.5R_M$. In their initial report, Mendillo et al. (1991) described the detection of Na emission out to 4 R_M (almost 7,000 km), and found that the radial dependence of intensity and hence column density (given the optically thin nature of the emissions) above the subsolar region is well fit by an R^{-4} power law. These data dramatically confirmed the reality of the nonthermal Na atom population discovered spectroscopically. Flynn & Mendillo (1993) extended this work with whole-Moon Na images. Figure 1.9 shows such an image.

Mendillo et al.'s images, like previous spectroscopic work (cf., Sprague et al. 1992), revealed that the Na distribution becomes progressively fainter and more extended toward both poles. Flynn & Mendillo (1995) found that the Na brightness profile can be fit to an $I(R,\chi)=I_0(\chi)R^{\alpha}(\chi))$ dependence, where χ is the solar zenith angle. For the quarter-Moon geometry they observed, they found $I_0=(1+6\cos^2\chi)$ kR and $\alpha(\chi)=-2(1+\cos^2\chi)$.

Continuing, Stern (1992) developed an independent imaging technique based around Na observations over the dark side of the lunar terminator, where surface illumination is limited to reflected Earthlight and the atmospheric Na can thus be detected directly against the disk. This technique complements the high-altitude coronagraphic imaging of Mendillo and co-workers by being able to obtain images quite close to the terminator, allowing Na profiles to be extended down to 50 km (0.03 R_M) altitude. Stern & Flynn (1995) reported an analysis of Na images made this way over a variety of latitudes in the northern lunar hemisphere. Applying a simple Maxwellian exosphere model, these workers confirmed that both hot and cold Na populations are required to adequately fit the radial intensity behavior. They also discovered that the mixing ratios and temperatures of the two components vary systematically with latitude such that the ratio of hot, coronal gas to warm thermal gas progressively increases as one moves toward the pole. See Figure 1.10.

More recently, Mendillo's team obtained images of the high-altitude Na exosphere during the 29 November 1993 (Mendillo & Baumgardner 1995) and 4 April 1996 (Mendillo et

al. 1997) lunar eclipses, revealing emission out to 10 R_M (at 10 R_M, 32 R of background-subtracted lunar emission was found). For the 1993 event, a full-Moon (i.e., eclipse) geometry revealed an R_{-2} power law brightness distribution, with no significant azimuthal asymmetry. For the 1996 eclipse, azimuthal symmetry was again observed. but a differing radial structure was seen: Inside 4 R_M the brightness declined like R^{-3}, indicating a bound population of Na atoms; outside 4 R_M the brightness declined like R^{-1} (much like a comet's freely escaping, spherically symmetric coma). In this case, the Na intensity profile $I(R,\chi)$ fit was determined to have $I_0 \approx 1$ kR and α=-2, independent of χ. Taking into account the differing observation geometry and the fact that the eclipse observations primarily sampled the terminator atmosphere (χ=90 deg), these observations are seen to be consistent with the $I(R,\chi)$ fit Mendillo et al. (1991) found from atmospheric imaging at quarter-Moon. Potter & Morgan's (1997a) success in obtaining near-surface Na images using a coronagraphic technique with narrow-band interference filters opens a new channel for additional imaging observations.

1.7 Groundbased Upper Limits on Other Neutral Species

Because the Apollo CCG total pressure measurements indicate surface number densities far in excess of the total number density of identified species, it seems that much of the lunar atmosphere remains compositionally unidentified. This conclusion has led to observations in search of the "missing species," as we now describe.

Flynn & Stern (1996) began this work with an extensive search for additional neutral species in the lunar atmosphere. This search was based on the naive, but reasonable first assumption of a simple stoichiometric metal-atom exosphere that reflects the surface elemental composition, adjusted for species loss times (with species brightnesses further adjusted for scale height and resonance fluorescence efficiency (g-factor) effects. Such a model predicts that relatively abundant lunar *surface* constituents such as Si, Al, Ca, Mg, Fe, and Ti should be more abundant in the lunar atmosphere than are either Na or K. Flynn & Stern (1996) investigated this hypothesis by searching for solar resonant scattering lines of nine metallic neutrals between 3700 and 9700 Å using the 2.7 m coudé and the 2.1 m Cassegrain Echelle spectrographs at McDonald Observatory. Spectra were taken 20 arcsec above the subsolar limb of the Moon near quarter phase on 30 July 1994 and 10–12 March 1995. Upper limits were obtained for the first time for the abundant lunar surface species Si, Al, Ca, Fe, Ti, Ba, and the alkali Li. Their results are summarized in Table 1.1 and Figure 1.11. In the cases of Si, Ca, Fe, and Ti, the derived upper limits were more than an order of magnitude lower than the simple stoichiometric model predicts. The upper limits for Li and Al are less constraining. These workers concluded that the stoichiometric Na:K ratio is peculiar in that the mechanism(s) that produce the lunar Na and K atmosphere somehow favor those atomic species over many other abundant lunar surface species. Imaging spectrograph observations at large distances from the Moon

during the 4 April 1996 lunar eclipse (Mendillo et al. 1997) also detected no emission other than Na in a wide, 5800–7700 Å bandpass.

In a later paper, Stern et al. (1997) reported using the Hubble Space Telescope's (HST's) Faint Object Spectrograph to make an initial mid-ultraviolet spectroscopic search for emissions from the lunar atmosphere. This spectrum revealed no emission lines, despite the fact that strong resonance emission transitions from the Al, Si, and Mg neutrals, and Mg^+, are present in the bandpass. The 5 sigma upper limits derived on the atmospheric abundances of each of these species, and OH (0-0), emission are also presented in Table 1.1. The most constraining upper limit they obtained was for Mg, which was found to be depleted by a factor of at least nine relative to model predictions which use the known abundance of Mg in the lunar regolith. These findings reinforce the conclusions of the groundbased search for neutral atoms in the lunar atmosphere: the missing species remain missing, and stoichiometry does not obtain.[12]

Flynn & Stern (1996) noted that the lack of stoichiometry may indicate that the very lunar surface may not have reached radiation exposure equilibrium. This could occur, for example, if meteoritic bombardment sufficiently gardens the lunar surface to result in a reduced effective surface age (Johnson & Baragiola 1991). In this case, solar wind sputtering yields would not approach stoichiometry and volatile species would dominate atmospheric metal abundances.

Alternatively, Na and K may be unique in their ability to sputter from refractory surfaces as atomic neutrals. Thus, the lack of other abundant surface species in the atmosphere may indicate that either thermal desorption or chemical sputtering (cf., Potter & Morgan 1997a), both of which favor high-vapor pressure species like Na and K, is occurring; or it may indicate that the other metal species may be preferentially injected as molecular fragments (e.g., CaO, TiO, TiO_2, etc.) rather than atoms. The latter possibility is now being actively pursued by using millimeter-wave telescopes to search for simple molecules in the lunar atmosphere.

In any case, the search for the missing components of the lunar atmosphere goes on.

1.8 Lunar Water

We now turn to the subject of lunar water. Although there has never been a confirmed detection of water or its dissociation products, H and OH in the lunar atmosphere, the possibility of cold-trapped deposits of H_2O ice has been a subject of scientific speculation

[12] Interestingly, searches for Ca (Sprague et al. 1992) and Li (Sprague et al. 1995) in Mercury's exosphere, and for a broad array of neutrals in Io's Na/K exosphere (Na et al. 1998) have also yielded negative results (cf., §4 for additional details).

for almost four decades. One reason for this long-standing interest is the obvious potential of H_2O as a resource available to human exploration of the Moon. A more scientific motivation would be the potential for study of the isotopic (i.e., D/H and $^{16}O/^{17}O/^{18}O$) abundances in the ice.

There is little question that a source of exogenous lunar water exists via deposition from the meteoritic complex and occasional cometary impacts. Morgan & Shemansky (1991) have estimated that the *meteoritic* H_2O source rate is of order 0.5–5 g s^{-1}. The *cometary* source, though highly sporadic, is thought to provide a time-averaged source rate of order 75 g s^{-1}. The surface reduction of oxygen-bearing minerals via solar wind bombardment (Thomas 1974) may provide a third, smaller source.

Thus, although the fact that a source of water to the Moon exists is incontrovertable (and therefore has deposited $\sim 10^{18-19}$ g onto the Moon over the last 4 Gyr), impacting water molecules must survive impact (avoiding both ionization and impact jetting) to be retained even briefly in the lunar environment. The molecules are then subject to photon-driven destruction as they transport across the Moon in a diffusive "search" for safe havens.

The key question then is how much of the H_2O which impacts the Moon actually survives to reach a cold trap reservoir. Morgan & Shemansky (1991) estimate the sticking fraction of water impacting in the meteoritic complex to be of order 25%. To avoid subsequent. and indeed rapid loss (the timescale for water destruction by UV sunlight at 1 AU is $\sim$1 day), the water molecules must find safe haven by random walking their way around the surface of the Moon's "griddle hot" surface until they find a cold trap.[13] The efficiency of this diffusive transport is not well established, but even if it is just 1%, then 10^{16-17} g of water should have migrated to the lunar poles over time, corresponding to some 100–1000 g cm^{-2} of water embedded in the traps (if no loss processes existed there to remove it).

Arnold (1979), Lanzerotti et al. (1981), and Morgan & Shemansky (1991) have each examined the possibility of stable cold traps ($25<T<95$ K) in the permanently shadowed floors of deep craters at the poles. They found that although such traps would indeed be thermally stable over billions of years as predicted by previous workers, both charged particle sputtering and Lyα-driven photodissociation (the Lyα being solar, and reaching the shadowed areas by scattering off H in the interplanetary medium) would still act as loss processes, etching away exposed deposits at the rate of $\sim$0.7 mm yr^{-1}. Hence, to achieve

[13] As to observationally based constraints, Morgan & Shemansky predict a typical subsolar limb brightness of 50 R of OH resulting from H_2O loss to photodissociation (the dominant loss mechanism). However, even the best existing observational constraint on OH, a 5σ upper limit of 67 R, obtained by HST (Stern et al. 1997), is not particularly useful, because HST's spectrometers were not allowed to point closer than 1.1 R_M above the surface, i.e., $\sim$1 OH scale height above the surface.

true stability, the water ice in polar deposits must be buried, and the question becomes whether the lunar burial rate is rapid enough to shelter it more rapidly than it is lost.

The issue of the viability of lunar polar ice deposits has long been data starved, but that situation is now changing. This began when Nozette et al. (1995) reported evidence for an ice-like scatterer of radio waves at the lunar south pole, detected through a bistatic radar experiment using the Clementine lunar orbiter. Although Nozette et al.'s report received much attention, was been called into question by Goldstone radar results reported by Stacy et al. (1997). At the root of this controversy is the fact that radar sounding of the lunar pole is both difficult, and radar signatures (unlike spectra, for example) do not succumb to unique interpretation, particularly with regard to chemistry.

The next data set expected to shed light on this issue will be provided by the Discovery Lunar Prospector's orbital mission, which carries a gamma ray/neutron spectrometer capable of directly detecting neutron emission from hydrogenated deposits down to depths of order 0.3–3 m, depending on the local surface dielectric constant and compaction state. Lunar Prospector is scheduled to be launched in early 1998.

1.9 AMPTE Detections of Lunar Ions in the Solar Wind

The final topic to be discussed in §1 is the detection of singly ionized atomic species that apparently originate at the Moon, in the solar wind near 1 AU.

As we will discuss in some detail in §3, the highly nonthermal populations of Na and K provide strong evidence for a nonthermal source mechanism, such as meteoroid impact or sputtering. This in turn naturally suggests the possibility that many other elements in the surface (the "very regolith") could also be present in the atmosphere. Elphic et al. (1991) studied these production processes in the lab using a simulated, keV-class He^{++}, Ar^{+} solar wind ion beam on lunar soil samples and sample simulants, and found a rich variety of sputter products, dominated by neutrals but containing a few percent ions by number.

About the same time that Elphic et al.'s work reached publication, Hilchenbach et al. (1991) announced the finding that their time-of-flight ion mass spectrometer (SULEICA) aboard the high Earth-orbiting AMPTE spacecraft had detected singly ionized solar wind pick up ions of lunar origin. As shown in Figure 1.12, the ion mass distribution detected by the AMPTE/SULEICA instrument (E/Q resolution ~10%) was dominated by peaks consistent with O^{+} (16 amu) and either Al (26 amu), Si (28 amu), or perhaps S (34 amu).[14] Although many heavy species would not have been detectable within AMPTE/SULEICA's

[14] Johnson & Sittler (1990) and Elphic et al. (1991) report that typical sputter products have excess energies of 5–10 eV; the escape energy for Si and Al ions from the lunar potential well is ≈1 eV.

E/Q bandwidth. Hilchenbach et al. (1991) reported that the instrument's upper range channel sensitive to singly ionized species with 40–60 amu, obtained evidence consistent with the marginal detection of Ar^+, Ca^+, and Fe^+. Hilchenbach et al. (1993) estimated that the 0.3 ions cm^{-2} s^{-1} sr^{-1} keV^{-1} flux they detected in the 23–37 amu "Al/Si" band corresponds to a source characteristic production rate of ~3–31 ions cm^{-2} at the Moon.

Shortly thereafter, Cladis et al. (1994) reported a detection (8σ) of singly ionized lunar pickup ions in the 23–40 amu range, using ISEE-1 spacecraft data, and described a set of transport calculations that verified the ability of lunar ions, created by an ion source like that observed in Elphic et al.'s laboratory experiments, to reach spacecraft in high Earth orbit with angular distribution and energy characteristics like those observed with AMPTE and ISEE-1.

Despite the fact that the transport of ions from the Moon to a spacecraft in high Earth orbit is dependent on many poorly known variables, the observational evidence supporting a lunar origin for these ions is strong: The ions were detected in a relatively narrow cone (~30 deg width) when the spacecraft was near apogee ($18.7R_E$), upwind of the Moon but outside the Earth's magnetospheric bowshock (Hilchenbach et al. 1991, 1993), such as one would expect from surface or atmospheric sputter products accelerated by the near-surface dayside lunar electric potential.

2.0 STRUCTURE AND DYNAMICS OF THE LUNAR ATMOSPHERE

It is easily demonstrated that the total number density at the base of the lunar atmosphere is so low that any atom or molecule traveling upward from the surface with $v>v_{esc}$ (2.38 km s^{-1}) is unlikely to suffer a collision with another gas atom or molecule.[15] Put another way, the mean free path in the lunar atmosphere greatly exceeds the atmospheric scale height; as such the atmosphere is an exosphere in which collisions play a very minor role, and structure and dynamics are controlled almost entirely by ballistic kinematics.

Owing to the fact that individual atoms and molecules do not commonly communicate via collisions, each gas species can be thought of as a separate lunar atmosphere with its own distinct structural and dynamical properties. Owing to this approximation, the literature is laced with the terminology of the "lunar atmospheres."[16]

---

[15] The lunar escape velocity corresponds to energy and gas temperature requirements of 0.03 eV/amu and 226 K/amu, respectively.

[16] It is often not appreciated that the lunar atmosphere is not strictly a perfect, collisionless exosphere. In fact, the mean free path against gas-gas collisions is of order 10^{11} cm; for the bound, thermal component of the lunar atmosphere the average distance traveled before loss to photoionization is sufficiently large (e.g., at 400 K: $\sim 4\times10^{10}$ cm for Ar,

The structure and dynamics of each of the species-segregated lunar atmospheres is controlled by the source rates and energetics, loss rates, gas-surface interaction physics, and transport susceptibility unique to that species.

In what follows here in §2, we review the essential details of the structure and dynamics of the lunar atmospheres, dividing them into two groups: the noble gas atmospheres discovered in the Apollo era, and the alkali atmospheres discovered and subsequently studied by groundbased techniques.

2.1 Lunar Ionospheric Dynamics: General Considerations

An important subtopic which is beyond the scope of this review, and which we do not discuss in detail is the dynamics of ions, which for the most part are formed as a result of neutral loss processes. Lunar ion dynamics are controlled by the force felt from the local electric field. This electric (**E**) field is usually dominated by the solar wind **E** field, except during magnetospheric passage each month, when it is dominated for a few days by the **E** field of the terrestrial magnetotail. The **E** field direction (except very very near the lunar surface) is essentially perpendicular to the solar wind (or magnetotail) velocity and the magnetic field. The scale lengths over which the **E** and **B** fields of the solar wind are comparatively uniform are of order 0.01 AU, roughly 10^3 times the radius of the Moon. Ions are accelerated either away from the Moon or toward it depending on the direction of the local **B** field, with on average about half of the ions being driven back to the lunar surface, where they are often implanted at high energies (Manka & Michel 1971). For ions traveling upward, escape to infinity is the result. For all but the lightest ions, the gyro radius is much greater than the lunar radius, and escape occurs within one gyro period. Readers interested in this topic are referred to Vondrak (1988).

2.2 The Dynamics and Structure of the Helium and Argon Exospheres

Our knowledge of the structure and dynamics of the helium and argon exospheres of the Moon are limited by the lack of detailed information on the energetics, and therefore the thermal distribution, of the lunar He and Ar gas. As a result, studies of the structure and dynamics of lunar He and Ar in the literature have assumed a purely thermal source population initially derived from surface desorption. This ignorance is partially compensated for by the fact that He and Ar are noble gases, which greatly simplifies their surface

---

$\sim 2\times10^9$ cm for Na, $\sim 1\times10^9$ cm for K) that a finite, nontrivial collision probability exists for each species. Crude scaling calculations reveal that Na and K atoms have an $\sim$1% probability of collision with another gas species prior to photoionization, and that an Ar atom has a probability of several tens of percent of suffering such a collision. Clearly, weak but nonzero gas-gas thermal and even chemical communication pathways do exist in the lunar atmosphere.

chemical interaction.

The assumption that the velocity distribution functions are purely thermal produces a simple hydrostatic equilibrium exosphere with scale heights H$\sim$1000 km and $\sim$50 km. respectively, for He and Ar at a daytime T=400 K. Radiation pressure and solar/terrestrial gravity affect the trajectories of He and Ar atoms, as shown by Hodges (1973, 1978). Here, however, we restrict our discussion to the near surface (e.g., bottom-most scale height) of the lunar He and Ar exospheres.

As early as the late 1960s, before any evidence for the lunar atmosphere was discovered, Hodges & Johnson (1968) demonstrated that in hydrostatic equilibrium, one would expect lateral flow in the lunar exosphere to establish a number density (n) distribution controlled by the relation $n\mathrm{T}^{5/2}$=constant. The discoveries of helium and argon in the early 1970s allowed this result to be tested. However, there is an important difference between He and Ar: He is so volatile (condensation temperature near 5 K) that it does not condense on the lunar nightside. In point of fact, helium number densities were observed to follow the prediction, producing a smooth and repeatable nighttime maximum in number density that was about 20 times that seen during the lunar daytime (the $n\mathrm{T}^{5/2}$=constant relation predicts a 26:1 increase).[17]

More specifically, Hodges et al. (1972a) has shown that the diffusion approximation of exospheric transport gives a source flux function ϕ for noncondensable gases like He of the form

$$\phi = \left(\frac{\alpha}{1-\alpha}\right)\left(\frac{n\bar{v}}{4}\right) + \left(\Omega\frac{d(nH)}{d\theta}\right) - \nabla_h^2 n\bar{v}H^2, \tag{2.1}$$

where α is the temperature-dependent sticking coefficient, $\bar{v}$ is the mean velocity of the gas molecules, Ω is the angular rate of rotation of the Moon, θ is the subsolar longitude, and ∇_h^2 is the horizontal component of the Laplacian operator in a Sun-referenced coordinate frame.

By contrast, argon adsorption becomes important 120 K, allowing it to accumulate on the nightside lunar surface. Consequently, whereas He gas should strictly follow the $n\mathrm{T}^{5/2}$=constant relation, the condensation sink for argon will break this relation. The argon condensation sink, coupled with the $n\mathrm{T}^{5/2}$=constant exosphere relation, predicts a distribution which peaks at the terminator, has a low (effectively zero) minimum on the nightside, and displays a secondary minimum near the subsolar point. As illustrated by Figure 1.3, this prediction appears to be borne out by ALSEP LACE nighttime data; however, its validation during the lunar day remains problematic owing to LACE saturation by Lunar Module outgassing between sunrise and sunset. One would expect that

[17] We point out that the total He column, $N = n\mathrm{H}$; since the scale height H$\propto$T but n$\propto\mathrm{T}^{-5/2}$, N$\propto\mathrm{T}^{3/2}$ and N_{night}:$\mathrm{N}_{day}\sim$7:1.

other condensable gases, such as CH_4, NH_3, and H_2O, would qualitatively behave like this Ar profile if they exist in the lunar atmosphere and are dominantly produced by thermal source processes.

2.3 The Dynamics and Structure of the Sodium and Potassium Exospheres

The structure and dynamics of the lunar Na and K exospheres had profited enormously from the rich data set of Na and K vertical profiles and Na images accumulated over the past decade (cf., §1). Among the most important findings in of the accumulated information is the fact that both Na and K atoms exhibit at least two distinct energy distributions: a bound, thermally surface-accommodated, "barometric" component, and a largely unbound, nonthermal "coronal" component. These two energy distributions display qualitatively different styles of transport and degrees of surface interaction during their generation at sources and their loss to sinks. Figure 2.1 illustrates these two styles of dynamics, and also provides a kind of schematic overview of many of the sources and sinks at work in the lunar atmosphere.

In §3 below, the various source mechanisms for the Na and K lunar exospheres will be discussed. Although photosputtering/desorption appears to dominate, all of these processes must operate at some level. It is therefore useful to briefly review the distinct energy distributions that each produces. *Photodesorption* produces a Maxwell-Boltzmann distribution with a characteristic temperature of 1000–2000 K. *Solar wind (i.e., ion) sputtering* produces a Sigmund-Thompson direct sputtering flux is characterized by a temperature distribution peak in the range of $2\text{–}6\times10^3$ K for sodium, and $4\text{–}12\times10^3$ K for potassium. *Meteoroid vaporization* typically produces a thermalized vapor with initial characteristic temperatures of $3\text{–}5\times10^3$K. *Thermal desorption*, which produces ballistic trajectories, is characterized by a daytime Maxwell-Boltzmann distribution with T$\approx$400 K, and T$\approx$80 K at night.

Only those atoms liberated in a thermal process will remain bound to the Moon in substantial numbers. Atoms liberated nonthermally are energetic enough to directly escape the lunar gravity field. Let us consider the energetic, nonthermal population first.

Once liberated, energetic Na and K neutrals are subject to two primary forces: gravity and radiation pressure. The gravitational force is dominated by the Moon's field, but is significantly influenced (particularly at high altitudes) by solar and terrestrial perturbation terms. Radiation pressure, which is effective only for atoms in sunlight, is of course dominated by the solar term, but a term due to lunar albedo pressure also plays a small role.

The radiation pressure acceleration a given atom feels depends on its resonance scattering cross section (i.e., the details of its quantum mechanical interaction with the ambient ra-

diation field). Importantly, the resonance scattering cross section depends on the atom's heliocentric radial velocity; this is because an atom traveling at a speed significantly different from rest will see the solar spectrum appropriately redshifted or blueshifted and will therefore experience flux at its photon resonant (i.e., Fraunhofer) frequencies that is increased over what it would see at rest, where the flux is limited to the level at the core of the solar Fraunhofer lines.

At zero velocity relative to the solar frame, sodium and potassium atoms feel accelerations of 2.7 cm s^{-2} and 3.1 cm s^{-2}, respectively. Variability up to ~50% over the course of a year around these nominal values is caused by (i) seasonal effects due to the Earth's motion about the Sun [18], (ii) orbital effects due to the Moon's motion around the Earth (1 km s^{-1} amplitude, period 29.5 days), (iii) source velocity effects (e.g., ion and photon sputtering produce a source peaked in the solar direction), and (iv) lunar rotation (4 m s^{-1} amplitude, 29.5-day period) effects; see Figure 2.2.

Now consider the cooler, thermal population. We begin with a heuristic discussion, and then proceed onward to a discussion of published model results. Owing to the much shorter flight times of the cooler, barometric component of the lunar Na and K atmospheres, these populations are subject to both smaller radiation force effects on their trajectories, and weaker solar/terrestrial gravitational perturbations. In effect, the barometric Na and K populations simply "hop" around the lunar dayside surface until they are either lost to ionization or find a temporary nightside refuge (i.e., until the Sun once again rises). As described by Hunten et al. (1988), at 400 K on the lunar dayside, the characteristic residence time for an adsorbed Na or K atom is <1 μs; near the terminator or in a shadow, a 100 K surface will produce a characteristic residence time on the surface of order 1 second; on the lunar nightside, temperatures below ~60 K will produce residence times in excess of 10^6 seconds, the timescale of a lunar night. During each residence on the surface, Na and K atoms can interact with the surface chemically and thermally, with the efficiency of these processes controlled by the local surface temperature, composition, and to a lesser extent, the physical microstructure of the residence site.

At T=400 K, a typical hop for Na and K atoms reaches an altitude near 130 km and 75 km, respectively, and displays a typical lateral range near 90 km for Na and 55 km for K. Taking a diffusion (i.e., random walk) approach, one easily finds that the characteristic transport time (R_M/v_{therm}) for an atom ballistically hopping over the lunar surface at T=400 K is ≈90 hours for Na and ≈200 hours for K. These values can be compared to their photoionization loss timescales of 15 and 10 hours, respectively. Such considerations

[18] This is an ≈2% effect due to radiation field dilution as the Earth moves between its perihelion and aphelion, and an even more important velocity-dependent effect of 0.5 km s^{-1} amplitude, with a positive extremum in the spring and a negative extremum in the fall.

imply that ballistically hopping Na and K atoms in the barometric population rarely transport over length scales comparable to the lunar radius. As a result, one expects that the barometric Na and K populations, which are derived from the surface (cf., §3), should show mare/highland compositional gradients reflecting the Na/Na and K/K abundance ratios between the mare and highland surface units. Owing to smoothing effects, this should be most evident in comparing lunar frontside and backside Na/K ratios, when that becomes possible.

Ip (1991) was the first to model the dynamics of the neutral Na and K exospheres in some detail, and predicted a comet-like structure with gross symmetry about the instantaneous lunar-solar line. Such a structure, Ip found, should be characterized by an atmospheric pause toward the Sun caused by radiation pressure reversal of trajectories, and a long, flowing atmospheric tail extending down-Sun behind the Moon. Based on the radiation pressure arguments outlined above, one expects the extent of the lunar Na and K envelopes to "breathe" with both lunar phase and season (the latter due to the Earth's motion around the Sun). The most extended lunar Na/K atmosphere is therefore predicted for the first, first quarter Moon of the spring; similarly, the most compact lunar Na/K atmosphere is predicted for the first, last quarter Moon of the fall. Observations by Mendillo et al. (1991) and Flynn & Mendillo (1993) have borne out these expectations.

A more recent and more complete model of lunar Na and K dynamics has been constructed and exploited by Smyth & Marconi (1995a); some resulting Na and K distributions are shown in Figure 2.3. Following Ip (1991), these workers produced a Monte Carlo-based source distribution; the model calculates the number density, column density, and brightness profiles of Na and K, once an atom is released from the surface, taking into account a full integration of the gravity and radiation pressure terms in the equation of motion; the lunar heliocentric velocity is accurately computed based upon Brown's theory. All Na and K sources were assumed on the surface (i.e., satellite orbits were not included). Gas-gas collisions were ignored, but gas-surface collisions were included, with free parameters used to explore the effects of varying the surface thermal accommodation and gas-surface sticking coefficients. During trajectory integration the model tracked the atom's position and turned off radiation pressure terms when the atom is in the Moon's shadow.

Many useful findings resulted from the exploitation of this model, including certain constraints on source processes which were described in §3 below. Smyth and Marconi's model found it necessary to have a "mildly" nonthermal (i.e., 1000 K source) in order to adequately fit observed Na altitude profiles. Additionally, in order to fit the tailward brightness lobe observed by Mendillo et al.'s wide-field Na imaging project, Smyth & Marconi (1995a) found it necessary to have a Na source flux that is rather sharply peaked around the subsolar point, with a subsidiary maximum over the morning terminator. The application of this model to noble gas dynamics in the lunar atmosphere would be worthwhile.

3.0 SOURCES, SINKS, AND RECYCLING OF NEUTRAL SPECIES

In this section we synthesize observations and theory in an attempt to describe what is known about the lunar atmosphere's sinks, sources, and recycling mechanisms.

3.1 Loss Mechanisms

We begin with loss mechanisms (also called sinks) in part because they are simpler and better understood than the lunar atmosphere's source mechanisms. Additionally, by discussing sinks first, we provide some important background for the discussion on sources later, in §3.2.

The loss rates in the lunar atmosphere are astonishingly high: A combination of SIDE measurements (Vondrak et al. 1974) and He gravitational escape rate estimates gives a total loss rate near $\sim$10 g s^{-1}. In effect, this high loss rate (compared to the $\sim 2\times10^7$ g total atmospheric mass) implies that losses in effect control the column density and equilibrium abundances of the tenuous lunar atmosphere.

No fewer than four loss mechanisms have been identified; we begin by briefly discussing the characteristics of each.

1. Gravitational Escape: Since the lunar atmosphere is an exosphere, in which the mean free path far exceeds the local scale height, atoms or molecules moving away from the Moon with radial velocities relative to the center of the Moon exceeding the lunar escape velocity, 2.38 km $sec^{-1}(R_M/R)^{1/2}$ (where R is altitude), are normally directly lost from the lunar atmosphere.[19] Exceptions to this occur if during "escape" either radiation pressure retards the velocity below the local escape speed, or the atom or molecule is ionized and driven back to the Moon. Neither of these exceptions is particularly important in the lunar case, and each serves only to perturb the escape flux slightly from its nominal value. Whether an atom or molecule achieves v_{esc} depends primarily on its initial speed when it is released from the its source, whether that is at the surface or in the atmosphere (e.g., due to photodissociation). As such, the time dependence of the gravitational escape mechanism directly depends on the number-weighted time dependence of the source mechanisms. Additionally, radiation pressure provides some acceleration to atmospheric species moving anti-sunward down the lunar exospheric tail, enhancing escape rates in this direction.

2. Ionization Loss: Atoms and molecules in the lunar atmosphere that become ionized

[19] The escape energies of H, He, Na, and K are 0.03 eV, 0.12 eV, 0.69 eV, and 1.2 eV, respectively.

are generally lost from the system.[20] This is because ionized constituents are accelerated beyond escape speed as they travel on the local solar wind electric field. Re-impact and implantation occurs for approximately half of the ions created at low altitudes (i.e., where the solid angle of the Moon fills half the sky), but becomes progressively less important with altitude as the solid angle of the "lunar obstacle" decreases. It is important to note, however, that this factor of 1/2 is a time average; at any given time and place the electric field is directed either toward or away from the surface and therefore channels all newly created ions there.

The only sources of ionization that are important in the lunar atmosphere are photoionization by solar UV, charge exchange, and solar wind impact ionization; the relative effectivity of each will be discussed below. All vary in concert with the 11-year solar cycle, and to a lesser degree with the 28-day solar rotation. Solar wind-driven charge exchange and electron impact additionally show a significant degree of short-term fluctuation, and are also (unlike photoionization) essentially curtailed during the $\approx$15% of each lunar orbit when the Moon is within the Earth's magnetotail. However, for the species and circumstances of interest to us, photoionization is always the dominant (i.e., fastest) ionization process.

3. Chemical Loss: Two types of chemical loss occur in the lunar atmosphere. The most important of these results from collision with the surface, which in some cases can result in chemical reactions leading to bonding to the surface before the atom is ballistically ejected again. Although this is probably not important for any of the five known lunar atmospheric species, it is believed to be an important mechanism for proton, H, He, and possibly oxygen loss from solar wind impingement on the Moon. Less important still is loss to chemical reactions occurring for gas-gas collisions. As discussed in §3, although the lunar atmosphere is an exosphere, few percent of the atoms resident there do suffer collisions with another atom before being lost to other processes. However,the cross sections for reactions to occur for many lunar species binary collisions (e.g., Ar-X, He-X, Na-Na, Na-K, K-K) are quite low, reducing the (already low) effectiveness of this process to act as a loss.[21] There is no important known time variability to chemical losses in the lunar atmosphere.

4. Condensation Loss: An important, if usually temporary, loss mechanism from the lunar atmosphere is loss to condensation. This occurs primarily on the lunar nightside, when species impacting after ballistic hops originating on the nightside become adsorbed in a shallow potential well, and as a result experience lattice residence times comparable to or in excess of the 14-day lunar night. The condensable lunar atmosphere species include Ar, Na, and K, as well as the (still undiscovered but no doubt present) H_2O from the meteoritic

[20] Molecules, if they present in the lunar atmosphere, would also be subject to loss by photon- or electron-impact disassociation.

[21] Of course, it is possible that highly reactive species could be found among the missing constituents of the lunar atmosphere.

complex. In most cases, species "lost" to condensation are regained after sunrise. and condensation loss should be considered a temporary sink, rather than a permanent one. However, if a condensable finds its way to a permanently shadowed polar cold trap (e.g., Arnold 1979; Morgan & Shemansky 1991), then it may succeed in being permanently lost.[22] Condensation loss probabilities are not significantly time variable.

Table 3.1 compares the key gravitational and ionization escape timescales for the known lunar atmospheric species, and water vapor. With the exception of He and T=1000 K ("hot") water[23], photoionization is always the dominant (i.e., fastest) loss process. Furthermore, all of the loss timescales are short, i.e., hours to weeks, showing definitively that all of the species in the lunar atmosphere are continuously being replenished.

Having said that loss timescales are short, however, it is important to recall the results obtained by observers (e.g., Sprague et al. 1992, Mendillo et al. 1993) that show the vertical distribution of Na and K in the lunar atmosphere is steeper than the R^{-2} distribution characteristic of a freely escaping atmosphere. While this is not true for He and Rn, it is probably true for Ar and H_2O, and implies that Na, K, Ar, and H_2O (if it exists) are largely bound. Furthermore, for all species except He, the ballistic hop time (minutes to hours, depending on the gas temperature) is short compared to the escape time, indicating that many hops occur before loss. This in turn implies that Na, K, Ar, and other heavies like H_2O that may exist, are "recycled" through the surface many times prior to loss; during this process they can experience thermal accommodation and/or re-emission by any of a number of nonthermal source processes, which we now describe.

3.2 Source Mechanisms

We now turn to a discussion of the sources which feed the lunar atmosphere. The seven sources proposed to date fall into four main categories: (1) thermal, (2) sputtering, and (3) meteoritic, and (4) interior release. Although new species, including H_2O (Thomas 1974), can be produced by chemical reactions with species adsorbed on the surface or in the crystal lattices, their ultimate release to the atmosphere must occur through some energetic process, such as thermal desorption, sputtering (including chemical sputtering), or meteoritic impact. Therefore, while the production of such species may be important in some instances, we do not discuss chemical production as a separate source process for the lunar atmosphere.

Concerning the atmospheric sources themselves, two facts are clear: Different kinds of source mechanisms are important for different species, and in general no single source

[22] The exception being if meteoritic impact or Lyman α driven photon sputtering off the interplanetary H results in subsequent release.

[23] And, we note, H and H_2 if they are exist there.

mechanism supplies any given species. Before critically discussing the importance of various sources for each species, we first describe the seven sources, organizing them into the five categories enumerated immediately above.

1. Thermal Sources: This mechanism, which is sometimes also called *thermal desorption*, involves sublimation from adsorption wells on grains at the very surface or within the upper regolith (to the depth that is in thermal contact with the diurnal cycle). It obviously follows a 29.5-day diurnal cycle, but has little or no time dependence, save the ≈4% peak-to-trough solar insolation variation as the Earth moves from its January perihelion to its July aphelion. Spatially, this source is concentrated on the dayside, and follows the form $S_{th}=C_x/t_{th}$, where C_x is the concentration of species x on the surface (number per unit area) and $t_{th}= 10^{-13}\exp(D/kT)$ seconds is the thermal desorption time; here D is a surface and species-dependent activation energy usually associated with a well depth (cf., Hunten et al. 1988) and kT has its standard meaning. Of course, T varies with solar zenith angle, and therefore with local time of day and latitude. In general, the combination of the exponential nature of t_{th} and the finite reservoir of gas adsorbed or condensed onto the surface implies that this source is primarily concentrated along the morning terminator, with substantially less strength across the dayside, and essentially no strength at night (except for noncondensables like H, He, H_2, O_2, and Ne). Local effects due to varying surface albedo, emissivity, conductivity, and terrain slope will occur. Further, the exponential dependence of this source makes it far stronger in equatorial latitudes than near the poles. This source produces an ensemble distribution set by the weighted average of thermal Maxwellians across the surface. Since the surface temperature maximum on the Moon is 400 K, this source will produce bound, ballistic atoms (or molecules) which (except for H, He, and H_2) have scale heights of tens of kilometers or less.

2. Sputtering Sources: Sputtering can be defined as the ejection of a species from a lattice site in the upper few monolayers of a surface owing to the injection of a discrete impulse of energy. Sputtering processes on the Moon have been a subject of interest since returned Apollo samples showed unusual compositions in the rims of grains and glasses (Kerridge & Kaplan 1978). The solar wind is known both to sputter material from the regolith and to implant material in and around the regolith (Hodges & Hoffman 1975). Effective yields obtained from the analysis of lunar samples indicates sputtering erosion of ~0.1–0.2 Å yr^{-1}, or ~10–100 g s^{-1} for the whole Moon. With regard to the lunar atmosphere, several types of sputtering have been discussed in the literature; these include: *photon sputtering* (also called photon-stimulated desorption), *charged particle sputtering* (e.g., due to incident, energetic e^-s, p^+s, or α particles), and *chemical sputtering.*[24]

Photon sputtering (McGrath et al. 1986; Morgan & Shemansky 1991) falls off with the

[24] Cosmic ray sputtering is not important, because the energy deposition occurs at depth, thereby preventing liberated species from escaping to the atmosphere.

cosine of the solar zenith angle, thereby creating a source which is essentially diurnal in character and concentrated at subsolar latitudes (which of course are seasonally dependent).[25] Laboratory studies of photon desorption (e.g., Townsend 1983; Wiens et al. 1993; cf.. also the review volume by Johnson 1990) demonstrate the Maxwellian nature of its source distribution, with characteristic temperature of ≈800–2000 K. This produces a velocity distribution that is intermediate between the thermal source and charged particle sputtering, and which can be moderately coronal, particularly for light species.

Charged particle sputtering (e.g., McGrath et al. 1986; Johnson & Lanzerotti 1986; Johnson & Baragiola 1991) also falls off with the cosine of the solar zenith angle, thereby also creating a source which is diurnal in character and concentrated at subsolar latitudes; local effects due to surface temperature and slope perturb this source distribution. Importantly, the solar wind charged particles that normally dominate the incident flux driving this source cannot reach the Moon during the few days each month when the Moon is within the Earth's magnetotail; the only available sources of charged particles during that time are electrons and ions trapped in the terrestrial magnetosphere. Charged particle sputtering produces a Sigmund-Thompson velocity distribution with characteristic speeds of 1–3 km s^{-1}; such velocities are sufficient to populate both high-altitude coronal trajectories and (for v>2.38 km s^{-1}) hyperbolic, direct escape orbits.

Chemical sputtering (cf., Roth 1983 for background on this process, or Potter 1995 for a short overview) results when a chemical reaction on the very lunar surface (e.g., due to incident solar wind H) has sufficient excess energy to desorb (as opposed to lattice eject) an atom or molecular fragment onto a ballistic trajectory; this process appears to offer particularly high yields for sputtered volatiles, and an at least partially accommodated thermal velocity distribution. Because exothermic reactions are required, it would not apply to noble gases. Chemical sputtering is much more temperature dependent than either photon or charged particle sputtering, because there is no photoelectric effect minimum energy to overcome; instead, there is a simple exp(D/kT) type activation barrier. Chemical sputter yields for relevant surface materials appear to peak in the 500–1000 K temperature range, which argues against it dominating the coronal Na or K yields on the Moon (but not for Mercury; Potter 1995). However, recent work on the variation of Na abundance with solar zenith angle (Potter & Morgan 1997a) provides some intriguing evidence that chemical sputtering may play a significant role with regard to lunar Na production; this is discussed at the end of this section.

---

[25] An important exception to this is that Lyman-α photons resonantly scattered of H in the interplanetary medium can and will induce sputtering of species with work functions below 10 eV at night and in the lunar polar regions. *Very* near the poles, and in permanently shadowed regions, Ly-α sputtering can dominate direct solar sputtering for some species (cf., Morgan & Shemansky 1991).

All types of sputtering on real (as opposed to simple, laboratory situation) surfaces are complex, and little quantifiable information has been developed on yield effects like surface roughness (which lowers sputter yields on real surfaces by factors of a few as sputter products encounter other grains while they attempt their exit to space), grain chemical heterogeneity, sputter site micro-slope, grain exposure dosage, and surface temperature; these circumstances prevent the easy quantification of sputter yields across the real Moon in space and time.

3. Meteoritic Sources: Meteorite impacts onto the lunar surface at velocities above a few km s^{-1} (the average lunar meteorite impacts at v≈15 km s^{-1}) produce both a cloud of impact-generated vapor and a source of hot or even molten surface material that will subsequently outgas until it cools. In both cases, the yields of various species depend on the energetics of the collision, the composition of the target site and the impactor, and (to a lesser degree) on the surface temperature, rock/soil ratio, and compaction state. Discussion of the meteoritic source of the lunar atmosphere can be found in papers including Morgan et al. (1989), Morgan & Shemansky (1991), Hunten et al. (1991), Sprague et al. (1992), Smyth & Marconi (1995a), and Cremonese & Verani 1997). We particularly wish to highlight the observations of Cremonese & Verani (1997), who reported a significant brightness enhancement (to 3.4–5 kR between 100 and 500 km altitude in D2 emission alone) during the Leonid meteor shower of 1997. Their observed brightness enhancement translates into unprecedented abundance and scale height increases of the lunar atmosphere.

The meteoritic source is the average over all impacts, which each produce a localized source for each species x of the form $S_{met}(x)=C_x V_x \eta$ where C_x is the weighted average concentration of x in the heated target and impactor material, V_x is the vapor production rate of species x in the heated material, and η is the fraction of vapor that escapes to the atmosphere. The temporal variation in this source (above the essentially constant background rate) is set by the crossing of the Earth and Moon through debris fields left in orbit by comets (so-called comet trails) and Earth-crossing asteroid collisions, with various well-known examples such as the Perseids occurring at predictable times each year. The strength of each "shower" depends on several factors, including where the Earth's orbit intersects the debris trail orbit, and can vary from year to year (the interested reader is directed to the relevant papers in the review volume by Rettig & Hahn 1996).

Because the debris trails have space cross sections that are orders of magnitude larger than the Moon, the resulting lunar source is spatially uniform on the velocity-forward hemisphere encountering the shower, and sharply curtailed on the shadowed hemisphere. The yield of vapor directly produced by meteoritic impact is somewhat uncertain, and will be ameliorated by local macroscopic and even microscopic roughness effects as species exit the impact site. Vapor escaping the impact site will display a thermal Maxwellian with characteristic temperatures of 2000–5000 K (e.g., Ahrens & O'Keefe 1971; Eichorn 1978).

Vapor produced subsequently by the outgassing of solid and melt material at the impact site will produce a weighted-average Maxwellian with temperatures ranging up to perhaps 3000 K. The meteoritic source will therefore produce both bound and directly escaping species. Vapor produced by the impact of secondaries (i.e., at velocities <2.4 km s^{-1}) will be colder than the vapor produced at the primary impact site. In general, atomic neutrals from the meteoritic impact source are expected to be dominated by volatile species such as alkalies, and sulfur, with molecular fragments due to metal oxides, H_2O (particularly for an icy impactor or an impact site in a polar cold trap), and other species appearing primarily as molecular fragments. As noted by Morgan & Killen (1996), the presence of refractory-rich grain coatings containing Al, Si, and Ca in lunar samples provides evidence that the most volatile components of the meteoritic vapor are preferentially lost to the atmosphere.

4. Internal Release Sources: Gas can be released from the lunar interior[26] by *vulcanism* (e.g., Taylor 1982), *seismically induced seepage* (Hodges et al. 1973), or *crustal diffusion* (e.g., Killen 1989). Of these, vulcanism is not important today, but may have been most important in the distant past (cf., §5.2). Further, Apollo seismic stations that reported data for over six years established that the Moon is essentially inactive, at least on those timescales, with only very minor (10^{7-9} erg), tidal stress-driven events having been observed from the interior (cf., Taylor 1982; Kaula et al. 1986). Further still, Killen's work has shown that crustal diffusion is not important on the Moon for Na and K, and our own thinking finds no reason it should be for any non-radiogenically produced species. As such, it appears that interior gas release is probably not very important today, and even then only for the observed atmospheric constituents with regard to radiogenic species. As to spatial concentrations, there are no definitive observations of sites of internal gas release (cf., §1.2 on LTPs) except in that Rn production was found to be correlated with the mare/highland boundaries (Gorenstein et al. 1974).

We now move from a discussion of the general attributes of each source, to a species-by-species discussion of which sources dominate. To do this, it is useful to make the now well-established distinction between *primary source* atoms and *recycling source* atoms, where the primary source(s) is/are responsible for initially liberating the constituent from the surface to the atmosphere, and the recycling source(s) is/are responsible for subsequent releases after each ballistic recontact with the surface.

The most relevant information concerning source mechanisms for each species has to do with the energetics of each species, which is determined (where possible) through measurements of the vertical distribution. This kind of information, however, is highly limited and only sparsely sampled in space and/or time for all known species, and is, in the case of

[26] Which we define for our purposes to be the region below the depth of penetration of the diurnal thermal wave.

Na and K, derived only through brightnesses of a 3-D structure seen projected on the sky. Additional information on sources comes from temporal and spatial variations of surface or near-surface abundances, and from the physical insights gained from our knowledge of the Moon and laboratory studies of the various source processes. These limitations in mind, we now briefly discuss the lunar atmospheric species, in order of their discovery:

Radon and Polonium: As summarized in §1.4, alpha particles resulting from the radioactive decay of ^{222}Rn and ^{210}Po were discovered and monitored by orbiting alpha particle spectrometers aboard the Apollo 15 and 16 Command Service Modules. Such species are indicative of seismic or volcanic outgassing, and it is therefore clear that the primary source of these species is internal release. Owing to the short half-lives, 3.8 and 138 days, respectively, as well as the 21-year half-life of the ^{210}Pb, the parent of ^{210}Po, it is also clear that this outgassing must have both been active during the Apollo missions, and have been ongoing for some time— presumably, it is quasi-continuous.[27]

An important characteristic of the Apollo observations was the spatial association of Rn and Po with specific (though differing surface) sites, such as the craters Aristarchus and Grimaldi (for Rn) and over mare/highland unit boundaries (for Po), that was reported (Bjorkholm et al. 1973; Gorenstein et al. 1973, 1974). Once released from the Moon as a gas, both Rn and Po will diffusively transport across the surface[28] until they are ultimately lost to either photoionization or radioactive decay; typical T=400 daytime ballistic hop lengths and altitudes will be of order 10 km and 3 minutes. Each species was detected in highl localized, ~150 km-wide bins which are small relative to its expected (many hundreds to >1000 km) transport length prior to alpha decay. In the case of the Rn, this was probably due to the fact that the localized sites of emission detected by Apollos 15 and 16 were in darkness, and therefore cold, at the time observed; Heymann & Yaniv (1971 give a prediction to this effect prior to the Apollo 15 Alpha Particle Spectrometer flight.[29]) Thus, the Rn, which is condensable on the cold nighttime surface, was almost certainly released since nightfall and would diffuse away later, after the Sun rose. As a result, one predicts that a thermally driven Rn recycling source is also important on the dayside, but this has not been observed.[30] It is puzzling why the Po, with its 138-day half-life, was found in localized concentrations near the edges of mare, unless actual primary emission

[27] However, it is puzzling that no coincident sources of seismic signals or ALSEP surface atmospheric signals were ever reported.

[28] Rn is a noble gas and therefore quite volatile; Po's volatility is of the same order as Na.

[29] These workers also predicted the possibility of a sunrise terminator peak, but this may have been too weak for the Apollo orbital instrumentation to detect.

[30] A sputter recycling mechanism can also be envisioned, but owing to the order of magnitude higher mass of Rn and Po, compared to Na and K, an equivalently energetic process would produce an ~10 times more compact corona, extending out only to ~1R_M.

fans were detected.

Helium: As described in §1.4, neutral ^{4}He was detected and monitored by the Apollo 17 LACE mass spectrometer during its 9 month (10 lunation) operational life. Potential primary sources include (i) outgassing of alphas from the radiogenic decay of ^{238}U and ^{232}Th in the lunar interior, and (ii) solar wind alpha particles, which impact the Moon at typical rates of $\sim 1\text{–}3 \times 10^{24}$ s^{-1}. Concerning the relative strengths of these sources, Hodges (1975) reported that the fraction of escaping radiogenic He is thought to be the same as that for ^{40}Ar, i.e., $\approx$10%. This leads to a radiogenic He loss rate of about 10^{23} atoms s^{-1}, which is about 10% of the solar wind alpha particle flux.

The good agreement between LACE measurements, and exospheric transport models fed by known He source rates from the solar wind, led Hodges & Hoffman (1974) to conclude that the primary source of the ^{4}He is solar wind alpha particles, which either are neutralized on impact (at typical energies of 4 KeV), or which release neutralized ^{4}He from the solar wind that was earlier-implanted and subsequently neutralized in grains. The case for a solar wind primary source is also supported by significant correlations of He abundance with solar wind flux and velocity (Hodges & Hoffman 1974, 1976).[31]

It is important to note, however, that because LACE could only obtain measurements at night, when the instrument and the site around it were in fact shielded from direct solar wind, typical He atoms detected by LACE must have been transported to the nightside and suffered recycling after of order 10 re-collisions with the lunar surface (recall, He is noncondensable). The probability of ionization loss after 10 ballistic hops (0.2 days) is negligible, but at 400 K, He Jeans escape losses are non-negligible (the escape time is comparable; see Table 3.1).[32] Although our scaling calculations here are crude, Hodges & Hoffman (1974) and then Hodges (1975) reported that their He abundance measurements with LACE were about 60% of the values their model predicted should be found. This led them to conclude that ~40% of the solar wind He impacting the Moon escapes at high velocity, either through spectral reflection of incident alpha particles off the surface, or through suprathermal release of He trapped within (at 4 KeV incident energies) soil grains (e.g., meteoritic, sputtering, etc).

To summarize, it seems clear that the primary source of lunar atmospheric He is the solar

[31] The transport time for He over a characteristic distance of R_M is of order 0.2 days. It is unfortunate that the K_p records available to LACE investigators were only daily averages. The correlation with the solar wind source through K_p would be better proven if a change in He abundance was seen after a delay by a characteristic transport timescale following a change in K_p.

[32] Escaping He atoms are primarily (>90%) lost to orbit around the Earth, where they typically survive for 6 months before being ionized (Hodges 1978).

wind, but perhaps 10% is due to interior outgassing (Hodges 1975). The ~40% He loss noted by Hodges & Hoffman during nightside measurements indicates some recycling loss, which is probably due to a combination of the initial reflection of neutralized ^{4}He off the surface, and later nonthermal emission from grains, and Jeans losses. It is unfortunate that the LACE instrument was not equipped to measure the energetics of the neutral species it detected.

Argon: As described in §1.4, argon was detected by the same Apollo 17 LACE instrument that detected lunar helium. About 90% of the argon detected was ^{40}Ar, which results from the decay of ^{40}K and therefore must ultimately be derived from the lunar interior, its primary source. (In contrast, the ^{4}He LACE detected is primarily derived from solar wind, as we described above.) The remaining ~10% of the LACE argon signal was ^{36}Ar, for which the parent source is the solar wind. LACE data indicate that the ^{40}Ar source rate is variable, suggesting that the release rate of Ar from the lunar interior is not steady. The average loss rate of Ar from the lunar atmosphere is near $1.5\text{–}2\times10^{21}$ s^{-1} (Hodges 1975, 1980).

The fact that LACE did detect an Ar wind blowing across the terminator (when LACE was still in darkness and its local surface site was still cold) provides direct evidence to support one's expectation that thermally desorbed Ar that is condensed on the nightside (where the probability of adsporption is ~30% and the mean thermal desorption time is ~1 day; Hodges 1975) is released and recycled onto the dayside through ballistic transport and thermal reaccommodation, prior to its ultimate loss by photoionization (after a characteristic exposure time of 25 days; cf., Table 3.1).[33] Hodges (1975) reports that the average Ar lifetime on the Moon is near 100 days, of which 80% is spent adsorbed on the lunar surface. As to nonthermal recycling sources, there is no clear indication of whether any nonthermal, coronal distribution of Ar exists (as we described in §2.2) because LACE was not capable of measuring the energetics of the argon atoms it detected.

Sodium and Potassium: The observations of Na and K were reviewed together in §1.6. Owing to fact that these species are both alkalies, and to the relative paucity of K data sets compared to Na data sets, we will restrict our discussion here to Na, but make the assumption that the same conclusions apply to K.

As we will describe, much controversy exists in the literature as to the relative importance of various source mechanisms for Na, and we will devote more space to Na sources than to any other lunar atmosphere species. This is of course ironic, since the Na and K are only trace species compared to the other known atmospheric constituents, and have far fewer geophysical implications than do lunar atmospheric He, Ar, and Rn. Still, the great mass

[33] The fact that this exposure time is so short provides convincing evidence that ^{40}Ar is being released from the Moon continuously or quasi-continuously.

of diverse data sets collected on Na (and K) since 1986 provide more grist for discussion than is possible for other atmospheric constituents, and we shall discuss these issues at great length now, relative to the mass fraction of the lunar atmosphere in alkali species.[34]

We begin by assessing the native reservoir of the Na observed in the lunar atmosphere. From the total mass of Na in the lunar atmosphere ($\approx 10^3$ g), a 50% day/night diurnal cycle, and sodium's lifetime in sunlight ($\approx$14 hours), one can compute that the present lunar atmosphere must be supplied with Na at the rate of $1 \sim 10^{-2}$ g s^{-1} (and roughly an order of magnitude smaller amount of K) from some quasi-steady long-term equilibrium; taking into account the time average 50% return of ionization losses to the surface (Manka & Michel 1971), this implies that over the age of the solar system $\approx 1 \times 10^{15}$ g of Na has been lost from the Moon, and therefore has been supplied from native reservoirs. The estimated uncertainties in this estimate are of order factors of two. Taking the average Na abundance in lunar soils (0.33% in highlands crust, 0.06% in the bulk Moon; Taylor 1982), this corresponds to the depletion of a regolith layer no more than 0.5 cm to a few cm deep, which is less than or comparable to a sputter-erosion depth of the lunar surface over the past 4 Gyr. Sputter erosion over 4 Gyr, equivalent to of a few centimeters of soil, should release $\sim 10^{15}$ g of Na.

Where could the Na have originated? In 4 Gyr, some $\approx 3 \times 10^{18}$ g of solar wind have impacted the Moon, of which at cosmogonic abundance (Allen 1973) $\approx 10^{14}$ g were in Na. Clearly, this source is insufficient. Morgan & Shemansky (1991) quote meteoritic plus comet impact source rates (we ignore hypothesized Frank/Swigarth small comets) of Na that are about 120 times higher than the solar wind source, i.e., $\approx 1.2 \times 10^{16}$ g over time; even if we ignore rare comet impacts, $\approx 8 \times 10^{15}$ g of meteoritic Na must have been deposited over time. Impacts also generate Na by vaporizing regolith. Vaporization yields are of order 2 to 5 times the impact mass at velocities characteristic of lunar impacts (cf., Haff et al. 1983), so if Na is released in atomic form (a reasonable assumption given its volatility), vaporization release of Na must dominate direct meteoritic import. Still more regolith Na will be released indirectly by impacts excavating and exposing fresh Na from depth, but how much is left exposed on the surface (or near, e.g., within reach of longer-term sputtering) is difficult to quantify.

Despite the extant uncertainties in Na supply estimates, it is clear that (1) solar wind Na is not sufficient to supply the lunar atmosphere, but it may be able to erode away enough surface to supply the requisite Na; (2) meteoritic Na is sufficient (by factors of several to ten) to supply the needed Na to support the lunar atmosphere for 4 Gyr; and (3) meteoritically generated regolith Na may provide up to several times more Na still. Clearly, the main source of the lunar atmospheric Na must be lunar Na from the regolith,

[34] Hunten has remarked several times that Bates himself made similar comments about Na in the Earth's upper atmosphere.

made available to the atmosphere via sputtering or impacts. A smaller but non-negligible source of Na must also be direct meteoritic/cometary Na imported in the impacts.

From the clear overabundance of Na supply rates compared to source requirements, one must conclude that either the present day Na loss rates are underestimated, or the source generation processes are inefficient, depleting only of order 3–10% of the Na supply made available over the past 4 Gyr. If the latter is true, then most of the Na generated over time must be sheltered from ionization loss either directly (i.e., by shadowing in the regolith) or by being bound to heartier molecular species, or both.

How is this Na initially injected into the atmosphere? Smyth & Marconi (1995a) have provided an excellent discussion demonstrating the wide range of rate uncertainties for the meteoritic, photon sputtering, and solar wind sputtering various source mechanisms. Their discussion demonstrates that even the average production rates for Na due to sources are too uncertain to allow us to distinguish between various candidate mechanisms on the basis of source rate considerations alone.

However, there are some key observational facts to aid us. One is that both thermally accommodated and suprathermal Na have been widely observed by spectroscopy and imaging experiments. Although various workers have shown that the Na brightness decreases steeply with angular distance from the subsolar point (i.e., in terms of solar zenith angle χ, like $\cos^2(\chi)$ (Mendillo & Baumgardner 1995; Flynn & Mendillo 1995; Potter & Morgan 1997a), Mendillo et al. (1997) caution that in certain geometric circumstances (e.g., quarter-Moon), this falloff in brightness and column density may simply reflect a geometric effect in the data, caused by a radiation pressure-driven lack of foreground and background Na along the observational line of sight.

A casual (or even dedicated!) reader of the literature will find many contradictory conclusions and even contradictory data sets concerning the primary (or direct) source of Na. This situation is clearly exacerbated by real time-variability effects in the solar wind, solar UV, and the meteoritic complex, as well as by relatively sparse sampling of a complex environment, and the maddening fact that both primary and recycling source Na is seen in every observation.[35] [36] What is clearly lacking is a long (e.g., several lunation) time base of densely sampled measurements at various latitudes.[37] Of course, even such a

[35] If only God would paint the atoms differently so we could tell who is on which team!

[36] Fore example, near the limb the airmass projection factor for Na, $\sqrt{2\ !pi\ R_M/H}$~6–15, implying that >80–90% of the Na atoms observed are actually foreground or background Na far removed from the surface.

[37] Additionally, it would be useful to obtain Na abundances over the lunar terminator, which would be useful for gauging how much condensed Na is thermally desorbed from the nightside surface on sunrise.

wonderful data set would have difficulties associated with the deconvolution of the Na line-of-sight observational path integral into a 3-D distribution. Truly the best experiment would involve a lunar orbiting spacecraft making Na and K measurements via both mass spectroscopy and spectroscopic tomography, all the while monitoring solar wind, solar UV, and meteoritic flux.

Since the prospect for either of the two data sets just described is not good on a timescale commensurate with the completion of this review, and may in fact be many years away, we will simply say what appears to be the case about the primary Na source mechanism(s). We order the points we make in descending order of our confidence in them:

- Several primary source mechanisms no doubt operate. These include meteoritic release, thermal desorption, and both photo- and charged-particle sputtering. The debate is about their relative importance in space and time.

- The relative importance of these sources is spatially dependent, following surface compositional trends, topographic factors (e.g., steep slopes), and latitude.

- The relative importance of the sources is temporally dependent, on both on lunar diurnal cycles and longer timescales.

- Some potential sources can be ruled out as being of widespread importance for Na production, these include internal outgassing/diffusion of Na from the regolith, and surface chemical reactions.

- Of the viable sources, only the meteoritic source likely operates to any significant degree on the lunar nightside or very close to the poles.

- The steep solar zenith angle dependence of the Na coronal-componet brightness indicates that, while meteoritic effects may be important for bringing Na to the very surface where it can be released, it cannot realistically be the dominate Na release mechanism on the dayside.

- The steep subsolar dependence of the Na thermal component brightness on subsolar latitude indicates that, of the viable sources that produce nonthermal production, neither meteoritic production nor simple thermal desorption is dominating the subsolar "Na fountain." This trend is, however, consistent with a chemical sputtering source, as demonstrated by the nice fit of $\ln(I_{Na}/\cos(\chi))$,[38] with T; the difficulty with this hypothesis is that Na chemical sputtering is thought to be efficient only at significantly

[38] Or equivalently, of $\ln(N_{Na}/\cos(\chi))$, the so-called "reduced column" (Potter & Morgan 1997a).

been detected around Ganymede, evidence for both an ionosphere (Gurnett et al. 1996) and auroral emissions (Hall et al. 1997) has been detected there. One fully expects to find SBEs around many planetary satellites and asteroids. Table 4.1 provides some useful comparisons between the known SBEs of the solar system.

As we have just noted, SBEs have been firmly detected around four solar system bodies to date.[42] Three of these SBEs, those surrounding Mercury, the Moon, and Io, can be grouped as "*refractory SBEs*" by virtue of the nature of the surfaces of these parent bodies; one expects that SBEs around asteroids would fall into this group as well. The SBE around Europa, however, is more properly classified as a "*volatile SBE*" by the nature of Europa's ice surface, and one expects that this class of SBE is common to the outer solar system. Beyond this simple classification, other subcategories also no doubt arise; e.g., whether the parent body has a significant dipole magnetic field (as Mercury, Io, and Europa do) or not (e.g., the Moon), whether or not the parent object is embedded in a planetary magnetosphere inducing significant charged particle bombardment onto the parent body's surface, or whether (as in the case of the four known SBEs) or not (e.g., in the case of weakly outgassing comets and small asteroids with R<10 km) gravity plays a significant role.

In the remainder of this section, we provide a brief review of the Europan SBE, and relatively detailed comparison of the lunar atmosphere to its closest analog among the discovered SBEs of the solar system: Mercury's.

4.1 Europa's SBE

The presence of a tenuous atmosphere surrounding Europa has been long suspected and discussed in the literature (cf., reviews in Burns 1986). However, indisputable evidence for this atmosphere was only obtained when Hall et al. (1995) and then Brown & Hill (1996) spectroscopically discovered gaseous O and Na, respectively.[43] Europa's atmospheric O is thought to be derived from sputtering of H_2O surface ice (cf., Johnson 1990); but a small fraction may also be derived from the photolysis of sublimated H_2O. The O neutrals detected by Hall et al. (1995) surrounding Europa is comparatively cold (T$\sim$200–1000 K) and at least partially gravitationally bound, as indicated by its moderate, $\sim$100 km scale height.

---

[42] The surface number densities at the base of Pluto's atmosphere and Triton's, roughly 10^{15} cm^{-3}, firmly establish their atmospheres as "conventional" collisional atmospheres, rather than SBEs.

[43] Similar searches for Na around Ganymede have yielded only upper limits (Brown 1997), indicating that Ganymede's Na column must be depleted by a factor of at least 13 relative to Europa.

In analogy to the lunar case, Europa's atmosphere contains distinct gas populations with different origins and energetics. The differences between Europa's O and Na SBEs can be briefly summarized as follows. In contrast to the O exosphere, Europa's Na exosphere is clearly a more energetic population, with emission having been detected as far as 25 R_{Europa} from the satellite. The total mass of O in Europa's atmosphere exceeds the Na mass by a ratio of 300:1. Furthermore, whereas Europa's O exosphere is thought to be derived from Europan H_2O ice, Europa's Na is suspected to be Ionian in origin, having been transported to Europa in Jupiter's magnetosphere, temporarily implanted in Europa's surface, and then re-released due to energetic particle sputtering.

4.2 Mercury's SBE and Its Relationship to the Moon

The closest available analog to the lunar atmosphere is the similarly tenuous surface boundary exosphere of Mercury. Here, we first briefly summarize the main attributes of Mercury's SBE. We then compare these attributes, as well as the circumstances affecting Mercury's SBE, and the physical processes at work there, to the lunar case. Unfortunately, space limitations prevent us from undertaking more than a cursory discussion; readers interested in a wonderful discussion of Mercury's atmosphere are referred to the long review by Hunten et al. (1988), and to the subsequent research papers cited in the final paragraph of this subsection.

Compositional Overview: After many unsuccessful attempts to detect an atmosphere surrounding Mercury by groundbased methods, ultraviolet instruments aboard the Mariner 10 Mercury multiple-flyby mission succeeded in discovering Mercury's atmosphere. As described by Broadfoot et al. (1974) and Broadfoot (1976), Mariner 10 detected neutral atomic H, He, and O. Of the three species detected by Mariner 10, oxygen is the most abundant, with $n \approx 4 \times 10^4$ cm^{-3} near the surface (cf., Table 4.2). UV occultation measurements by Mariner 10 set a strict upper limit of 10^{-12} bar on the total atmospheric surface pressure near the terminator. Other UV measurements set upper limits on CO, H_2, H_2O, Ne, Ar, Xe, and C abundances in the daytime atmosphere (cf., Broadfoot et al. 1976).

Later, in the mid-1980s, both Na and K neutrals were discovered (Potter & Morgan 1985).[44] One should note the far higher abundance of Na and K in Mercury's atmosphere than the Moon's. Sprague et al. (1993) and Sprague et al. (1996) have reported searches for both Ca and Li, but obtained only upper limits. Table 4.2 summarizes the species detections in Mercury's atmosphere, and compares these to lunar abundances. Although the strong case for "missing mass" and therefore undiscovered species that exists in the lunar atmosphere (cf., §1) does not exist at Mercury (because there is no total surface pressure measurement, only an upper limit), the Mariner 10 surface pressure upper limit

[44] It was this discovery of Na and K at Mercury that motivated searches for and the discovery of the same species at the Moon two years later.

does allow for about 100 times the total number density that is present in the combined inventory of species detected to date. Given this, and the relatively incomplete state of sensitive searches for other species, we would find it surprising if other neutral species were not present in the Mercurian SBE, particularly molecular ones.

Vertical and Lateral Distributions: We now turn to other aspects of Mercury's atmosphere. We begin with thermal distributions. Mariner 10 established that the vertical distribution of daytime He above the subsolar region appears to be nicely fit by a monothermal distribution with T=575 K, the vertical distribution of H apparently requires both hot (T$\approx$ 420 K) and (T$\approx$110 K) cold components. Puzzlingly, the cold component is colder than predicted for the surface under the measurement, and suggests a nightside-like thermal source. Groundbased studies reveal that the daytime Na and K atmospheres exhibit T$\approx$500 K, but extended, nonthermal components may also exist (Hunten 1992). In this regard, one might ask whether Mercury has a large, faint extended Na coma like that of the Moon. The answer appears to be yes. Monte Carlo codes developed and explored by Ip (1993) and Smyth & Marconi (1995b) indicated several years ago that it is possible to generate such an extended coma with source rates consistent with what is required to maintain the observed Na emissions at Mercury. Now, quite recently, Potter & Morgan (1997b) have obtained Na images showing evidence for such an extended coma.

Turning to lateral distributions, one expects a similar distinction between condensable and noncondensable species as in the lunar atmosphere (see §2). Thus, He, which is not condensable, should be conserved according to the standard $nT^{-5/2}$=constant exospheric conservation law, and the other known species, all of which are condensable, should show daytime maxima and nighttime cold trapping. Despite this simple expectation based on the lunar analogy, things are more complex. Concerning helium, the $nT^{-5/2}$=constant law predicts a night/day density asymmetry of 150, but Mariner 10 data show that only a 50:1 density asymmetry exists. This is almost certainly due to uncertainties in our understanding of the interaction of He gas with Mercury's surface, and in particular implies that He's thermal accommodation to the surface is inefficient (Smith et al. 1978).

Turning to Na and K, for which only daytime data exist (since they are detected by resonance fluorescence), strong (e.g., 5:1) morning/afternoon abundance variations have been reported (Sprague et al. 1996). More surprising, however, are the observations of fascinating localized Na and K spatial variations (the so-called Na and K "clouds," sometimes occurring in north-south pairs) seen at high latitudes over the past several years (Potter & Morgan 1990; Sprague 1990; Sprague et al. 1997). The ultimate cause of these features has not been firmly established, but solar UV, Mercury magnetospheric/auroral (Potter & Morgan 1990), and local surface concentration enhancements (perhaps associated with radar bright terrains that may even be sources of vulcanism; Slade et al. 1992; Butler et al. 1993) have been suggested as potential causal mechanisms; we discuss this topic again

a few paragraphs below.

Sources and Sinks: As in the classic picture of any SBE, the abundance and distribution of the constituent species in Mercury's atmosphere must be controlled by a balance between sources and sinks, as modified by surface recycling interactions, and dynamical effects (e.g., gravity, radiation pressure) during transport. Detailed knowledge about this interplay is severely limited at Mercury, owing to the paucity and limited resolution of available observational data sets, and to fundamental uncertainties about the nature and composition of Mercury's surface, the meteoritic environment at Mercury, and the detailed structure and variability of Mercury's magnetosphere (Goldstein et al. 1981; Ip 1993; also Vilas et al. 1988). Despite these limitations, however, some qualitative information is available.

Concerning sources, it is clear that the ultimate source of much of Mercury's atmospheric H must be the solar wind, but H (and O) probably is also derived from the photodissociation of H_2O imported by the meteoritic complex and (rare) cometary impacts. Mercury's He must be supplied by some combination of solar wind capture and internal outgassing. Na and K must be derived from a combination of surface release and meteoritic import, but the relative importance of charged particle sputtering, chemical sputtering, thermal desorption, photon sputtering, and meteoritic impact is essentially unconstrained (and likely to be highly time variable). An excellent discussion of the current state of knowledge/ignorance in this area is given in Potter (1995).

Loss processes for the gases in Mercury's SBE include photoionization, photodissociation (for molecules, if present), Jeans escape (particularly important for H and He), and radiation pressure loss. Concerning radiation pressure, it is important to point out that Mercury's elliptical orbit drives a strong and complex cycle of both distance and velocity effects that contribute to strong effective photon intensity, and therefore radiation pressure variations (e.g, Ip 1986; Smyth 1986; Smyth & Marconi 1995b). Early on, Potter & Morgan (1987) confirmed such suspicions observationally by demonstrating that Mercury's Na column is inversely proportional to the instantaneous radiation pressure felt by Na atoms as Mercury travels along its orbit.

Comparison to the Lunar SBE: As we compare Mercury to the Moon, we see both similarities and differences. Somewhat similar rosters of species have been detected in both SBEs, but as shown in Table 4.2, the abundances of all known atmospheric constituents are higher at Mercury (note also that Mercury's H and O have no counterpart at the Moon).[45] So too, as shown in Table 4.3, the Na/K ratios at Mercury are significantly higher than in the lunar atmosphere. Higher abundances, combined with the fact that neutral lifetimes are much shorter on Mercury than on the Moon, provide strong circumstantial evidence that

[45] In fact, at Mercury, the Na D lines become moderately optically thick, with *tau* of order 1.

source rates must be higher at Mercury, and/or the recycling processes more effective.[46] Yet another similarity is that both the lunar and Mercurian SBEs show strong temporal and spatial variability, but this is not surprising given the tenuous, low-inertia nature of SBEs in general.

The physics that drives Mercury's atmosphere is strongly modified, relative to the lunar case, by a combination of Mercury's higher gravity, its closer position to the Sun (affecting thermal conditions, and incident photon fluxes), its order-of-magnitude more severe orbital distance and velocity variations, and particularly fundamentally, by the presence of a planetary dipole field and its consequent magnetosphere.

Mercury's higher gravity results in a shorter time of flight for bound atoms on ballistic trajectories between encounters with the surface. A consequence of this is that an atom experiences fewer encounters with solar photons during each ballistic hop. This, and the shorter lifetimes against photoionization resulting from Mercury's smaller heliocentric distance, serve to counteract the higher radiation pressure forces on atoms at Mercury.

As we just noted, the decreased heliocentric distance of Mercury compared to the Moon induces much shorter surface residence times between bounces of atomic species on the surface, which may create a larger thermalized population of atoms at Mercury. Mercury's smaller heliocentric distance (combined with its albedo) also causes its surface temperature to be much hotter (725 K, subsolar) than on the Moon (400 K, subsolar). This higher temperature causes more rapid outgassing of volatile or semivolatile constituents, increases the thermal scale height in the daytime atmosphere, and modifies the timescales required for both thermal accommodation and lateral transport. Owing to the strong dependence of outgassing rates on temperature, Mercury's higher surface temperature may be a (or the) significant cause of the striking difference in Na/K ratios between the Moon and Mercury. (See Table 4.3; notice there that the lunar and Mercurian values, though different, bracket the solar value).

The presence of a magnetic field at Mercury that is capable of standing off the solar wind most of the time (e.g., Hood & Schubert 1979), and creating a magnetospheric cavity whose importance cannot be underestimated when the lunar and Mercurian cases are compared. In addition to standing off the solar wind, and therefore reducing the effectivity of solar wind sputtering onto the surface, Mercury's magnetic field acts to prevent direct ion loss to the solar wind, and establishes a magnetospheric reservoir of ions and electrons.[47] As such, the presence of an internal dynamo essentially eliminates the importance of the Manka-Michel solar wind loss mechanism (which is so important at the Moon) at Mercury,

[46] Taking Na as an example, the typical global average source rates are roughly $\sim 5 \times 10^3$ and $\sim 2 \times 10^6$ cm^{-2} s^{-1}, respectively.

[47] Mercury's magnetosphere is also a potential generator of polar auroral phenomena.

and instead causes photo-ions and charge exchange ions to be essentially ubiquitously recycled to the surface, where they are later re-neutralized. This is very likely a major cause of the more effective recycling of atmospheric species discussed above.

One might expect that a combination of magnetospheric processes, and the effects of Mercury's elliptical orbit on photon and charged particle fluxes, radiation pressure, and meteoritic impact rates and energetics, would generate some significant time variability in Mercury's atmosphere.[48] This time variability has in fact been observed. A dramatic example of this kind of variability is the localized Na and K "emission cloud" enhancements observed at Mercury (Potter & Morgan 1990; Sprague et al. 1997). These enhancements may be related to known changes in the direction of the interplanetary electric field relative to Mercury's magnetosphere, which may cause large enhancements in the amount of recycled Na^+ brought to Mercury's surface (Hunten & Sprague 1997). Ion neutralization on impact, and either immediate return to the atmosphere as neutrals, or storage in localized cold spots to be released upon heating, may be responsible for some or all of the localized, short-lived Na bright spots seen in recent imaging experiments (Potter & Morgan 1990, 1997b). More observations are needed to improve our knowledge about the variability of Mercury's atmosphere.

As we conclude this discussion, we must admit the obvious: The way in which the various differing factors between Mercurian and the lunar cases affect the distribution, sources, sinks, and recycling of Mercury's atmosphere is complex, and far from satisfactorily understood. However, the literature contains some important papers that may lead to a deeper understanding. We refer the reader to Goldstein et al. (1981) concerning H and He; Ip (1993) and Smyth & Marconi (1995b) on radiation acceleration; Potter & Morgan (1990) and Sprague (1993) on magnetospheric recycling of Na; Sprague (1990) and Killen & Morgan (1993) for the suggested crustal diffusion source; and Killen & Morgan (1993) and Smyth & Marconi (1995b) for general models of the combined effects of several mechanisms.

5.0 SPECIAL TOPICS

In this final section before closing, we briefly touch on two little-studied but interesting topics regarding the lunar atmosphere: the impact of human exploration on the native lunar atmosphere, and the likely content and history of the lunar atmosphere over the past 4.6 Gyr, including impact-driven transients which have probably increased its bulk by orders of magnitude for short periods. We begin with a review of the literature available on human impacts.

[48] The planet's 3:2 spin:orbit coupling might also expected to play a role.

5.1 Past and Potential Human Impacts

As we noted above, the rate of supply of gases to the native lunar atmosphere is of order 10 g s^{-1}, and the total mass of the atmosphere is only $\sim 10^7$ g. Because this atmosphere has so little mass, it is particularly susceptible to human influence. This was dramatically demonstrated by the simple fact that each Apollo lunar landing mission deposited $\sim$0.2 lunar atmosphere mass in rocket exhaust and spacecraft effluents (Vondrak 1974, 1988). See Figure 5.1. Of course, this gas was lost to space on a few ionization timescales, but the effects of repeated landings in the period 1969–1972 severely hampered ALSEP measurements of the lunar atmosphere (see §1).

Any future, intensive lunar exploration phase using rocket-based technologies and involving currently foreseen technologies[49] would involve substantial gas injection to the lunar atmosphere, severely perturbing its native state. Additionally, if the average injection rate were to exceed $\sim$1 kg s^{-1}, affecting the pristine environment's suitability for some kinds of astronomical observations (Burns et al. 1988; Fernini et al. 1990).

The "good" news about the present, low-mass state of the lunar atmosphere as regards to human contamination is twofold: The atmosphere is optically thin to the photons and charged particles which drive the naturally cleansing loss processes, and its escape time is short. As a result of these factors, the whole ensemble of gas molecules on the dayside are subject to photoionization loss. This is why the effects of each Apollo landing were seen to dissipate over timescales of a few lunations.

Vondrak's work (1974, 1988), however, has shown that it would not be difficult to transform this situation into a different one. Making simple calculations about an increasingly dense, idealized (i.e., oxygen) lunar atmosphere, Vondrak found that as the number density of the lunar atmosphere increases, the exobase eventually rises above the surface, in effect shielding the atmosphere below it from escape, and thereby dramatically lengthening the time required for it to recover to the native state. More specifically, as shown in Figure 5.1, Vondrak found that for source injection rates $\gtrsim$ 60 kg s^{-1} (corresponding to a total atmospheric mass $>10^8$ kg, roughly 10^4 the present mass), the atmosphere switches from being photoionization loss dominated to being thermal escape (Jeans 1923) dominated, with a consequent increase in characteristic escape time from tens of days to hundreds of years.

These considerations emphasize how fragile the native lunar environment is, and how easily human activities, even in the name of science, can affect this ancient wilderness.

[49] Not to mention the mining activities envisioned by some groups.

5.2 The Primordial Lunar Atmosphere and More Recent Transients

Today the lunar atmosphere is a rarefied surface boundary exosphere, but simple considerations demonstrate that it could not have always been so thin. Cast into its simplest form, one finds three major epochs in the history of the lunar atmosphere. These are illustrated in Figure 5.2. During Epoch I the Moon's surface was still hot from formation and displayed widespread exposed surface magmas. The atmosphere during this period, prior to final crustal formation, was a thick, thermally supported rock vapor pressure atmosphere. During Epoch II, which spanned the period from the end of the last magma ocean and the formation of the lunar crust ~4.4 Gyr ago, until the tailoff of large impacts ~3.4–3.0 Gyr ago, the lunar atmosphere stochastically fluctuated between an SBE state and thicker environments owing to the effects of vulcanism and impacts. During Epoch III, which stretches down to the present, the lunar atmosphere should be correctly called a time-averaged SBE (as should other SBEs) in which the rarefied SBE is occasionally exceeded owing to occasional impacts or internal outgassing events.

To our knowledge, no discussion of the long-term time evolution has ever been presented, and there is no body of research into its properties. Therefore, in this subsection, we briefly sketch a few interesting details concerning the thicker atmospheres that have existed during Epochs I–III, with the hope that it will spur further research into this natal but fascinating subject area. We discuss each of the three atmospheric epochs in turn.

Epoch I: The Thick Primordial Lunar Atmosphere. Geochemical evidence from lunar samples provides convincing support to the idea that accretional heating induced an early lunar epoch initially exhibiting either widespread or global magma oceans which later declined to magma seas and eventually to ponds as they cooled. Such surface magmas, with characteristic temperatures of 1000–2500 K, must have acted as sources of rock vapor, consisting primarily of silicon, aluminum, magnesium, sulfur, and iron oxides. As a purely illustrative example, consider the magnitude and characteristics of a purely SiO_4 vapor envelope around the Moon. At a canonical magma temperature of 1500 K, the saturation vapor pressure of SiO_4 is 100 bars— under these conditions the lunar atmosphere would be about as thick as Venus's present atmosphere! The scale height of this atmosphere would be of order 75 km; the radiative output of the hot Moon under these conditions would be $\sim 10^{26}$ (T/1500 K)^4 erg s^{-1}.

One would expect this atmosphere to have displayed complex chemical and dynamical processes. These processes would have been affected by the ancient Moon's closer position to the Earth, and the ancient Sun's lower bolometric but higher UV luminosity (e.g., Kasting & Grinspoon 1991). The investigation of the chemical and dynamical environment of this atmosphere is beyond the scope of this review.

Because the escape parameter Λ of the massive Epoch I lunar atmosphere would have been $\sim$20, escape would not have been hydrodynamic, but would instead be dominated by the standard Jeans process and scavenging by solar wind and solar UV. Following Vondrak (1974), we estimate the combined atmospheric loss rate under these circumstances to have been of order 100 g s^{-1}. Since a 100 bar lunar atmosphere would have had a mass near 10^{24} g, almost 100 times the mass of the present-day terrestrial atmosphere, its escape timescale would have been of order 10^{13}–10^{14} years, far exceeding the age of the solar system. As such, this atmosphere would have remained in place as long as its underlying source (exposed, hot magma) was extant on the surface to a degree capable of sustaining the equilibrium vapor pressure. Throughout this epoch, the massive lunar atmosphere would have shielded the underlying "surface" from many impacts (though not from the infalling mass deposition itself), and may (particularly in its waning days) have created geochemical or geophysical evidence of its presence.

Even if localized hot magma pools existed on the surface (i.e., a lunar-like Io), a massive atmosphere could not have existed unless it remained hot enough to prevent widespread condensation (i.e., a rock rain). Borrowing from the literature on the evolution of terrestrial rock vapor atmospheres after giant impacts (e.g., Sleep et al. 1989), we find that the radiative timescale on which a rock vapor atmosphere thermally collapses from 1500 K is about 0.5 years. Thus, the demise of this atmosphere most likely occurred when the lunar crust formed ($\sim$4.4–4.3 Gyr ago; Taylor 1982), cutting off the overlying atmosphere from the necessary heating source.

Epoch II: The Era of Thick-Atmosphere Transients. Subsequent to the era of a sustained, thick lunar atmosphere, there must have been an era during which occasional large (e.g., large crater- or basin-forming) impacts either punctured the thin crust overlying subsurface magmas, or which themselves created regional-scale magma lakes. Lunar geochronology suggests that this era persisted until 3.8–3.4 Gyr ago. Sample dating of basalts (see Taylor 1982) provides ample radiometric evidence that mare basalts, and therefore mare vulcanism, persisted until $\sim$3.1 Gyr ago. From this we conclude that throughout the period from $\sim$4.4 Gyr ago when the crust solidified until $\sim$3.1 Gyr ago when vulcanism effectively terminated, the Moon had a thin, volcanically supported atmosphere which was punctuated by brief ($\sim 10^3$ yr?) and increasingly rare transients to high-mass states created by the dramatic but declining effects of large impacts.

A crude (and perhaps grossly inaccurate) scale for the "background" mass of this atmosphere would be the expected output from a single significant volcano, which might produce a steady-state atmosphere of order 10^{14} g and a pressure of order 10^{-8} bars; such an envelope would display a column mass of 3×10^{-4} g cm^{-2} and a number density of order 10^{11}–10^{12} cm^{-3}. As such, it would not be an SBE, but a conventional (though quite thin) collisional atmosphere. Vondrak's (1974) calculations indicate an escape rate of order 10^4

g s^{-1}, which gives a crude loss timescale (in the absence of replenishment) of a few years to a few tens of years. The exploration of this fascinating environment, including the attributes and possible signatures of the punctuated intrusions of more massive atmospheric transients owing to impacts during Epoch II deserves further study.

Epoch III: Transients from the Modern Lunar Atmosphere. The boundary between Epochs II and III might be crudely defined as occurring when the lunar atmosphere first became an SBE for a timescale comparable to the timescale between major impacts. Based purely on the lunar cratering chronology established from Apollo-era data, this probably occurred of order 3 Gyr ago. Since then, the lunar atmosphere has probably appeared, on average, much as it does today, with only brief, occasional transients to higher mass states, which occur when significant impacts (or perhaps rare, significant internal gas releases) occur.

How often do important transient excursions occur? We consider here only impact-generated transients, and adopt the following criteria for "interesting" cases. Criterion 1 is that the lunar atmosphere increases by an order of magnitude in mass to $\sim 10^8$ g; such an event would be dramatic, but the atmosphere would remain an SBE. Criterion 2 is met by an impact that would transition the atmosphere out of the SBE regime. This requires a minimum total atmospheric mass of order 10^{10} g.

For impacts onto rock at speeds of order 7–25 km s^{-1}, as would be produced by objects in the Earth orbit crossing population, models predict the formation of 1–5 times the mass of the impactor in vapor (Gault 1973; Haff et al. 1983), with characteristic temperatures of 2000–5000 K. The escape speed from the Moon (2.38 km s^{-1}) equates to a gas thermal temperature of ≈16,000 K, which little of the vapor would reach (O'Keefe & Ahrens 1982; Morgan & Shemansky 1991); ionization effects do not become important at vapor temperatures below 20,000 K. Therefore, to first order, essentially all of the vaporized mass remains as a neutral gas and is initially retained, and impactors of scale 3×10^8 and 3×10^{10} g are required to satisfy criteria 1 and 2, respectively.[50] For impactor densities of 3 g cm^{-3} the impactor radii corresponding to these masses would be only ≈2 and ≈10 meters, respectively. Recent calculations of the Earth-crossing impactor population and lunar impact rates (e.g., Bottke et al. 1994; Rabinowitz et al. 1994) differ by factors of a few. Still, however, such results are useful for providing a feel for the frequency of impacts that generate interesting atmospheric transients. For impactors with radii of 2 m and 10 m, the predicted mean times between impacts on the Moon are of order 5–10 years, and 100–200 years, respectively. By comparison, a comet impact is estimated to occur every $\sim 10^7$ years (Shoemaker 1983) and to generate $10^{16.6-17.5}$ g of vapor, corresponding to a microbar-class atmosphere; a Tycho-generating impactor occurs of order every $\sim 10^8$ years and generates an atmospheric mass of order $10^{19.5-20.5}$ g, which would generate a

[50] Cometary impacts at characteristic speeds of 30–50 km s^{-1} would import several times more energy per gram and require proportionately smaller impactors.

millibar-class transient atmosphere.

Again following Vondrak's escape rate calculations, transient atmospheres with masses of 10^8 g would be lost on timescales of a few months. Transient atmospheres with masses of 10^{10} g would decline in a few days back below the SBE boundary (owing to the development of an optically thick envelope and higher exospheric temperatures), further declining to the ambient (i.e., present) quasi-state environment in a few years.[51] Crudely speaking, the duty cycle for significant lunar atmospheric transients above the current environment is of order 0.1–3%, which is surely nontrivial.

The fact that the modern lunar atmosphere routinely exhibits transients of this magnitude, and in fact briefly exits the SBE regime of order every 100–200 years, is not generally recognized. This, like the more severe departures of the lunar atmosphere from its present environment that occurred early in lunar history, deserves more rigorous investigation.

6.0 OUTLOOK

The lunar atmosphere is tenuous indeed: Upper limits derived by Apollo-based instruments indicate that the entire native envelope weighs only ~100 tons. However, the complexity and scientific value of this atmosphere is not commensurate with its low mass.

Tenuous as it may be, the lunar atmosphere contains vital information about the location of near-surface volatiles, including water, acts as a reservoir of gases released from the interior, and may even mirror the composition of certain surface-lying mineralogical units. Furthermore, as described in §4 above, the lunar atmosphere is the most accessible of the solar system's surface boundary exospheres, and offers a rich variety of physical processes to study as analogs to other SBEs across the solar system. An important advantage of the Moon for such studies is that, unlike any other similarly exposed planetary surface, we enjoy abundant surface samples and orbital geochemical data that provide key "boundary conditions" to the physics and chemistry at work.

As one example, consider surface sputtering. Owing to its nature as a surface boundary exosphere, chemical reactions between lunar atmospheric species and the lunar surface serve to modify the atmospheric composition and to control the transport physics of mobile species. Because sputtering and micrometeorite impacts are major neutral and ion gas production sources, studies of the lunar atmosphere offer to improve knowledge about the rate and kind of weathering processes that affect uppermost planetary regolith. Such

[51] A comet impact event atmosphere would likely take of order 10^3 years to decline back to the SBE boundary; a Tycho-forming event atmosphere would likely take of order 10^6 years to decline back to the SBE boundary.

weathering is driven by the constant rain of charged particle and photon radiations from the Sun; radiation is known to modify the color, albedo, and microphysical structure of planetary surfaces (e.g., Johnson 1990). These data provide important information which. when coupled to atmospheric measurements allow direct solution for weathering yields, as a function of surface composition, temperature, and microphysical roughness. Once these are established, lunar surface weathering rates can then be used to translate atmospheric abundances on other planets and satellites into surface elemental compositions.

A second example concerning the value of the lunar atmosphere as it applies to other problems in planetary science is that the lunar atmosphere exhibits neutral gas densities ($\sim 10^{4-5}$ cm^{-3}) characteristic of cometary comae, thereby offering the opportunity to study the physical regime of a "gravitationally bound cometary coma." Numerous other examples exist as well.

Despite the great progress made in recent years concerning the nature and attributes of the lunar atmosphere, we remain fundamentally ignorant of the basic processes at work there. The first-order questions that remain to be resolved include:

- *What is the full composition of the lunar atmosphere?*
- *Why are so many expected neutral atomic species, like H, O, and Mg, missing?*
- *What are the dominant source and sink mechanisms for the major species?*
- *How does the composition and structure vary spatially and temporally?*
- *Do internal gas-release events correlate with certain surface features?*

These issues can only be resolved by obtaining more and better data of several kinds.

With regard to groundbased efforts, it would be particularly useful to obtain more sensitive upper limits on additional species in the lunar atmosphere, and to obtain temporally dense Na and K data sets spanning a full lunation. A concerted effort using modern detectors and large-database management techniques to search for, and determine the occurrence frequency, of LTPs would also be highly productive.

With regard to spacebased missions, we look forward to the results of the NASA *Lunar Prospector* mission's second-generation alpha particle emission spectrometer Ra/Rn/Po survey, as well as the mission's neutron spectrometer search for polar H_2O ice deposits. Additional insights into the composition of the lunar atmosphere are likely to be obtained by spectroscopic studies using HST, and the upcoming FUSE and AXAF missions as well.

However, the most valuable experiments that can be envisioned would involve placing a

suite of optical and mass spectrometers in lunar orbit (or even on the surface) aboard a clean spacecraft. Such a mission could easily be accomplished in the next few years.

In the more distant future, we envision an even more ambitious prospect: the active perturbation of the lunar atmosphere as a tool for studying the response of surface boundary exospheres to specific stimuli. Such experiments, for example involving temporary compositional and density modifications, are possible only as a result of the lunar atmosphere's low mass, and would open an exciting new era of laboratory-style atmospheric studies on a planetary scale.

ACKNOWLEDGMENTS

I want to thank my collaborators and colleagues including Brian Flynn, Dick Hodges, Don Hunten, Melissa McGrath, Mike Mendillo, Tom Morgan, Drew Potter, and Ann Sprague for many useful discussions over the years. I also thank Ann Sprague for providing material for Tables 4.2 and 4.3.

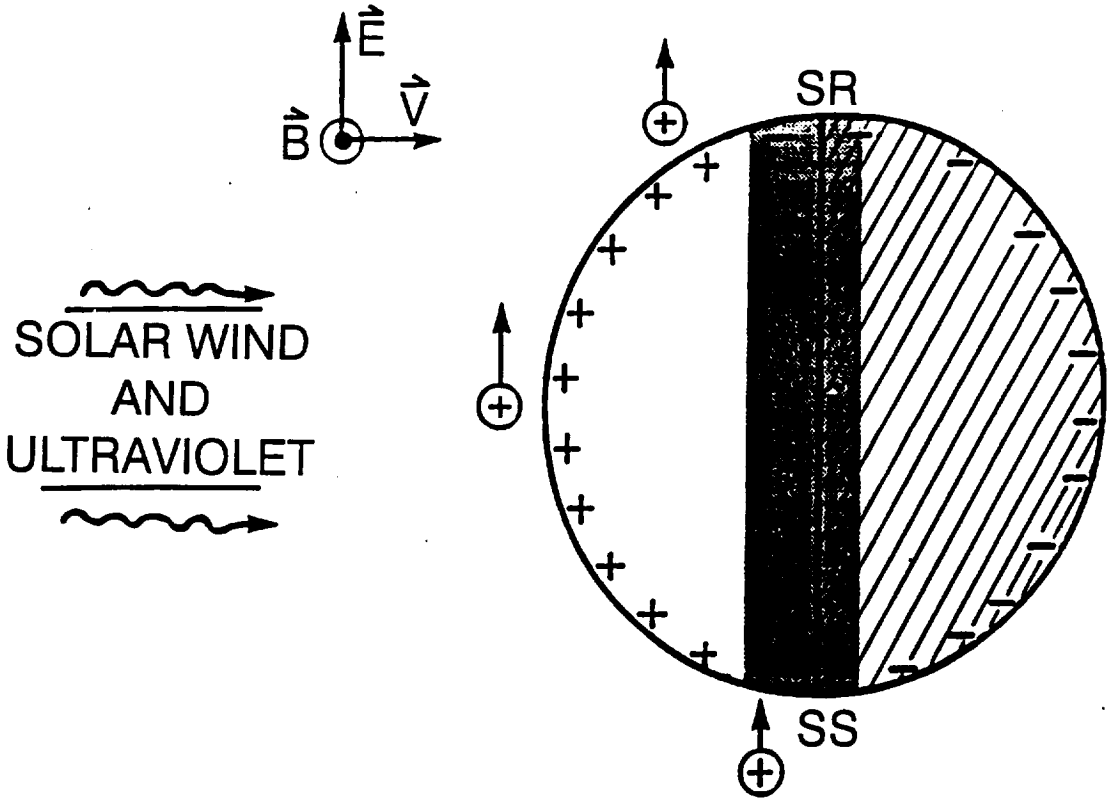

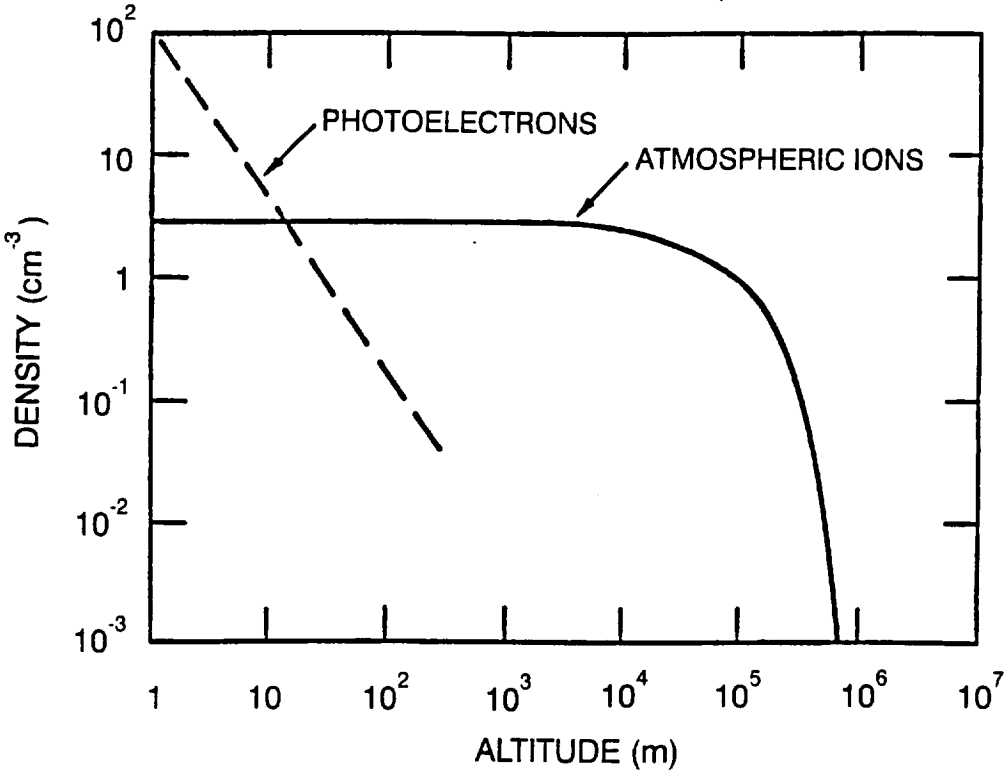

FIG. 1.1

TA000023

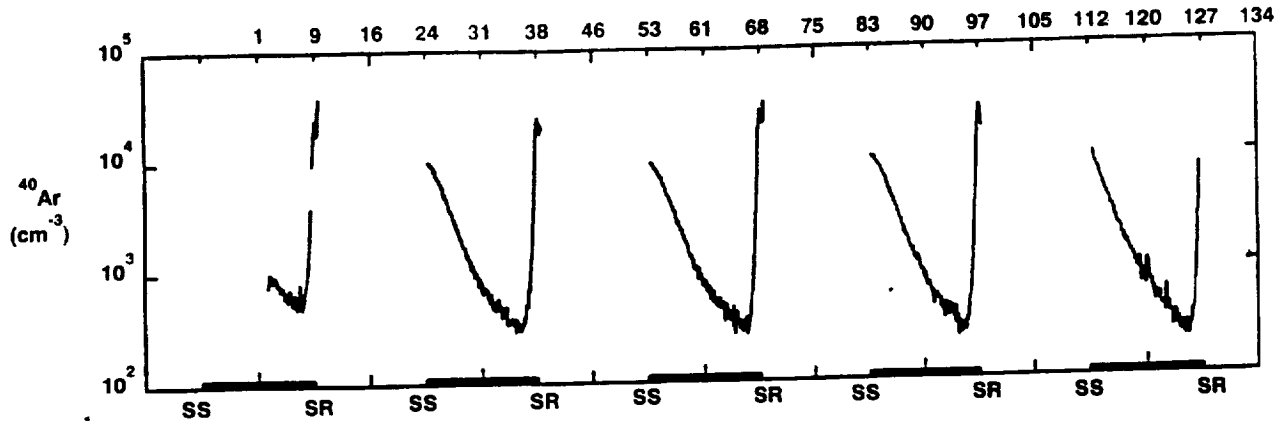
1 9 16 24 31 38 46 53 61 68 75 83 90 97 105 112 120 127 134
10^5
10^4
10^3
10^2
^{40}Ar
(cm^{-3})
SS SR SS SR SS SR SS SR SS SR

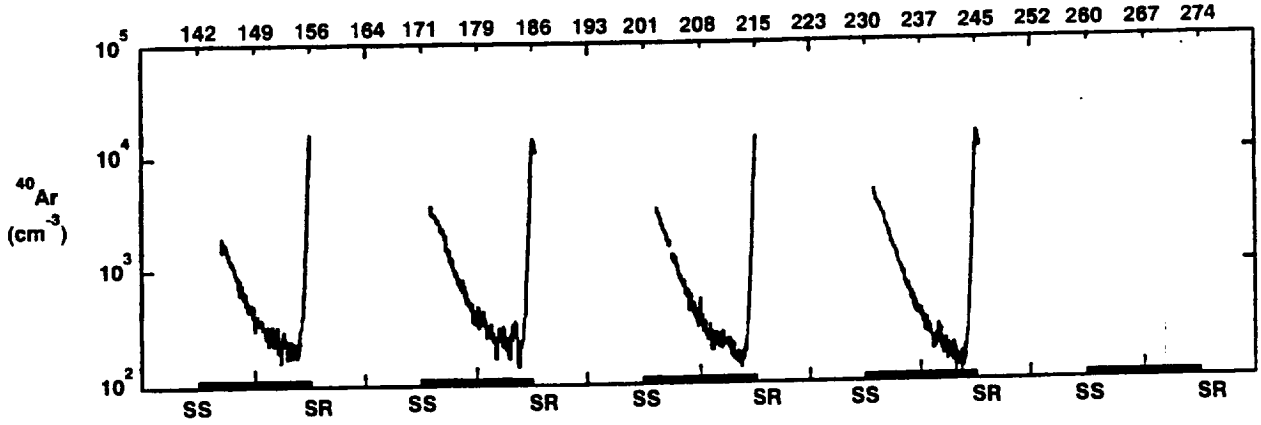
142 149 156 164 171 179 186 193 201 208 215 223 230 237 245 252 260 267 274
10^5
10^4
10^3
10^2
^{40}Ar
(cm^{-3})
SS SR SS SR SS SR SS SR SS SR

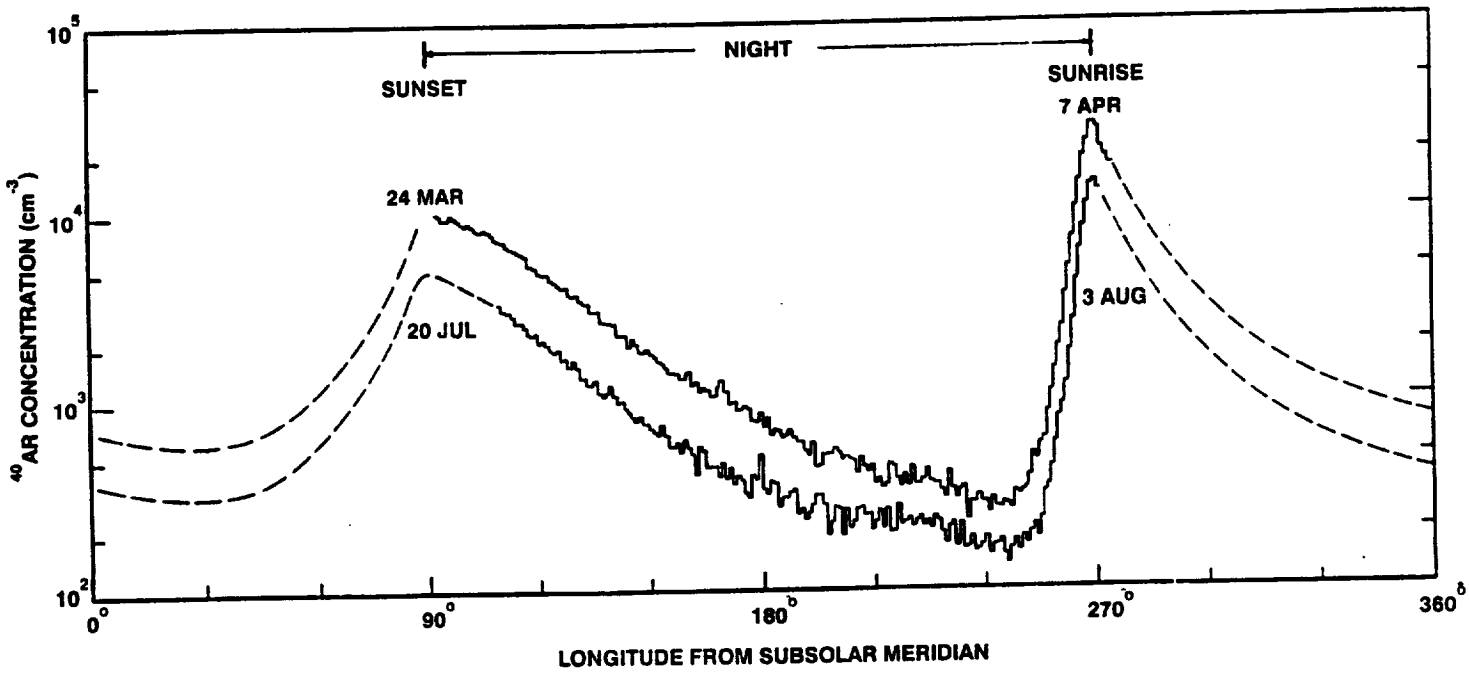
NIGHT
SUNSET
SUNRISE
7 APR
24 MAR
20 JUL
3 AUG
10^5
10^4
10^3
10^2
^{40}AR CONCENTRATION (cm^{-3})
0° 90° 180° 270° 360°
LONGITUDE FROM SUBSOLAR MERIDIAN

FIG. 1.2

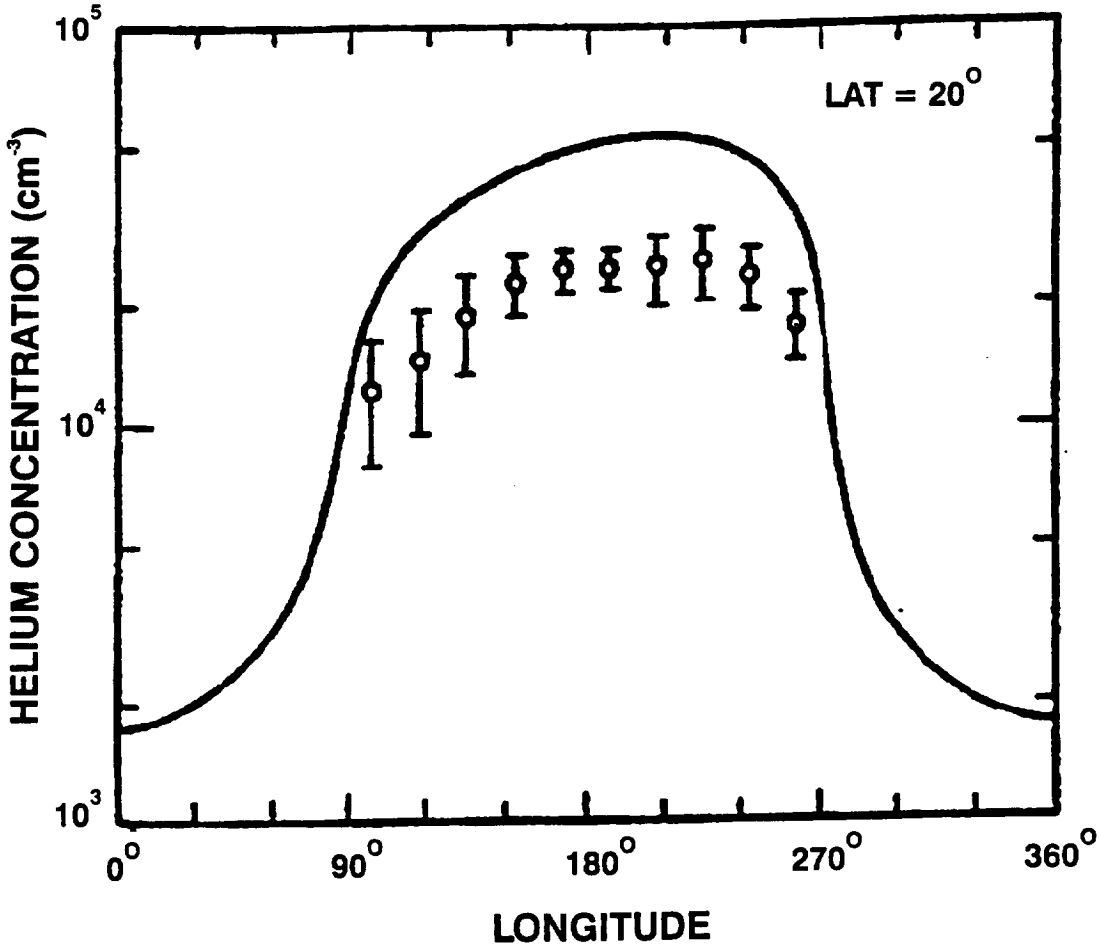

TA000025

FIG. 1.3

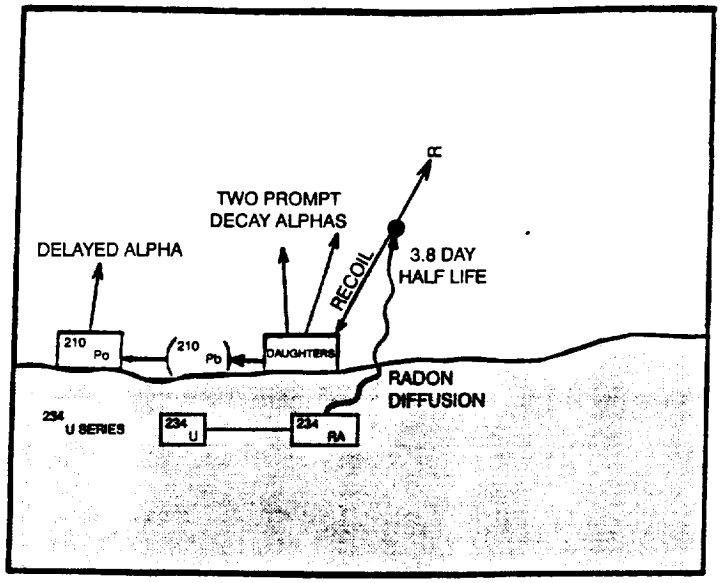

APPOLLO 15 ALPHA PARTICLE SPECTROMETER

DISTRIBUTION OF DEVIATIONS FROM THE WHOLE MOON AVERAGE FOR RADON-222 (+DAUGHTERS) DATA FROM 111 GET TO 220 GET

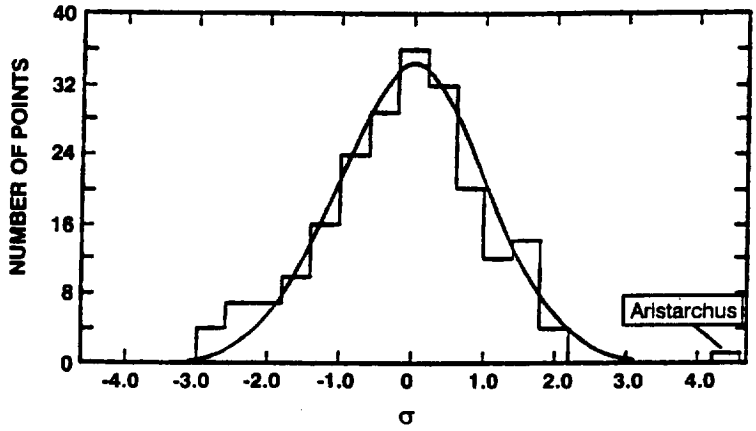

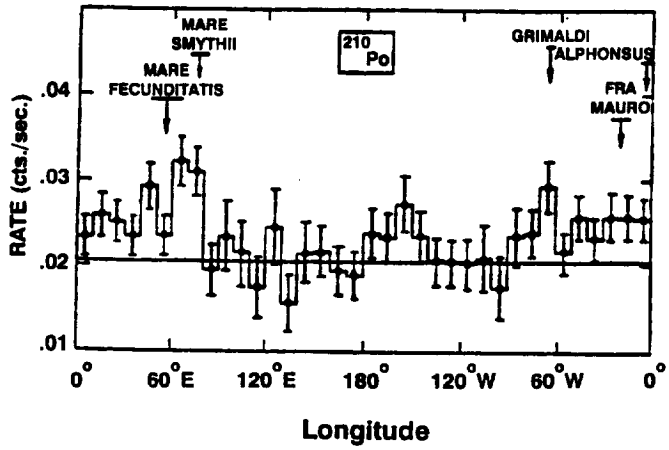

FIG. 1.4

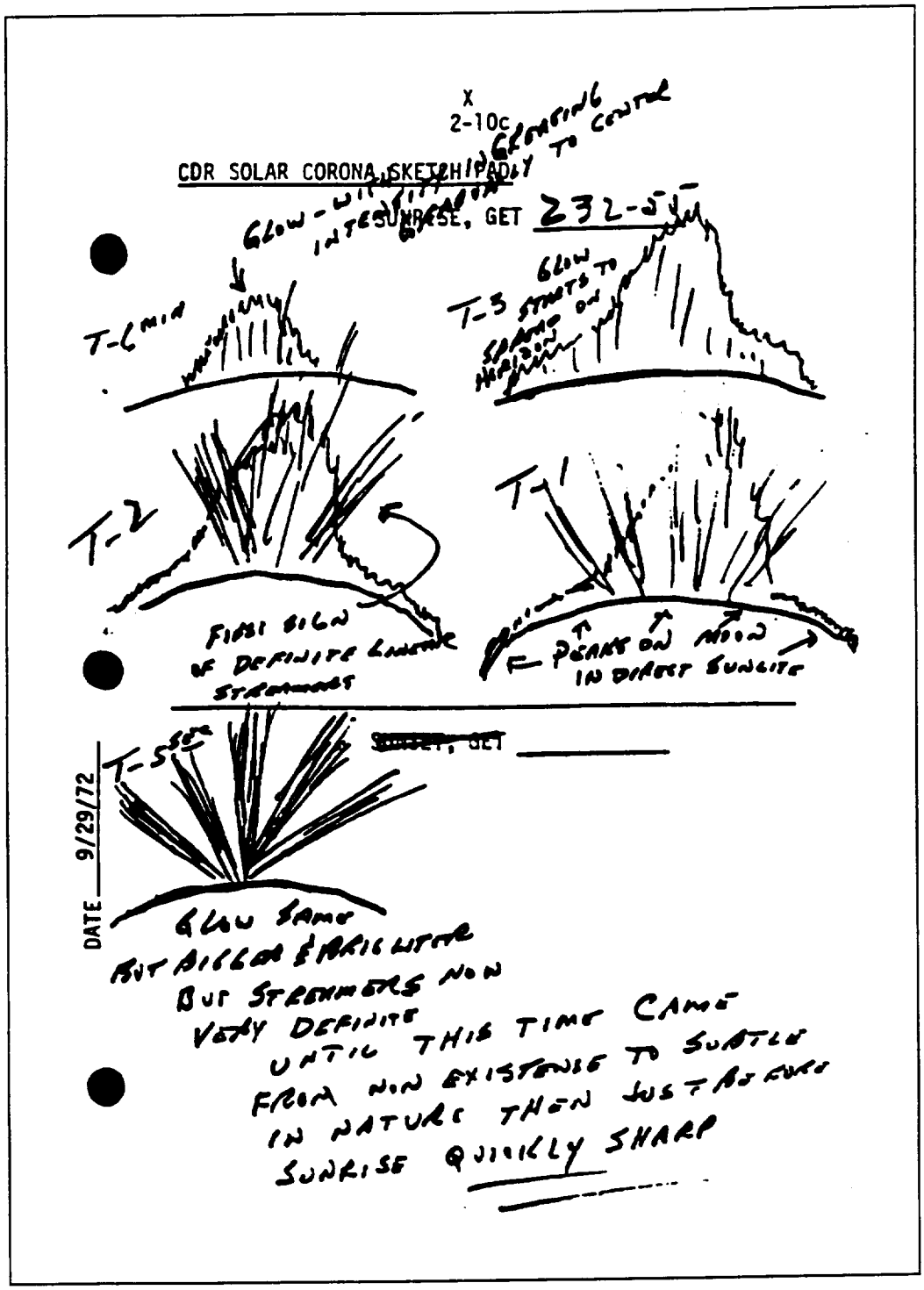
X
2-10c
CDR SOLAR CORONA SKETCH
T-6 MIN
T-3
T-2
T-1
FIRST SIGN OF DEFINITE LUNAR STREAMERS
PEAKS ON MOON IN DIRECT SUNLITE
T-5
DATE 9/29/72
GLOW SAME BUT BIGGER & BRIGHTER
BUT STREAMERS NOW VERY DEFINITE
UNTIL THIS TIME CAME FROM NON EXISTENCE TO SUBTLE IN NATURE THEN JUST BECAME SUNRISE QUICKLY SHARP

FIG. 1.5

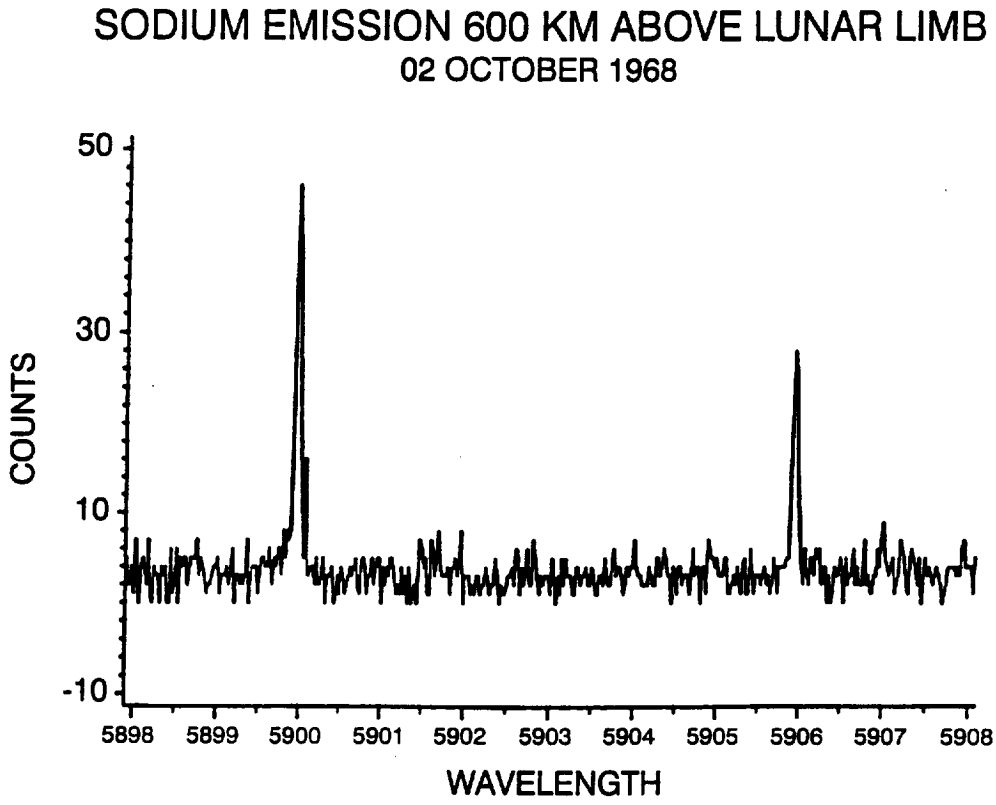

FIG. 1.6

TA000028

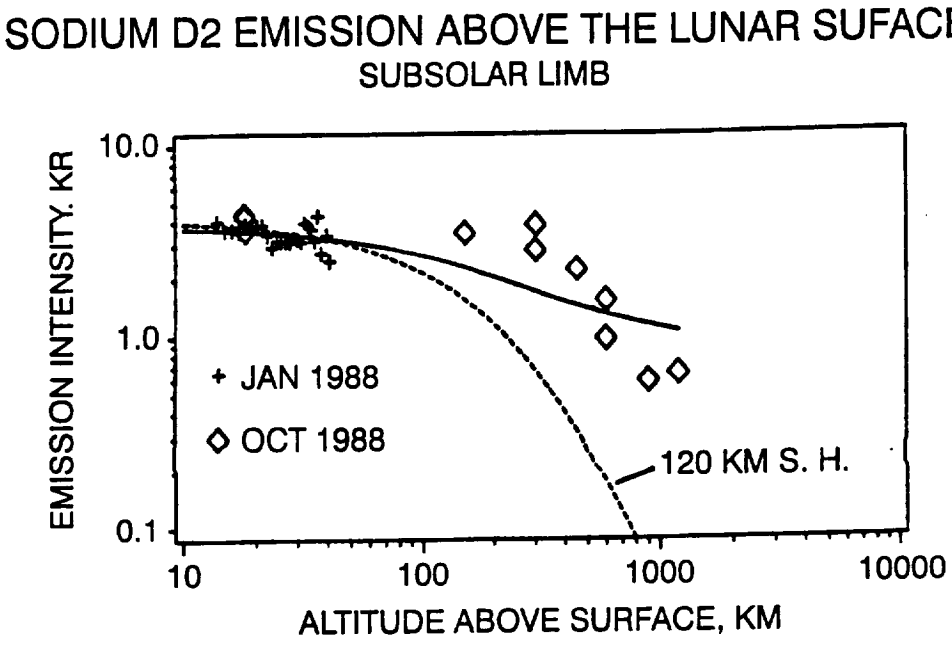

FIG. 1.7

TA000029

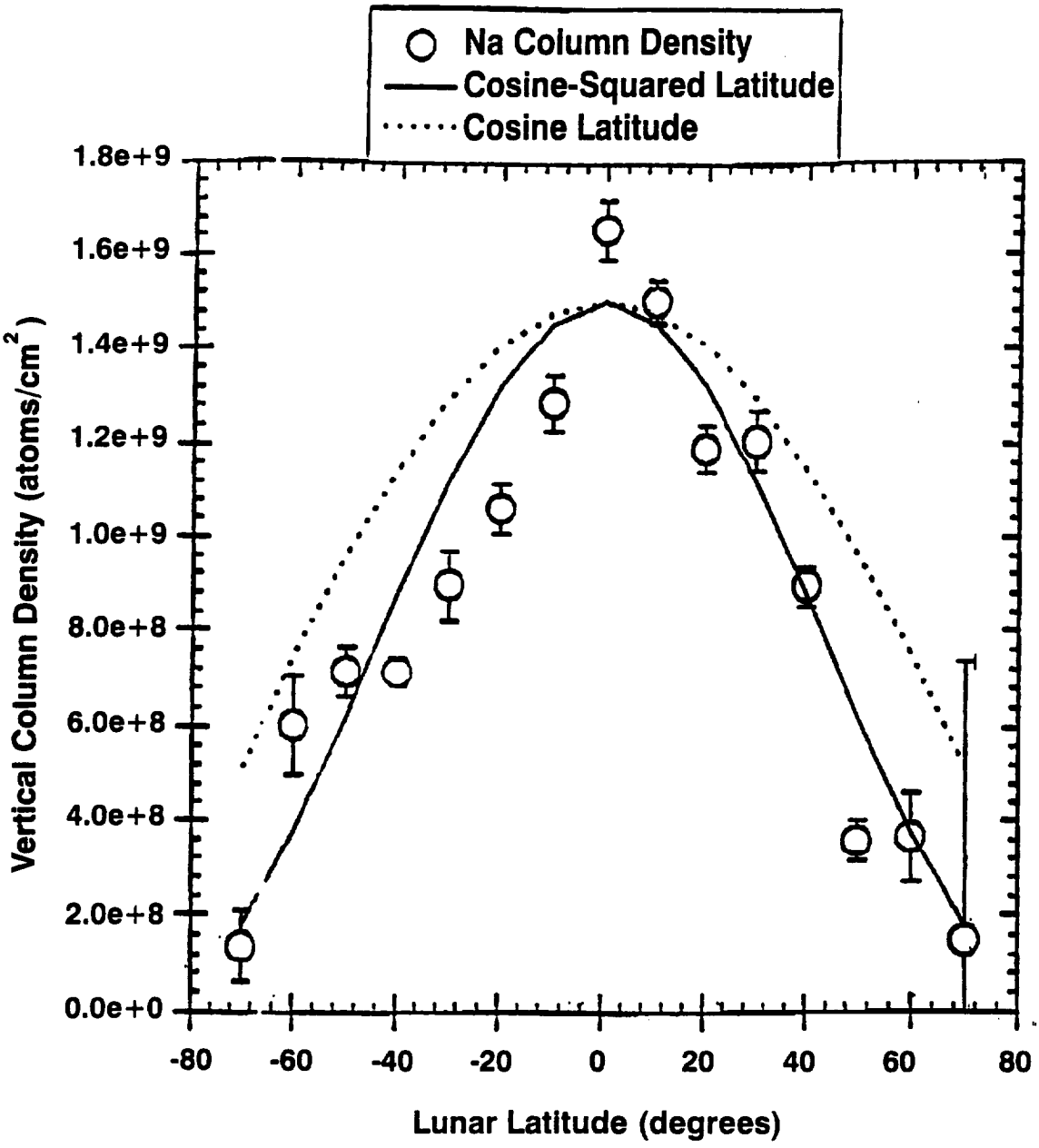
Na Column Density
Cosine-Squared Latitude
Cosine Latitude
1.8e+9
1.6e+9
1.4e+9
1.2e+9
1.0e+9
8.0e+8
6.0e+8
4.0e+8
2.0e+8
0.0e+0
Vertical Column Density (atoms/cm^2)
-80
-60
-40
-20
0
20
40
60
80
Lunar Latitude (degrees)

FIG. 1.8

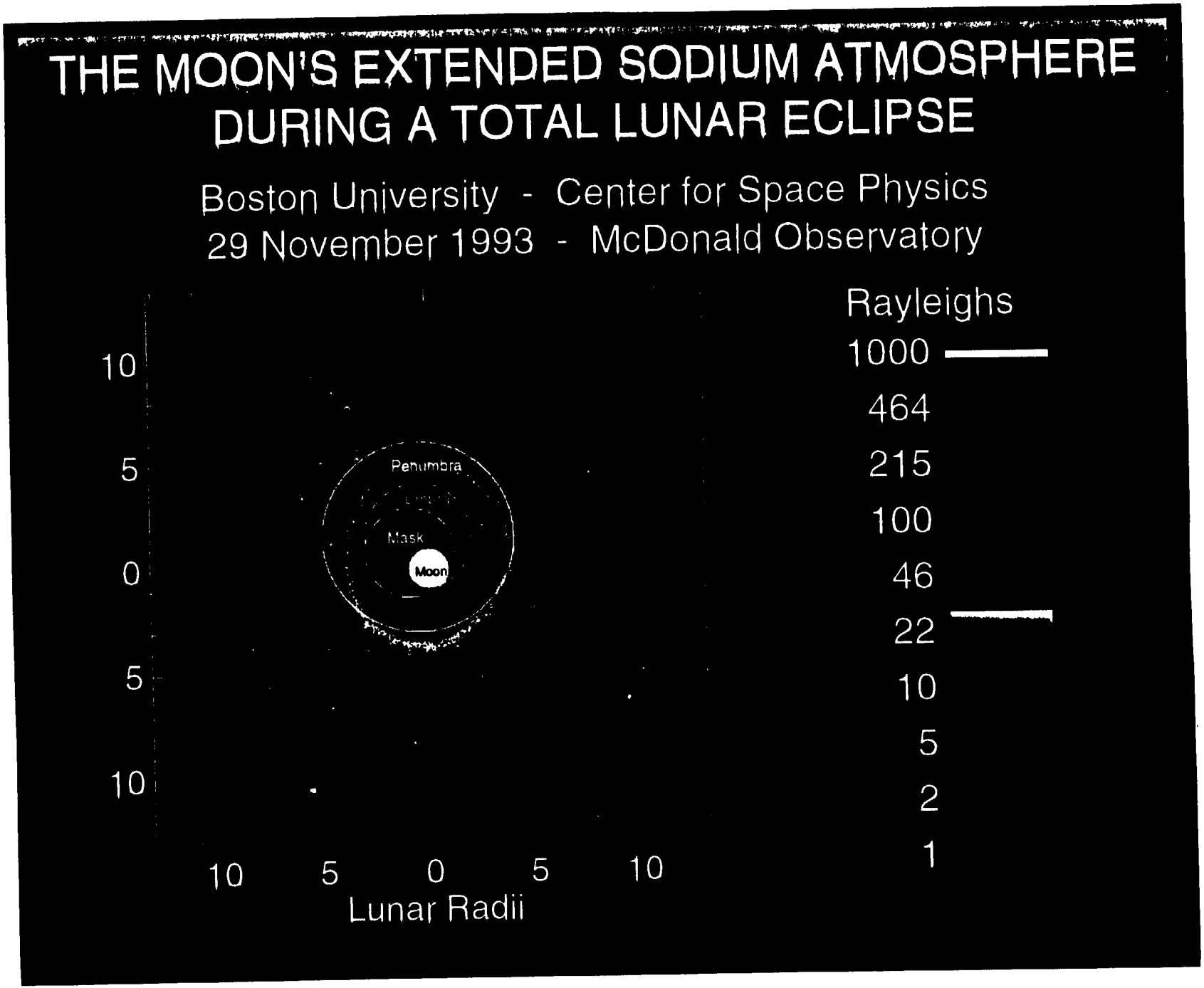
THE MOON'S EXTENDED SODIUM ATMOSPHERE
DURING A TOTAL LUNAR ECLIPSE
Boston University - Center for Space Physics
29 November 1993 - McDonald Observatory
Rayleighs
1000
464
215
100
46
22
10
5
2
1
Penumbra
Mask
Moon
10
5
0
5
10
10
5
0
5
10
Lunar Radii

FIG. 1.9

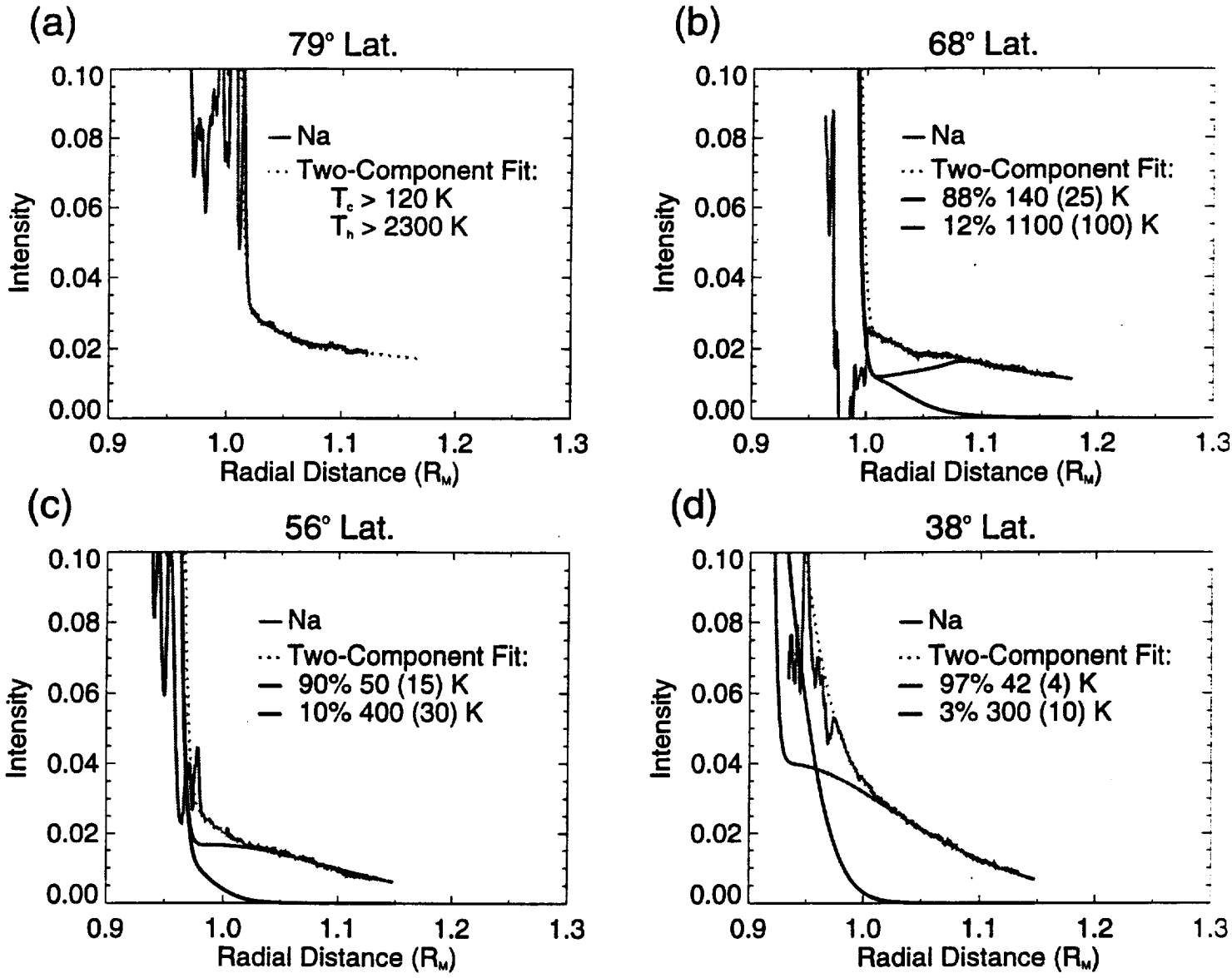
(a)
79° Lat.
— Na
··· Two-Component Fit:
T_c > 120 K
T_h > 2300 K
(b)
68° Lat.
— Na
··· Two-Component Fit:
— 88% 140 (25) K
— 12% 1100 (100) K
(c)
56° Lat.
— Na
··· Two-Component Fit:
— 90% 50 (15) K
— 10% 400 (30) K
(d)
38° Lat.
— Na
··· Two-Component Fit:
— 97% 42 (4) K
— 3% 300 (10) K
Intensity
Radial Distance (R_M)
0.00
0.02
0.04
0.06
0.08
0.10
0.9
1.0
1.1
1.2
1.3

FIG. 1.10

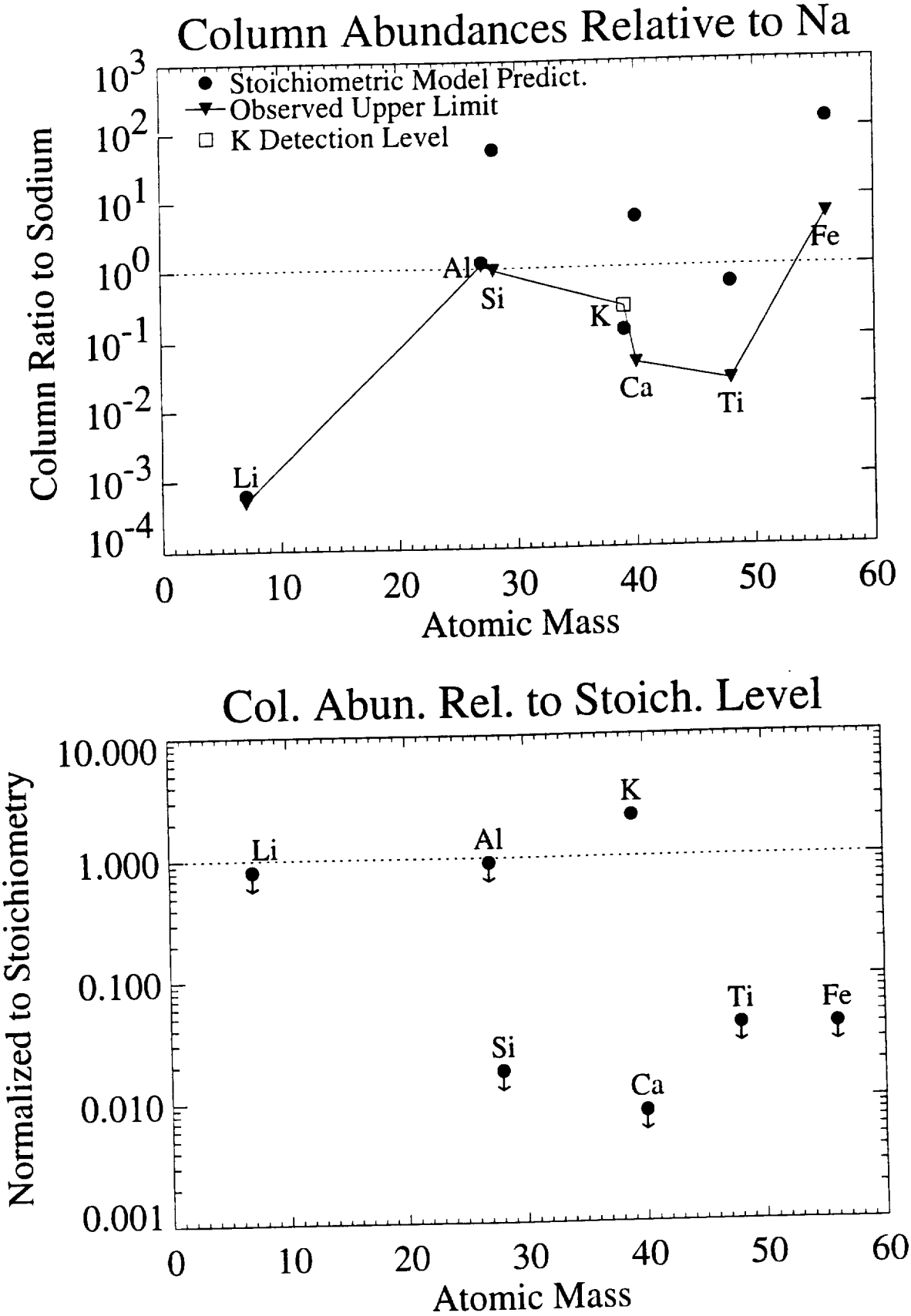
Column Abundances Relative to Na
Stoichiometric Model Predict.
Observed Upper Limit
K Detection Level
Column Ratio to Sodium
10^3
10^2
10^1
10^0
10^{-1}
10^{-2}
10^{-3}
10^{-4}
Li
Al
Si
K
Ca
Ti
Fe
0
10
20
30
40
50
60
Atomic Mass
Col. Abun. Rel. to Stoich. Level
Normalized to Stoichiometry
10.000
1.000
0.100
0.010
0.001
Li
Al
K
Si
Ca
Ti
Fe
0
10
20
30
40
50
60
Atomic Mass

FIG. 1.11

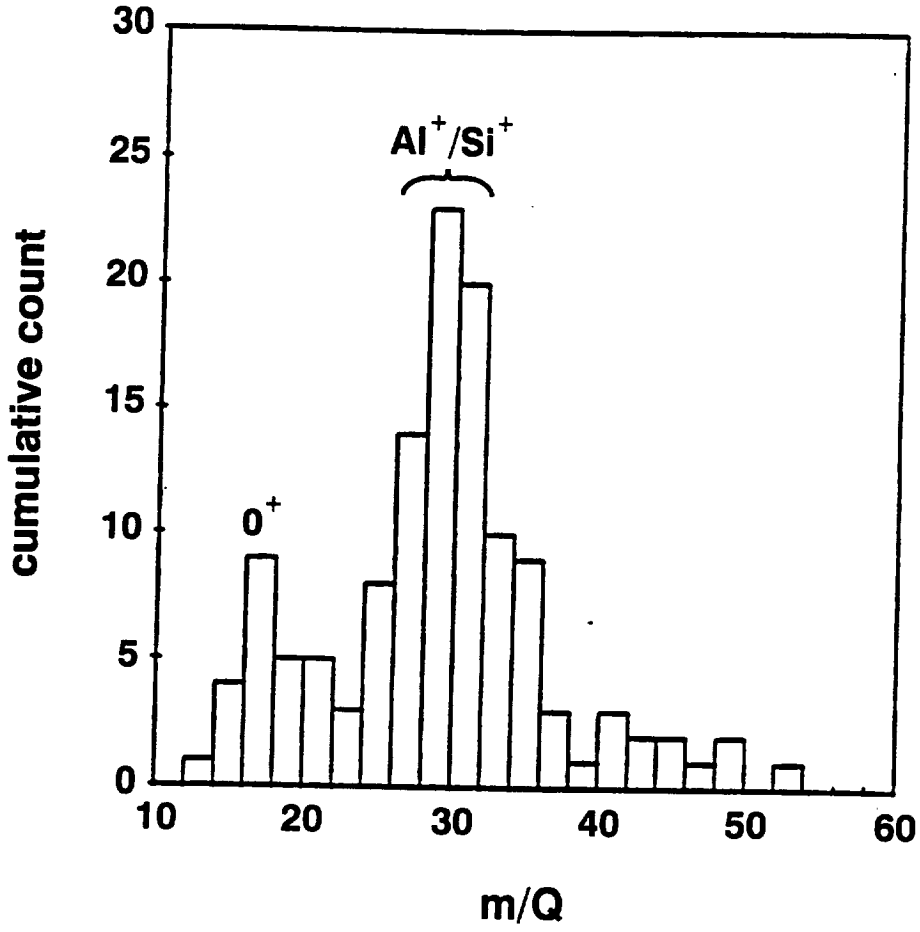

FIG. 1.12

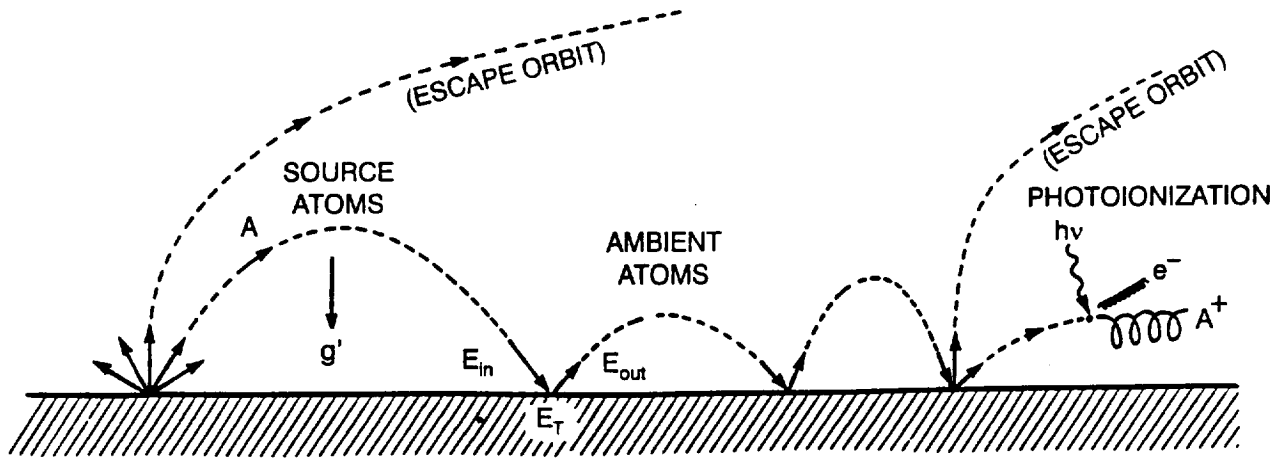
(ESCAPE ORBIT)
SOURCE ATOMS
A
g'
E_in
AMBIENT ATOMS
E_out
E_T
(ESCAPE ORBIT)
PHOTOIONIZATION
hν
e⁻
A⁺

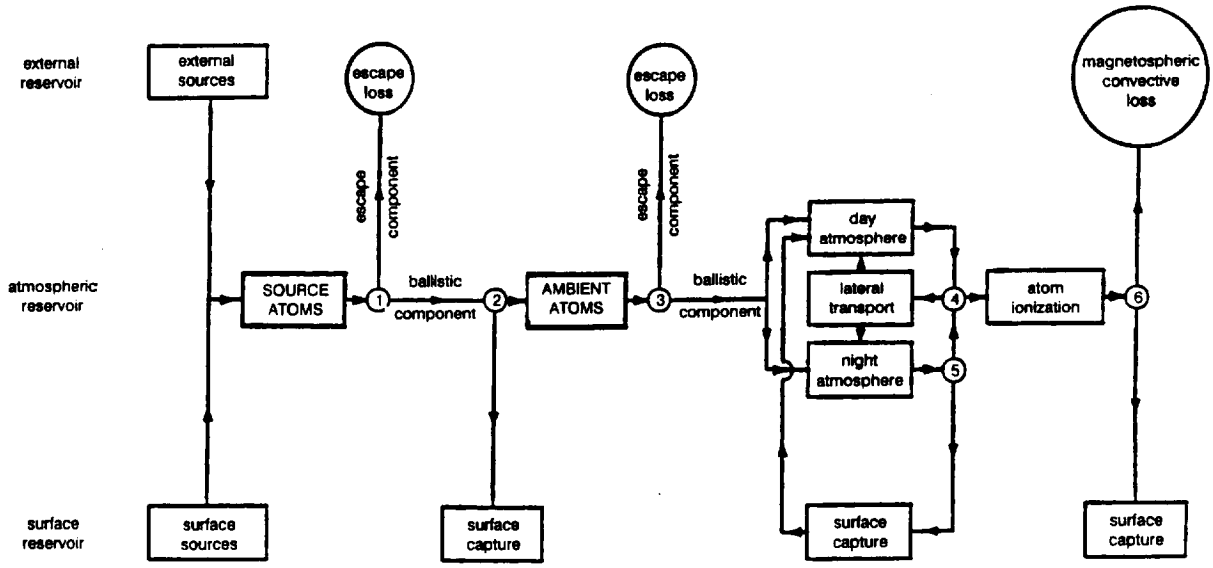
external reservoir
external sources
escape loss
escape component
escape loss
escape component
magnetospheric convective loss
atmospheric reservoir
SOURCE ATOMS
1
ballistic component
2
AMBIENT ATOMS
3
ballistic component
day atmosphere
lateral transport
night atmosphere
4
5
atom ionization
6
surface reservoir
surface sources
surface capture
surface capture
surface capture

FIG. 2.1

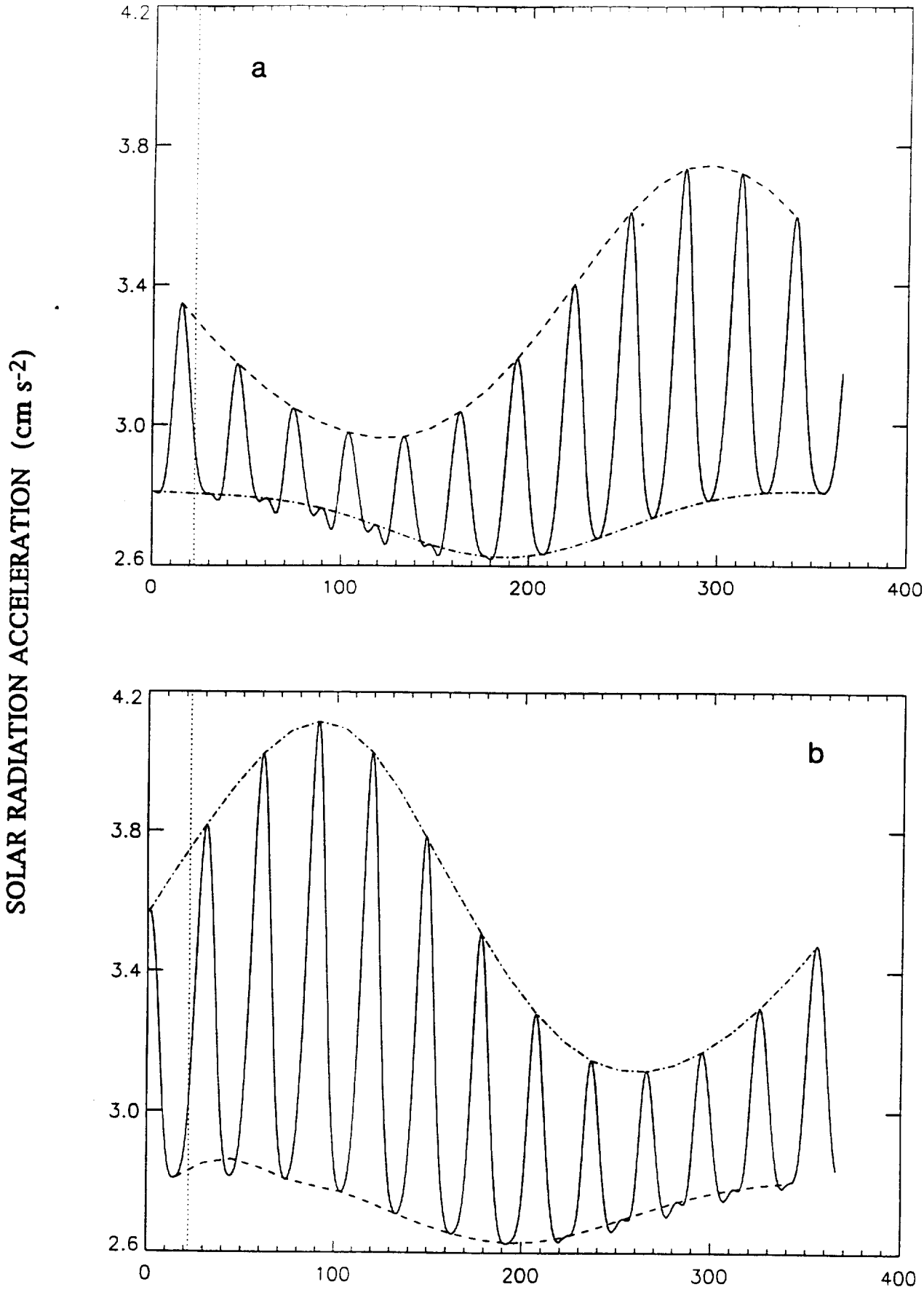
a
b
4.2
3.8
3.4
3.0
2.6
0
100
200
300
400
SOLAR RADIATION ACCELERATION (cm s-2)
DAY OF YEAR 1993

FIG. 2.2

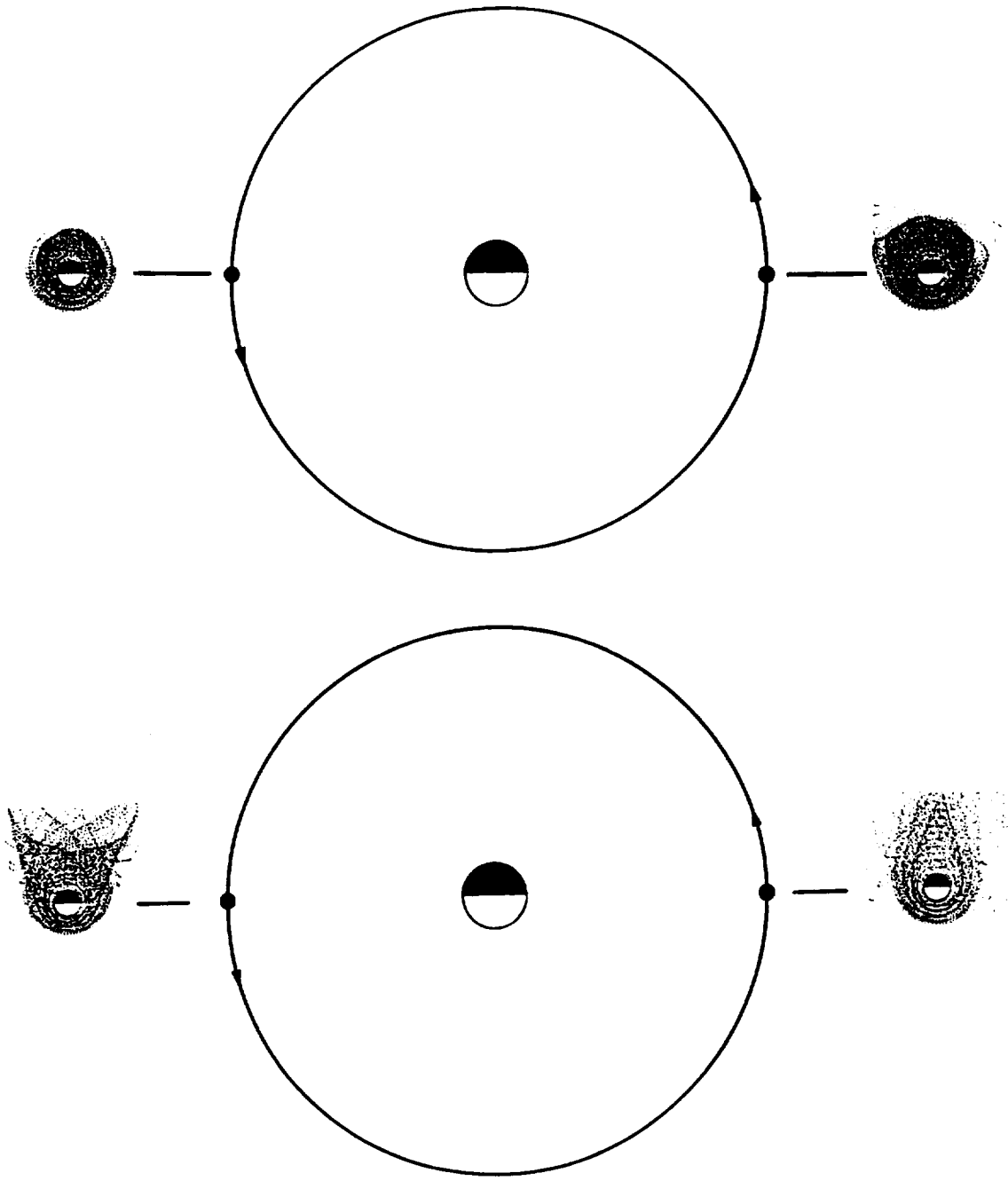

FIG. 2.3

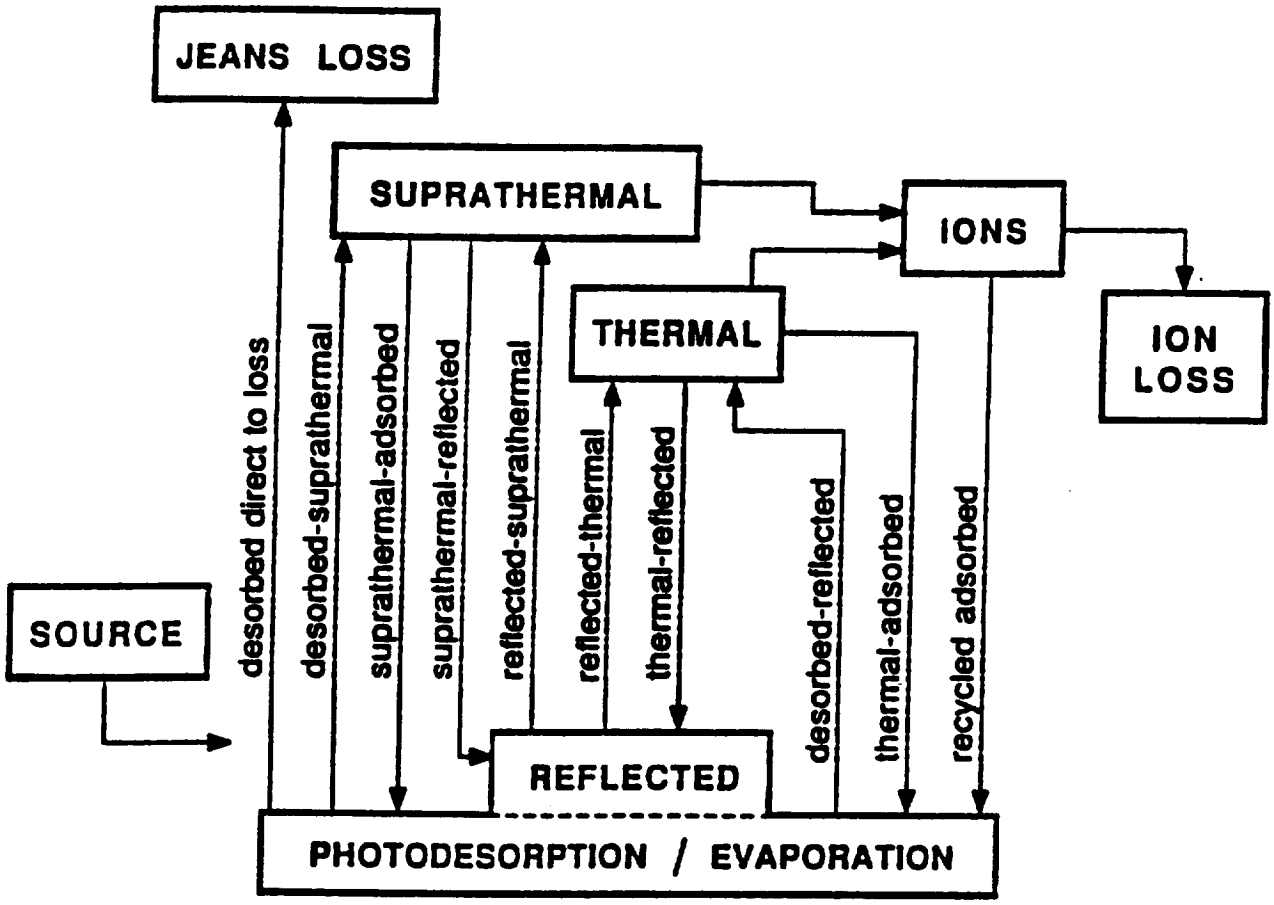

FIG. 3.1

TA000035

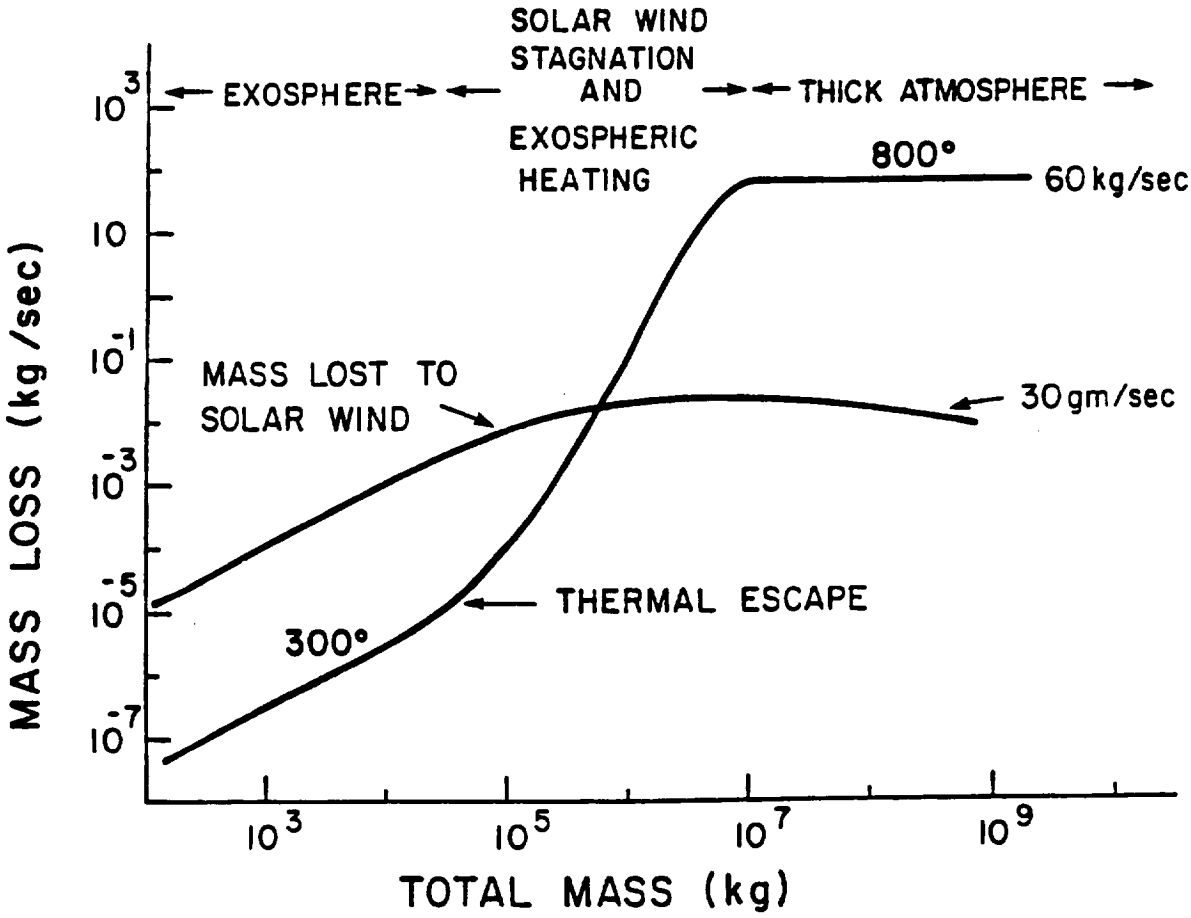

FIG. 5.1

TA000036

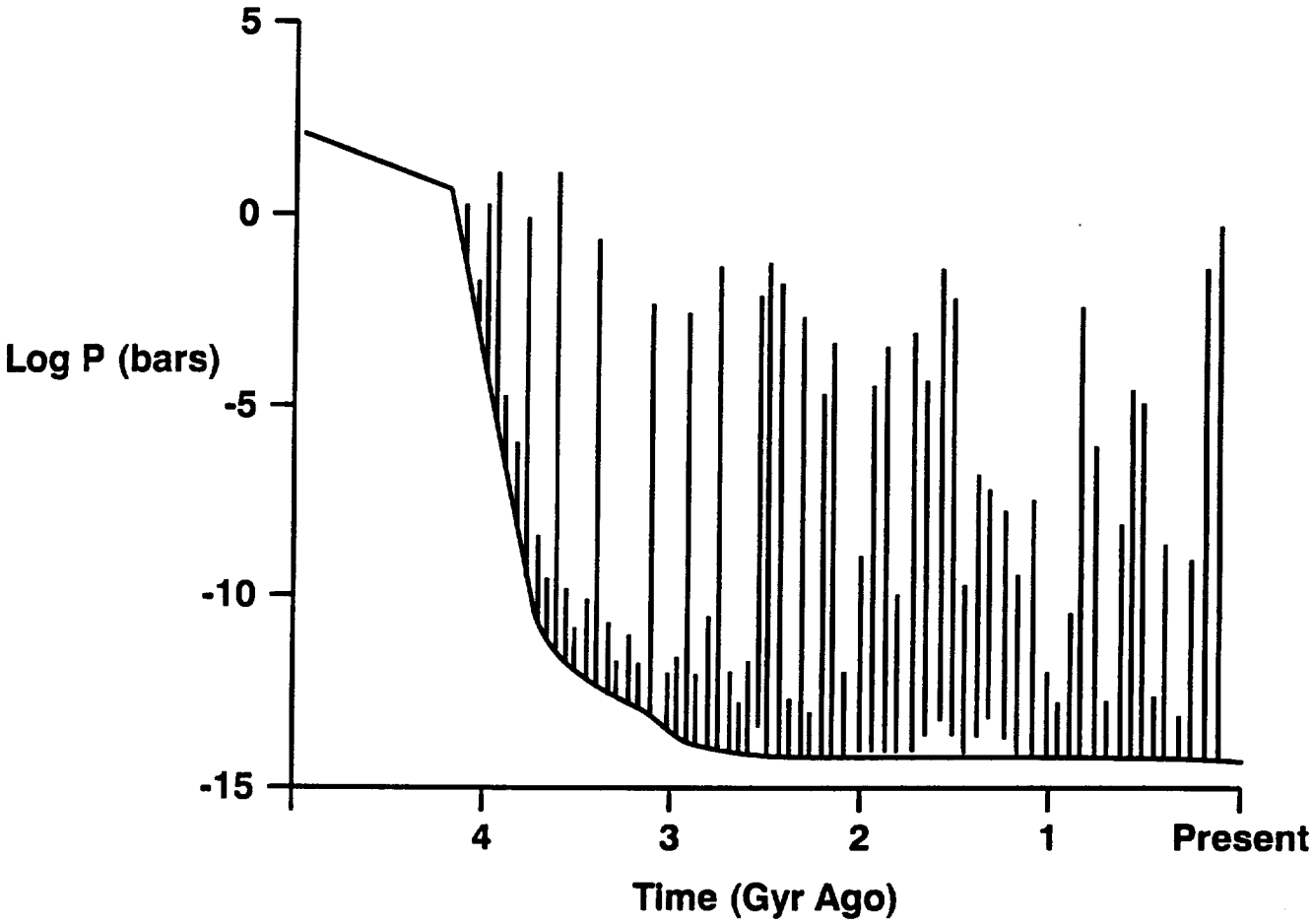

FIG. 5.2

TA000037

Table 1.1
Native Lunar Atmospheric Species: Abundances

Species	Detection Method	Number Density	Reference
He	LACE Mass Spectroscopy	2×10^3, 4×10^4 (day, night)	Hoffman et al. (1973)
Ar	LACE Mass Spectroscopy	1×10^5, 4×10^4 (day, night)	Flynn (1997), Hoffman
Rn	Alpha Particle Spectroscopy	variable	Gorenstein et al. (197
Na	Groundbased Spectroscopy (5890 Å)	070	Potter & Morgan (19
K	Groundbased Spectroscopy (7699 Å)	017	Potter & Morgan (19
H	Apollo 17 UV Spectroscopy (1216 Å)	<017 (3σ)	Feldman & Morrison
O	Apollo 17 UV Spectroscopy (1304 Å)	<500 (3σ)	Feldman & Morrison
N	Apollo 17 UV Spectroscopy (1200 Å)	<600 (2σ)	Fastie et al. (1973)
C	Apollo 17 UV Spectroscopy (1657 Å)	<200 (3σ)	Feldman & Morrison
S	Apollo 17 UV Spectroscopy (1474 Å)	<150 (3σ)	Feldman & Morrison
Kr	Apollo 17 UV Spectroscopy (1236 Å)	<20,000 (2σ)	Fastie et al. (1973)
Xe	Apollo 17 UV Spectroscopy (1470 Å)	<3000 (3σ)	Feldman & Morrison
H_2	Apollo 17 UV Spectroscopy (1462 Å)	<9000 (3σ)	Feldman & Morrison
CO	Apollo 17 UV Spectroscopy (1510 Å)	<14,000 (3σ)	Feldman & Morrison
Si	Groundbased Spectroscopy (3906 Å)	<048 (5σ)	Flynn & Stern (1996)
Al	Groundbased Spectroscopy (3962 Å)	<055 (5σ)	Flynn & Stern (1996)
Ca	Groundbased Spectroscopy (4227 Å)	<001 (5σ)	Flynn & Stern (1996)
Fe	Groundbased Spectroscopy (3859 Å)	<380 (5σ)	Flynn & Stern (1996)
Ti	Groundbased Spectroscopy (5036 Å)	<001 (5σ)	Flynn & Stern (1996)
Ba	Groundbased Spectroscopy (5536 Å)	<0.2 (5σ)	Flynn & Stern (1996)
Li	Groundbased Spectroscopy (6708 Å)	<0.01 (5σ)	Flynn & Stern (1996)
Al	HST UV Spectroscopy (3092 Å)		Stern et al. (1997)
Mg	HST UV Spectroscopy (2852 Å)		Stern et al. (1997)
OH	HST UV Spectroscopy (3085 Å)		Stern et al. (1997)

Notes: (1) In all cases, only the best existing upper limit is quoted on a given species. (2) All species number densities are quoted as dayside values unless otherwise noted. (3) Daytime contaminants detected by Apollo instruments not included. (4) Number densities for Feldman & Morrison (1991), Flynn & Stern (1996), Stern et al. (1997) all adjusted to an exospheric temperature of T=400 K.

Table 3.1
Characteristic Loss Timescales in the Lunar Atmosphere

Species	Thermo-Gravitational (390 K)	Thermo-Gravitational (1000 K)	Photoionization	e^- Impact
He	0.2 d	0.04 d	162 d	2900 d
Ar	500 Myr	03 yr	025 d	0550 d
Na	011 Kyr	23 d	0.6 d	0015 d
K	011 Gyr	16 yr	0.4 d	0010 d
H_2O	175 yr	06 d	029 d	0165 d

Notes: (1) Ionization loss timescales are in the presence of their respective sources and ignore shadowed time. (2) Despite not being discovered, water is included for reference; the dominant loss timescale for H_2O in the lunar atmosphere is its 1.2-day photodissociation timescale. (3) Radon is not listed because the excess energy of emission is greater than the lunar escape speed, escape is instantaneous.

Table 3.2
Surface Residence Times and Solar Zenith Angles for Lunar Sodium

T (K)	t_r (sec)	Lunar Solar Zenith Angle (deg)
300	3×10^5	80
400	7	00
500	0.01	N/A

Table 3.3
Reservoir, Source, and Sink Overview

Species	Reservoir	Primary Source	Sinks
He	Solar Wind	Thermal Desorption	Jeans Escape
	Lunar Interior	Sputtering	
Ar	Lunar Interior	Thermal Desorption	Photoionization
Rn	Lunar Interior	Outgassing	Decay Half-life
Po	Lunar Interior	Outgassing	Photoionization
Na, K	Lunar Regolith	Sputtering	Photoionization
	Meteorites/Comets	Thermal Desorption	
	Solar Wind		

Note: secondary entries indicate the secondary reservoirs or processes.

Table 4.1
Detected Surface Boundary Exospheres: Some Relevant Attributes

Object	Species Detected	Gravity ($cm\ s^{-2}$)	Dipole **B** (nT)	Total Detected Surface Number Density (cm^{-3})
Mercury	He, Na, K	372	~330	8×10^4 (day)
Moon	He, Ar, Rn, Po, Na, K	163	<0.2	2×10^5 (night)
Io	SO_2, SO, S, O, Na, K	187	~1500	10^{13} (max)
Europa	O, Na	281	<240	$10^{7.5}$

Table 4.2
Daytime Atmospheric Constituents: The Moon and Mercury

Species	Mercurian (cm^{-3})	Lunar (cm^{-3})
H	200	<17
He	6×10^3	2000–40,000
O	$\leq 4 \times 10^4$	<500
Na	2×10^4	70
K	500	17
Ar	$< 3 \times 10^7$	4×10^4
Total	5×10^4	8×10^4

Notes: (1) Abundances are average daytime abundances. (2) Abundances for H, He, O, and Ar at Mercury are from Broadfoot et al. (1976), for Na, K at Mercury are from Potter & Morgan (1985, 1986) and Sprague et al. (1990, 1997). (3) Abundances for H, He, O, and Ar for the Moon are from Hodges et al. (1973), for Na, K at the Moon see Potter & Morgan (1988a). (4) Adapted with permission from Hunten & Sprague (1997).

Table 4.3
Comparative Mercurian and Lunar Sodium and Potassium Abundance Ratios

Species	Solar (cm^{-3})	Mercurian (cm^{-3})	Lunar (cm^{-3})	Mercury/Moon Ratio
Na	6×10^4	4×10^4	70	~600
K	4×10^3	500	17	~030
Na/K Ratio	14	~80	~4	——

Note: Solar system abundances are per 10^6 Si atoms. This table is adapted from Hunten & Sprague (1997).

Figure List

1.1. On the lunar ionosphere (adapted from Vondrak 1988). Upper panel: Schematic representation of the sources of electric fields near the northern hemisphere of the Moon. The interplanetary field arises due to the motion of the solar wind magnetic field; the lunar surface field arises from surface charges. The terminator is the shaded area, labelled with SR=sunrise, and SS=sunset. Bottom panel: Schematic from SIDE data representing the variation in photoelectrons and lunar atmospheric ions with altitude.

1.2. Apollo 17 LACE argon data; adapted from Hodges (1975). The dashed lines represent model fits for the daytime atmosphere, which LACE could not measure owing to saturation effects (see text).

1.3. Apollo 17 LACE helium data; adapted from Hodges (1975). The data (with error bars) show the average synodic variation in lunar He; the (solid line) model fit is a model distribution for a solar wind source of 1.35×10^7 cm^{-2} s^{-1}.

1.4. Top panel: schematic representing the ^{238}U decay chain that results in the production of ^{222}Rn and later, ^{210}Po. Middle panel: The distribution of ^{222}Rn counts over the whole Moon during Apollo 15, showing the distinct deviation of the Aristarchus region (at right). Lower panel: ^{210}Po count rates measured over the lunar surface. Adapted from Gorenstein et al. (1974).

1.5. Sketches drawn by Apollo 17 astronaut E. Cernan of sunrise drawn from lunar orbit; the times in minutes and seconds refer to the time (e.g., T-6 min) before sunrise. Adapted from McCoy & Criswell (1976).

1.6. Reduced Potter and Morgan spectrum of the lunar sodium D lines, measured 600 km above the equatorial bright limb.

1.7. Sodium 5890 Å D2-line intensity above the subsolar limb, demonstrating the presence of both cool and hot thermal components (solid line); for comparison, the dotted line shows the fit attained if only a thermal component with a 120 km scale height were present. Adapted from Potter & Morgan (1988b).

1.8. Potter & Morgan's (1997) demonstration that the Na column density varies with latitude (and thus solar zenith angle) like $\cos^2(\chi)$.

1.9 Mendillo et al. (1993) wide-field Na Image.

1.10 Radial intensity cuts from four sodium images. Each image was corrected for vignetting, bias, gain, and scattered light. Plotted with each cut is the best two-temperature fit. In panel (a), 3σ lower limits for each temperature are given, where σ is the random

error in the data. In panels (b)-(d), the 3σ uncertainties in each temperature are given in parentheses. Each temperature component is shown individually along with the combined fit. The percentages for each temperature refer to the fractional abundances at the surface. Adapted from Stern & Flynn (1995).

1.11 Line-of-sight column abundances at 40 km above the límb for Si, Al, Ca, Fe, Ti, and Li relative to Na from both the stoichiometric model (filled circles) and the observations (triangles). The detected value for K is within a factor of 2 of the predicted stoichiometric value. *Bottom*: Ratios of observed upper limit column abundances to predicted values. A ratio of unity indicates stoichiometric behavior relative to Na. Arrows denote that values are upper limits in the cases of Si, Al, Ca, Fe, Ti, and Li. Note that the K value is within a factor of 2 of unity.

1.12 Charge-to-mass (M/q) spectra from the AMPTE SULECA instrument showing the detection of lunar ions when it was downstream of Moon; adapted from Hilchenbach et al. (1991).

2.1. Upper panel: The dynamics of transport in the lunar atmosphere. Bottom panel: The interchange of gases between reservoirs, sources, and sinks. Adapted from Smyth & Marconi (1995a).

2.2. Variation in solar radiation pressure on Na atoms as a function of time in 1993, showing both the effect of the monthly lunar orbit, and longer-term annual variations driven by the Earth's orbit. Upper panel: For Na atoms initially moving toward the Sun at 1 km s^{-1}; for Na atoms initially moving away from the Sun at 1 km s^{-1}. Adapted from Smyth & Marconi (1995a).

2.3. Comparison of the spatial character of the lunar Na and K atmospheres at first and last quarters. Upper panel: sodium; lower panel: potassium. These particular calculations were run for surface atom ejection speeds of 2.0 km s^{-1}; 259 atoms were used in this Monte Carlo simulation, the position of each being shown every 900 seconds. The lunar velocity at first and last quarters are -1.5 km s^{-1} and +1.5 km s^{-1}, respectively. Adapted from Smyth & Marconi (1995a); the distance to the Sun and the scale of the Sun are not to scale relative to the Moon and the lunar atmosphere, which are to scale with one another.

3.1. Illustration of the competing source mechanism concept; adapted from Sprague et al. (1992).

5.1. Loss rates for a 16 amu lunar atmosphere (model) as a function of atmospheric mass. Adapted from Vondrak (1974).

5.2. Schematic illustrating the three epochs of the lunar atmosphere,.

References

Ahrens, T.J., and J.D. O'Keefe, xxx, *The Moon*, 4, 214-xxx, 1971.

Allen, C.W., *Astrophysical Quantities*, London, The Athlone Press, 1973.

Arnold, J.R., Ice in the polar regions, *J. Geophys. Res.*, 86, 5659-5668, 1979.

Benson, J., J.W. Freeman, and H.K. Hills, The lunar terminator ionosphere, *Proc. 6th Lunar. Sci. Conf.*, 3013-3021, 1975.

Berg, O.E., A lunar terminator configuration, *Earth. Plan. Sci. Lett.*, 39, 377-381, 1978.

Berg, O.E., H. Wolf, and J. Rhee, Lunar soil movement registered by the Apollo 17 cosmic dust experiment, *Interplanetary Dust and Zodiacal Light*, edited by H. Elssser and H. Fechtig, Springer-Verlag, New York, 233-237, 1976.

Bjorkholm, P., L. Golub, and P. Gorenstein, The distribution of Rn and Po on the lunar surface as observed with the alpha particle spectrometer, *Proc. 4th Lunar Sci. Conf., Geochim. Cosmochim. Acta.*, 3, xxx-xxx, 1973.

Bottke, W.F., Jr., M.C. Nolan, R. Greenberg, and R.A. Kolvoord, Collisional lifetimes and impact statistics of near-earth asteroids, *Hazards due to Comets and Asteroids*, edited by T. Gehrels, The University of Arizona Press, Tucson, 337-357, 1994.

Broadfoot, A.L., Ultraviolet spectroscopy of the inner solar system from Mariner 10, *Rev. Geophys. Space Phys.*, 14(4), 625-627, 1976.

Broadfoot, A.L., S. Kumar, M.J.S. Belton, and M.B. McElroy, Mercury's atmosphere from Mariner 10: Preliminary results, *Science*, 185, 166-169, 1974.

Broadfoot, A.L., D.E. Shemansky, and S. Kumar, Mariner 10: Mercury atmosphere, *Geophys. Res. Lett.*, 3, 577-580, 1976.

Brown, M.E., A search for sodium atmosphere around Ganymede, *Icarus*, 126, 236-238, 1997.

Brown, M.E., and R.E. Hill 1996, Discovery of an extended sodium atmosphere around Europa, *Nature*, 380, 229-231, 1996.

Brown, M.E., and Y.L. Yung, Io, its atmosphere and optical emissions, *Jupiter*, edited by T. Gehrels, 1102-1145, The University of Arizona Press, Tucson, 1976.

Buratti, B., et al., Clementine evidence of lunar transient phenomena, in prep., 1998.

Burns, J.A., and M.S. Matthews, (Eds.) *Satellites*. The University of Arizona Press. Tucson, 1986.

Burns, J.O., I. Fernini. M. Sulkanen, N. Duric, and J. Taylor, Artificially-generated atmosphere near a lunar base. *Lunar Bases & Space Activities in the 21st Century*, Symposium sponsored by NASA, et al., Paper No. LBS-88-024, Houston, Texas, April 5-7, 1988.

Butler, B., D. Muhleman, and M. Slade, Mercury: Full-disk radar images and the detection and stability of ice at the north pole, *J. Geophys. Res.*, 98, 15,003-15,023, 1993.

Cameron, W.S., Comparative analyses of observations of lunar transient phenomena, *Icarus*, 16, 339-387, 1972.

Cameron, W.S., Report on ALPO lunar transient phenomena observing program, *JALPO*, 25(1-2), 1-14, 1974.

Cameron, W.S., Manifestations and possible sources of lunar transient phenomena (LTP), *The Moon*, 14, 187-199, 1975.

Cameron, W.S., Lunar transient phenomena catalog, *NSSDC/World Data Center A for Rockets & Satellites*, publication 78-03, 1978.

Carruthers, G.R., and T. Page, Far UV camera/spectrograph, *Apollo 16 Preliminary Science Report*, NASA SP-315, NASA, Washington, D.C., 13-1-13-13-14, 1972.

Cladis, J.B., W.E. Francis, and R.R. Vondrak, Transport toward earth of ions sputtered from the Moon's surface by the solar wind, *J. Geophys. Res.*, 99(A1), 53-64, 1994.

Cremonese, G., and S. Verani, High resolution observations of the sodium emission from the Moon, *Adv. Space Res.*, 19, xxx-xxx, 1997.

Criswell, Horizon-glow and the motion of lunar dust, *Photon and Particle Interactions with Surfaces in Space*, edited by R.J.L. Grard, 545-556, Dordrect-Holland, Reidel Publishing Company, 1973.

Dollfus, A., A new investigation of an atmosphere in the neighborhood of the Moon, *Comptes Rendus*, 234, 2046, 1952.

Dollfus, A., Polarization of light scattered by solid bodies and natural clouds, *Ann. Astrophys.*, 19, 83-113, 1956.

Eichorn, G., Heating and vaporization during hypervelocity particle impact, *Planet. Space Sci.*, 26, 463-467, 1978.

Elphic, R.C., H.O. Funsten, III, B.L. Barraclough, D.J. McComas, M.T. Paffett, D.T. Vaniman, and G. Heiken, Lunar surface composition and solar wind-induced secondary ion mass spectrometry, *Geophys. Res. Lett.*, 18(11), 2165-2168, 1991.

Fastie, W.G., P.D. Feldman, R.C. Henry, H.W. Moos, C.A. Barth, G.E. Thomas, and T.M. Donahue, A search for far-ultraviolet emissions from the lunar atmosphere, *Science*, 182, 710-711, 1973.

Feldman, P.D., and Morrison, D., The Apollo 17 ultraviolet spectrometer: Lunar atmosphere measurements revisited, *Geophys. Res. Lett.*, 18, 2105-2109, 1991.

Fernini, I., J.O. Burns, G.J. Taylor, M. Sulkanens, N. Duric, and S. Johnson, Dispersal of gases generated near a lunar outpost, *J. Spacecraft*, 27(5), 527-538, 1990.

Fessenkov, V.C., On the mass of the Moon's atmosphere, *Astron. J. Soviet Union*, 20, 1, 1943.

Flynn, B., Orfeus II FUV spectrographic observations of the lunar atmosphere, *Bull. Am. Astron. Soc.*, 190, 42.01, xxx-xxx, 1997.

Flynn, B., and M. Mendillo, A picture of the Moon's atmosphere, *Science*, 261, 184-186, 1993.

Flynn, B., and M. Mendillo, Simulations of the lunar sodium atmosphere, *J. Geophys. Res.*, 100, 23,271-23,278, 1995.

Flynn, B.C., and S.A. Stern, A spectroscopic survey of metallic species abundances in the lunar atmosphere, *Icarus*, 124, 530-536, 1996.

Freeman, J.W., Jr., Energetic ion bursts on the nightside of the Moon, *J. Geophys. Res.*, 77(1), 239-243, 1972.

Freeman, J.W., Jr., and J.L. Benson, A search for gaseous emissions from the Moon, *Phys. Earth Planet. Inter.*, 14, 276-281, 1977.

Freeman, J.W., Jr., and H.K. Hills, The Apollo lunar surface water vapor event revisited, *Geophys. Res. Lett.*, 18, 2109-2112, 1991.

Freeman, J.W., Jr., H.K. Hills, R.A. Lindeman, and R.R. Vondrak, Observations of water vapor ions at the lunar surface, *The Moon*, 8, 115-128, 1973.

Gault, D.E., Displaced mass, depth, diameter, and effects of oblique trajectories for impact craters formed in dense crystalline rocks, *The Moon*, 6, 32-34, 1973.

Gold, T., xxx, *Monthly Notices Roy. Astron. Soc.*, 115, 585-604, 1955.

Goldstein, B.D., S.T. Suess, and R.J. Walker, Mercury: Magnetospheric processes and the atmospheric supply and loss rate, *J. Geophys. Res.*, 86, 5485-5499, 1981.

Gorenstein, P. and P.J. Bjorkholm. Detection of radon emanation from the crater Aristarchus by the Apollo 15 alpha-particle spectrometer, *Science*, 179, 792-794, 1973.

Gorenstein, P., L. Golub, and P.J. Bjorkholm, Spatial features and temporal variability in the emission of radon from the Moon: An interpretation of results from the alpha particle spectrometer, *Proc. 4th Lunar Sci. Conf., Supplement 4, Geochim. Cosmochim. Acta.*, 3, 2803-2809, Pergamon Press, New York, 1973.

Gorenstein, P., L. Golub, and P.J. Bjorkholm, Detection of radon emission at the edges of lunar maria with the Apollo alpha-particle spectrometer, *Science*, 183, 411-413, 1974.

Gurnett, D.A., W.S. Kurth, A. Roux, S.J. Bolton, and C.F. Kennel, Galileo plasma wave observations in the Io plasma Torus and near Io, *Science*, 274(5286), 391-392, 1996.

Haff, P.K., et al., Ring and plasma: The enigma of Enceladus, *Icarus*, 56, 426-438, 1983.

Hall, D.T., D.F. Strobel, P.D. Feldman, M.A. McGrath, and H.A. Weaver, Detection of an oxygen atmosphere on Jupiter's moon Europa, *Nature*, 373(6516), 677-679, 1995.

Heiken, G., D. Vaniman, and B.M. French, *Lunar Sourcebook*, Cambridge University Press, Cambridge, England, 1991.

Herring, J.R., and A.L. Licht, Effect of the solar wind on the lunar atmosphere, *Science*, 130, 206, 1959.

Heymann, D., and A. Yaniv, Distribution of radon-222 on the surface of the Moon, *Nature Phys. Sci.*, 233, 37-39, 1971.

Hilchenbach, M., D. Hovestadt, B. Klecker, and E. Mbius, Detection of singly ionized energetic lunar pick-up ions upstream of earth's bow shock, *Proceedings Solar Wind Seven*, edited by E. Marsch and G. Schwenn, Pergamon Press, Goslar, Germany, 1991.

Hilchenbach, M., D. Hovestadt, B. Klecker, and E. Mbius, Observation of energetic lunar pick-up ions near earth, *Adv. Space Res.*, 13(10), 321-324, 1993.

Hinton, F.L., and D.R. Taeusch, Variation of the lunar atmosphere with the strength of the solar wind, *J. Geophys. Res.*, 69, 1341-1347, 1964.

Hodges, R.R., Jr., Formation of the lunar atmosphere, *The Moon*, 14, 139-157, 1975.

Hodges, R.R., Jr., Gravitational and radiative effects on the escape of helium from the Moon, 9th Lunar and Planetary Science Conference, Houston, Texas, March 13-17, 1978, Vol. 2 (A79-39176 16-91), Pergamon Press, New York, 1749-1764, 1978.

Hodges, R.R., and J.H. Hoffman, Implications of atmospheric Ar escape on the interior structure of the Moon, *Proc. 6th Lunar Sci. Conf.*, 3039-3047, 1975.

Hodges, R.R., and F.S. Johnson, Lateral transport in planetary exospheres, *J. Geophys. Res.*, 73, 7307-7317, 1968.

Hodges, R.R., J.H. Hoffman, T.T.J. Yeh, and G.K. Chang, Orbital search for lunar volcanism, *J. Geophys. Res.*, 77, 4079-4085, 1972.

Hodges, R.R., J.H. Hoffman, F.S. Johnson, and D.E. Evans, Composition and dynamics of the lunar atmosphere, *Proc. 4th Lunar Sci. Conf.*, 2865-2864, 1973.

Hodges, R.R., J.H. Hoffman, and F.S. Johnson, The lunar atmosphere, *Icarus*, 21, 415-xxx, 1974.

Hoffman, J.H., R.R. Hodges, Jr., and D.E. Evans, Lunar atmospheric composition results from Apollo 17, *Proc. 4th Lunar Sci. Conf., Geochim. Cosmochim. Acta.*, 3, xxx-xxx, 1973.

Hood, L.L., and G. Schubert, Inhibition of solar wind impingement on Mercury by planetary induction currents, *J. Geophys. Res.*, 84, 2641-2647, 1979.

Hunten, D.M., The equilibrium of atmospheric sodium, *Planet. Space Sci.*, 40, 1607-1614, 1992.

Hunten, D.M., and A.L. Sprague, Origin and character of the lunar and mercurian atmospheres, *Adv. Space Res.*, 19, 1551-1560, 1997.

Hunten, D.M., and L.V. Wallace, Resonance scattering by mercurian sodium, *Astrophys. J.*, 417, 757-761, 1993.

Hunten, D.M., T.H. Morgan, and D. Shemansky, The Mercury atmosphere, *Mercury*, edited by F. Vilas, C.R. Chapman, and M.S. Matthews, 562-612, The University of Arizona Press, Tucson, 1988.

Hunten, D.M., R.W.H. Kozlowski, and A.L. Sprague, A possible meteor shower on the Moon, *Geophys. Res. Lett.*, 18, 2101 - 2104, 1991.

Hunten, D.M., R.W.H. Kozlowski, and A.L. Sprague, xxx *J. Geophys. Res.*, 18, 2101-2104, 1992.

Ip, W.H., The sodium exosphere and magnetosphere of Mercury, *Geophys. Res. Lett.*, 13, 423-426, 1986.

Ip, W.H., The atomic sodium exosphere/coma of the Moon, *Geophys. Res. Lett.*, 18, 2093-2096, 1991.

Ip, W.H., On the surface effects of magnetospheric charged particles at Mercury, *Astrophys. J.*, 418, 451-456, 1993.

Jeans, J., *The Dynamical Theory of Gases*, Cambridge University Press, New York, 1923.

Johnson, F.S., Lunar atmosphere, *Rev. Geophys. Space Phys.*, 9(3), 813-823, 1971.

Johnson, F.S., J.M. Carroll, and D.E. Evans, Lunar atmosphere measurements, *Proc. 3rd Lunar Planet. Sci. Conf.*, 2231-2242, 1972.

Johnson, R.E, *Energetic charged-particle interactions with atmospheres and surfaces*, Springer-Verlag, New York, 1990.

Johnson, R.E., and R. Baragiola, Lunar surface: sputtering and secondary ion mass spectrometry, *Geophys. Res. Lett.*, 18(11), 2169-2172, 1991.

Johnson, R.E., and L.J. Lanzerotti, Ion bombardment of interplanetary dust, *Icarus*, 66, 619-624, 1986.

Johnson, R.E., and E.C. Sittler, Jr., Sputter-produced plasma as a measure of satellite surface composition: The Cassini mission, *Geophys. Res. Lett.*, 17, 1629-xxx, 1990.

Kasting, J.F. and D.H. Grinspoon, The faint young sun problem, *The Sun in Time*, edited by C.P. Sonett, M.S. Giampapa, and M.S. Matthews, The University of Arizona Press, Tucson, 1991.

Kaula, W.M., M.J. Drake, and J.W. Head, The moon, *Satellites*, edited by J.A. Burns and M.S. Matthews, The University of Arizona Press, Tucson, 581-628, 1986.

Kerridge, J.F., and J.R. Kaplan, Sputtering: Its relationship to isotopic fractionation on the lunar surface, *Proc. 9th Lunar Sci. Conf.*, Lunar Planetary Institute, Houston, 1687-1709, 1978.

Killen, R.M., Crustal diffusion of gases out of Mercury and the Moon, *Geophys. Res. Lett.*, 16, 171-174, 1989.

Killen, R.M., and T.H. Morgan. Maintaining the Na atmosphere of Mercury, *Icarus*, 101, 293-312, 1993.

Kozlowski, R.W.H., A.L. Sprague, and D.M. Hunten, Observations of potassium in the tenuous lunar atmosphere, *Geophys. Res. Lett.*, 17, 2253-2256, 1990.

Kozyrev, N.A., and Priroda, 84, *Sky and Telescope*, 18, 561, March 1959.

Lanzerotti, L.J., W.L. Brown, and R.E. Johnson, Ice in the polar regions of the Moon, *J. Geophys. Res.*, 88, 3949-3950, 1981.

Lin, R.P., and K.A. Anderson, Observations of magnetic merging and the formation of the plasma sheet in the earth's magnetotail, *J. Geophys. Res.*, 82(19), 2761-2773, 1977.

Manka, R.H., and F.C. Michel, Lunar atmosphere as a source of lunar surface elements, *Proc. 2nd Lunar Sci. Conf.*, 1717-1728, 1971.

McCoy, J.E., Photometric studies of light scattering above the lunar terminator from Apollo solar corona photography, *Proc. 7th Lunar Sci. Conf.*, xxx-xxx, 1976.

McCoy, J.E., and D.R. Criswell, Evidence for a high altitude distribution of lunar dust, *Proc. Fifth Lunar Conf., Supplement 5, Geochim. Cosmochim. Acta*, 3, 2991-3005, 1974.

McGrath, M.A., R.E. Johnson, and L.J. Lanzerotti, Sputtering of sodium on the planet Mercury, *Nature*, 323, 694-696, 1986.

Mendillo, M., and J. Baumgardner, Constraints on the origin of the Moon's atmosphere from observations during a lunar eclipse, *Nature*, 377, 404-406, 1995.

Mendillo, M., J. Baumgardner, and B. Flynn, Imaging observations of the extended sodium atmosphere of the Moon, *Geophys. Res. Lett.*, 18, 2097- 2100, 1991.

Mendillo M., B. Flynn, and J Baumgardner, Imaging experiments to detect an extended sodium atmosphere on the Moon, *Adv. Space Res.*, 13(10), 313-319, 1993.

Mendillo M., J. Emery, and B. Flynn, Modeling the Moon's extended sodium cloud as a tool for investigating sources of transient atmospheres, *Adv. Space Res.*, 19, 1577-1586, 1997.

Middlehurst, B.M., An analysis of lunar events, *Rev. Geophys.*, 5, 173-189, 1967.

Morgan, T.H., and R.M. Killen, A non-stoichiometric model of the composition of the atmospheres of Mercury and the Moon, *Planet. Space Sci.*, xx, xxx-xxx, 1996.

Morgan, T.H., and D.E. Shemansky, Limits to the lunar atmosphere, *J. Geophys. Res.*, 96, 1351-1367, 1991.

Morgan, T.H., H.A. Zook, and A.E. Potter, Production of sodium vapor from exposed regolith in the inner solar system, *Proc.19th Lunar Planet. Sci. Conf.*, 297-304, 1989.

Mukherjee, N.R., Solar-wind interactions: Nature and composition of lunar atmosphere. *The Moon*, 14, 169-186, 1975.

Na, C.Y., L.M. Trafton, E.S. Barker, and S.A. Stern, A search for new species in Io's atmosphere, *Icarus*, submitted, 1997.

Norton, R.H., J.E. Guinn, W.C. Livingston, G.A. Newkirk, and H. Zirin, Surveyor 1 observations of the solar corona, *J. Geophys. Res.*, 72(2), 815-817, 1967.

O'Keefe, J.D., and T.J. Ahrens, Cometary and meteorite swarm impact on planetary surfaces, *J. Geophys. Res.*, 87(B8), 6668-6680, 1982.

Pomalaza-Diaz, J.C., Measurement of the lunar ionosphere by occultation of the Pioneer 7 spacecraft, *Stanford Electronics Lab. Sci. Rep. No. SU-SEL-67-095*, 1967.

Potter, A.E., Chemical sputtering could produce sodium vapor and ice on Mercury, *Geophys. Res. Lett.*, 22, 3289-3292, 1995.

Potter, A.E., and T.H. Morgan, Discovery of sodium in the atmosphere of Mercury, *Science*, 229, 651-653, 1985.

Potter, A.E., and T.H. Morgan, Potassium in the atmosphere of Mercury, *Icarus*, 67, 336-340, 1986.

Potter, A.E., and T.H. Morgan, Variation of sodium on Mercury with solar radiation pressure, *Icarus*, 71, 472-477, 1987.

Potter, A.E. and T.H. Morgan, Discovery of sodium and potassium vapor in the atmosphere of the Moon, *Science*, 241, 675-680, 1988a.

Potter, A.E. and T.H. Morgan, Extended sodium exosphere of the Moon, *Geophys. Res. Lett.*, 15, 1515-1518, 1988b.

Potter, A.E., and T.H. Morgan, Evidence for magnetospheric effects on the sodium atmosphere of Mercury, *Science*, 248, 835-838, 1990.

Potter, A.E. and T.H. Morgan, Observations of the lunar sodium exosphere, *Geophys. Res. Lett.*, 18, 2089-2092, 1991.

Potter, A.E. and T.H. Morgan, xxx, *J. Geophys. Res.*, 18, 2089-2092, 1992.

Potter, A.E. and T.H. Morgan, Variation of lunar sodium emission intensity with phase angle, *Geophys. Res. Lett.*, 21, 2263 - 2266, 1994.

Potter, A.E., and T.H. Morgan, Coronagraphic observations of the lunar sodium exosphere near the lunar surface, *J. Geophys. Res.*, submitted, 1997a.

Potter, A.E., and T.H. Morgan, Evidence for suprathermal sodium on Mercury, *Adv. Space Res.*, 19(10), 1571-1576, 1997b.

Rabinowitz, D.L., E. Bowell, E.M. Shoemaker, and K. Muinonen, xxx, *Hazards Due to Comets and Asteroids*, edited by T. Gehrels and M. Matthews, The University of Arizona Press, Tucson, 1994.

Reasoner, D.L., and W.J. Burke, Characteristics of the lunar photoelectron layer while in the geomagnetic tail, paper presented at the *Sixth ESLAB Symposium*, Noordwijk, Holland, 26-29, September 1972.

Rennilson, J.J., and D.R. Criswell, Surveyor observations of lunar horizon-glow, *The Moon*, 10, 121-142, 1974.

Rettig, T.W., and J.M. Hahn, Eds., *Completing the Inventory of the Solar System, A Symposium Held in Conjunction with the 106th Annual Meeting of the ASP held at Lowell Observatory, Flagstaff, Arizona, 25-30 June 1994*, Volume 107, Astronomical Society of the Pacific, San Francisco, CA, 1996.

Roth, J., Chemical sputtering, sputtering by particle bombardment II, edited by R. Gehrisch. *Topics in Applied Physics*, 52, Springer-Verlag, 91-145, 1983.

Severny, A.B., E.I. Terez, and A.M. Zvereva, Preliminary results obtained with an astrophotometer installed on Lunokhod 2, *Space Research XIV*, Akademic-Verlag, Berlin, xxx-xxx, 1974.

Shoemaker, E.M., Asteroid and comet bombardment of the Earth, *Ann. Rev. Earth Planet. Sci.*, 11, 461-494, 1983.

Shoemaker, E.M., et al., Surveyor 7 Mission Report, Part 2, Science Results, *JPL Tech. Rep. 32-1264*, 9-76, 1968.

Singer, S.F., Atmosphere near the Moon, *Astronaut. Acta*, 7, 135, 1961.

Siscoe, G.L., and N.R. Mukherjee, Upper limits on the lunar atmosphere determined from solar-wind measurements, *J. Geophys. Res.*, 77(31), 6042-6051, 1972.

Slade, M., B. Butler, and D. Muhleman, Mercury radar imaging: Evidence for polar ice,

Science, 258, 635-640, 1992.

Sleep, N.H., K.J. Zahnle, J.F. Kasting, and H.J. Morowitz, xxx, *Nature*, 342, 139-144, 1989.

Smith, G.R., D.E. Shemansky, A.L. Broadfoot, and L. Wallace, Monte Carlo modeling of exospheric bodies: Mercury, *J. Geophys. Res.*, 83, 3783-3790, 1978.

Smyth, W.H., Nature and variability of Mercury's sodium atmosphere, *Nature*, 323, 696-699, 1986.

Smyth, W.H., and M.L. Marconi, Theoretical overview and modeling of the sodium and potassium atmospheres of the Moon, *Astrophys. J.*, 443, 371-392, 1995a.

Smyth, W.H., and M.L. Marconi, Theoretical overview and modeling of the sodium and potassium atmospheres of Mercury, *Astrophys. J.*, 441, 839-864, 1995b.

Sprague, A.L., A diffusion source for sodium and potassium in the atmospheres of Mercury and the Moon, *Icarus*, 84, 93-105, 1990.

Sprague, A.L., xxx, *J. Geophys. Res.*, 98, 1231-xxx, 1993.

Sprague, A.L., R.W.H. Kozlowski, and D.M. Hunten, Caloris Basin: An enhanced source for potassium in Mercury's atmosphere, *Science*, 249, 1140-1143, 1990.

Sprague, A.L., R.W.H. Kozlowski, D.M. Hunten, W.K. Wells, and F.A. Grosse, The sodium and potassium atmosphere of the Moon and its interaction with the surface, *Icarus*, 96, 27-42, 1992.

Sprague, A.L., R.W.H. Kozlowski, D.M. Hunten, and F.A. Grosse, An upper limit on neutral calcium in Mercury's atmosphere, *Icarus*, 104, 33-37, 1993.

Sprague, A.L., D.M. Hunten, and K. Lodders, Sulfur at Mercury, elemental at the poles and sulfides in the regolith, *Icarus*, 118, 211-215, 1995.

Sprague, A.L., D.M. Hunten and F.A. Grosse, Upper limit for lithium in Mercury's atmosphere, *Icarus*, 123, 345-349, 1996.

Sprague, A.L., D.M. Hunten, R.W.H. Kozlowski, F.A. Grosse, R.E. Hill, and R.L. Morris, Observations of sodium in the lunar atmosphere during International Lunar Atmosphere Week, 1995, *Icarus*, 120, xxx-xxx, 1997.

Stern, S.A., Imaging detection of atmospheric sodium over the lunar terminator, *Proc. LPSC*, XXIII, xxx-xxx, 1992.

Stern, S.A., and H. Campins, Chiron and the Centaurs: Escapees from the Kuiper Belt. *Nature*, 382, 507, 1996.

Stern, S.A. and B.C. Flynn, Narrow-field imaging of the lunar sodium exosphere. *Astron. J.*, 109, 835-841, 1995.

Stern, S.A., J.W. Parker, T.H. Morgan, B.C. Flynn, D.M. Hunten, A.L. Sprague, M. Mendillo, and M.C. Festou, An HST search for magnesium in the lunar atmosphere. *Icarus*. 127, 523-526, 1997.

Taylor, S.R., *Planetary Science: A Lunar Perspective*, Pergamon, New York, 1982.

Thomas, G.E., Mercury: Does its atmosphere contain water?, *Science*, 183, 1197-1198, 1974.

Townsend, P.C., xxx, *Sputtering by Particle Bombardment*, edited by R. Behrich, Springer-Verlag, Berlin, 147-xxx, 1983.

Tyler, A.L., R.W.H. Kozlowski, and D.M. Hunten, Observations of sodium in the tenuous lunar atmosphere, *Geophys. Res. Lett.*, 15, 1141-1144, 1988.

Vondrak, R.R., Creation of an artificial lunar atmosphere, *Nature*, 248, 657-659, 1974.

Vondrak, R.R., Upper limits to gas emission from lunar transient phenomena sites, *Phys. Earth Planet. Inter.*, 14, 293-298, 1977.

Vondrak, R.R., Lunar base activities and the lunar environment, *Lunar Bases & Space Activities in the 21st Century*, Symposium sponsored by NASA, et al., Paper No. LBS-88-098, Houston, Texas, April 5-7, 1988.

Wiens, R.C., D.S. Burnett, W.F. Calaway, and M.J. Pellin, xxx, *Bull. American Astron. Soc.*, 25, 1089-xxx, 1993.

Williams, R.J., and J.J. Jadwick, *Handbook of Lunar Materials*, Report NASA-RP-1057, NASA, Washington, DC, 1980.

Zook, H.A., A.E. Potter, and B.L. Cooper, Lunar horizon glow: New evidence from Clementine, *Int. Lunar Expl. Conf.*, San Diego, CA, 14-16 (limited distribution), November, 1994.

Zook, H.A., A.E. Potter, and B.L. Cooper, The lunar dust exosphere and Clementine lunar horizon glow, *Proc. 26th Lunar Planet. Sci. Conf.*, 1995.